



**WITS**  
UNIVERSITY

**Detecting peat degradation using low altitude remote sensing technologies**

**Mathapelo Petunia Chauke (1109434)**

A research report submitted to the Faculty of Science, University of the Witwatersrand, Johannesburg, in partial fulfilment of the requirements for the degree of Master of Science (Geographical Information Systems and Remote Sensing) at the School of Geography, Archaeology & Environmental Studies

**Supervisor:** Prof. MAM Abd Elbasit (*Sol Plaatje University*)

**Co-Supervisor:** Prof. E. Adam (*University of the Witwatersrand*)

**29 SEPTEMBER 2021**

### *Declaration of Originality*

I Mathapelo Petunia Chauke, declare that this research report is my work, except where otherwise acknowledged and appropriately referenced. It is being submitted for the degree of *Master of Science in Geographical Information Systems and Remote Sensing* to the University of the Witwatersrand, Johannesburg. It has not been submitted before for any degree or examination at any other University.

*MP Chauke*

---

Signature of Student

29th      **day of**      September 2021      **at the**      University of the Witwatersrand

## Acknowledgements

I want to thank **God**, the **Almighty**, He who is "**I AM**" for the grace and mercy that he has showered into my life, this research, and all the success that I have accomplished. To my family (*L. Chauke, J. Chauke, N. Moyana, S. Chauke*), friend (*M. Khanyile*) and mentors (*T. Layne and T. Naidoo*), I offer great gratitude for the support, words of encouragement, caring, and love they have given me throughout the research progress and completion. 'I thank you all.'

I give my most significant appreciation to my supervisor from Sol Plaatje University, *Prof. MAM Abd Elbasit*, and a co-supervisor from the University of the Witwatersrand, *Prof. E. Adam*, for their patience, assistance, for pushing me at times when I derailed from the research; most of all, the support they have given to me through all the research stages, from the proposal stage to a full research report completion. I also want to thank the Agricultural Research Council-Institute for Soil, Climate, and Water (ARC-SCW) for giving me access to their laboratories for experimental analysis.

I am highly honoured by all the sponsors who have helped me fund my studies, i.e., tuition, accommodation, and research necessities. Many thanks to the National Research Foundation (NRF) ~ Scarce Skills Development Funds Masters Scholarships 2019/20 for funding my tuition fees; I am grateful for the financial assistance.

A special thank you to Water RDI Roadmap 2019/20 Postgraduate Student Bursary from Water Research Commission (WRC) to fund my accommodation and my research essentials. The Water RDI program provided financial support for my academics and delivered training workshops (hosted by GreenMatter) to enrich one soft skill. That is, build self-confidence, self-acceptance, self-awareness, self-management, and leadership skills (which taught one that leadership is not about being in power but the ability to communicate and convince people to work towards a common goal).

I am grateful to the Water Research Commission for funding this research as part of the "Multi-Platform Remote Sensing Tools for Peat Fire Detection and Monitoring" project (Project No. K5/2836).

I am beyond grateful and honoured to be allowed to learn, up-skill myself, and complete my master's degree (MSc in GIS and Remote Sensing).

## **Abstract**

Peatlands are rare and unique in South Africa; they occur in patches and stripes at the valley bottom. They are mostly found in the wet eastern and southern parts of the country and are characterised as groundwater-dependent ecosystems. South Africa's peatlands are at risk as a result of improper management and use. These include growing population demand for pumping of underground water, peat mining, the invasion of infrastructure and species, and agricultural use. Amongst others, these peats are vulnerable to peat fires during extreme drought conditions or after the groundwater level has been artificially lowered/draind. Peat fires are spontaneous ground fires that arise on the floor of forests that produce much heat without flames (smouldering).

This research aims to assess peatland degradation using low altitude remote sensing technologies, unmanned aerial vehicles (UAVs) in South African peatlands by: (1) Establishing peat thermal and moisture contents at a small scale, (2) Identifying peat dryness/peat moisture using TIR and NIR, and (3) Determining the extent of peat fires by integrating multispectral data and investigating thermal anomalies. Remote sensing of peatlands can help develop an understanding of threats to peatlands and treatments to manage them sustainably. It can also help to secure and define areas that are not accessible. Satellite data can help establish the extent of peatlands and the impact of fire disturbance on peatland ecosystems and the atmosphere (smoke affecting the air quality).

The study investigated two peat sites (Molopo and Molemane) situated within the hydrological karst region, making them vulnerable to degradation when disturbed by economic activities such as natural resources. Molemane is a peat that has not been significantly affected by the destruction of cultivation/drainage. In contrast, Molopo is peat that a recent forest fire has severely damaged.

The results show that the predicted soil moisture has a maximum Perpendicular Soil Moisture Index (PSMI) maximum value of 0.78 for Molopo and a maximum value of 0.71 PSMI at Molemane. The results indicate a lower level of peat moisture at the Molopo peat site than Molemane since Molopo is regarded as dry peat.

The Temperature Vegetation Dryness Index (TVDI) also points out that Molemane is more pristine than Molopo. Molopo peat has a higher value of TVDI (0.61) than Molemane,

which has a 0.51 TVDI average value. PSMI and TVDI have been used to establish maps of peat moisture's spatial distribution across the Molopo and Molemane peat sites.

The results from the study showed that: TVDI and PSMI can measure (1) dry area hot spots, which indicated that both PSMI and TVDI can be used for peatland degradation monitoring, although they showed some discrepancies in the spatiotemporal characteristics of peat dryness of the two peat areas; and (2) that ground measured peat moisture had better correlations to PSMI than to TVDI, indicating that there were more statistically significant relationships between PSMI and peat moisture and that PSMI is a more reliable indicator for assessing peat dryness. The study shows that peat moisture is a reliable proxy for peatland dryness level. This proxy can be monitored cost-effectively using UAVs equipped with infrared cameras.

### **Keywords**

PSMI, TVDI, peat fires, smouldering, spectral, thermal imaging, infrared cameras, multispectral, peat moisture, low-altitude remote sensing, UAV

# TABLE OF CONTENTS

<b>Detecting peat degradation using low altitude remote sensing technologies</b> .....	i
<i>Declaration of Originality</i> .....	ii
Acknowledgements .....	iii
Abstract .....	iv
List of Figures .....	viii
List of Tables .....	x
List of Acronyms .....	1
Examiner’s Corrections Highlighter Colour .....	3
CHAPTER ONE: INTRODUCTION .....	4
1. General Introduction .....	4
1.1. Peatland functions and characteristics .....	4
1.2. The rationale for the study .....	5
<b>1.3. Problem Statement</b> .....	7
1.4. Aims and objectives .....	8
<b>1.5. Research Questions</b> .....	8
1.6. Research report outlines .....	8
CHAPTER TWO: LITERATURE REVIEW .....	10
2. General Overview of Peatland Systems .....	10
2.1. Distribution of Peatland Systems in South Africa .....	11
2.2. Importance of Peatland Systems .....	12
2.3. Soil Moisture and Thermal Indices .....	14
2.4. Mapping and monitoring peatland degradation .....	17
<b>2.5. Conclusion of the Literature Review</b> .....	22
CHAPTER THREE: RESEARCH METHODOLOGY .....	25
3. Materials and Methods .....	25
3.1. Study Site .....	25
3.2. Ground data measurements .....	27
3.3. Laboratory experiment setup .....	30
3.4. Unmanned Aerial Vehicle (UAV) monitoring system .....	31
<b>3.5. Statistical Analysis</b> .....	36
CHAPTER FOUR: RESULTS .....	38
4. Peat properties at the laboratory experiment scale .....	38
4.1. Peat soil moisture and thermal properties .....	38

4.2.	The behaviour of ignition front or front movement in peat samples.....	41
5.	Soil moisture estimates using thermal infrared (TIR) and near-infrared (NIR).....	42
5.1.	Relationship between vegetation and TIR .....	42
5.2.	Comparison between PSMI and TVDI.....	44
5.3.	Validation of imagery derived soil moisture data with ground measured soil moisture content .....	47
CHAPTER FIVE: DISCUSSION.....		48
6.1.	Laboratory Experiment .....	48
6.1.1.	Peat moisture estimation (Laboratory-Based).....	48
6.1.2.	Peat moisture and thermal characteristics (Ground-based and laboratory-based) .....	48
6.1.3.	Spread of peat fire under different moisture .....	49
6.2.	UAV Application .....	50
6.2.1.	UAV images for peatland monitoring.....	50
6.2.2.	Estimation of peat moisture using UAV data .....	51
CHAPTER SIX: CONCLUSION AND RECOMMENDATIONS .....		53
7.1.	Conclusion of the study .....	53
7.2.	Recommendations and future studies.....	54
REFERENCES .....		55
APPENDICES .....		63
Appendix A: Figures.....		63

## List of Figures

<b>Figure 1:</b> Brief explanation of the chapters.....	9
<b>Figure 2:</b> Rietvlei Reserve peatland, indicating peat thickness (Grundling <i>et al.</i> , 2017, 4).....	10
<b>Figure 3:</b> The spatial distribution of the peatland in South Africa (Grundling <i>et al.</i> , 2017).....	12
<b>Figure 4:</b> Peat formation factors/ indicators, and sensors that can assess the indicators as a function of spatial scale (after Minasny <i>et al.</i> , 2019) .....	13
<b>Figure 5:</b> In a summary, the data required for peatland monitoring (FAO, 2020).....	23
<b>Figure 6:</b> Map depicting the study area of interest and the two peatlands selected for the study .....	26
<b>Figure 7:</b> Wetland Vegetation distribution of North West Province, South Africa .....	27
<b>Figure 8:</b> Ground measurements tools .....	28
<b>Figure 9:</b> Schematic diagram of the peat burn experiment, a. 20cm x 20cm x 5cm open-top box; b. Peat soil (wet/dry soil moisture); c. Electrical heating coil; d. infrared camera and a thermal camera (FLIR Systems).....	30
<b>Figure 10:</b> Equipment for performing laboratory experiments .....	31
<b>Figure 11:</b> Unmanned Aerial Vehicle (UAV) with available sensors utilised to monitor the peat conditions.....	32
<b>Figure 12:</b> Ground Measurements and Flying Area for Molopo (a.) and Molemane peat sites (b.); Flight Plan for Molopo (c.) and Molemane peat sites (d.) .....	34
<b>Figure 13:</b> Brief process followed from data acquisition to data analysis .....	34
<b>Figure 14:</b> Bulk density for Molopo and Molemane wet and dry samples(g/cm <sup>3</sup> ).....	38
<b>Figure 15:</b> The relationship between front movement, soil moisture, and temperature during peat ignition for Molemane sample with a gravimetric moisture content of (a.) 30% and (b.).130% MC .41	
<b>Figure 16:</b> Molopo samples indicating the relationship between temperature and distance from the ignitor with a gravimetric moisture content of (a) 45% MC and (b) 88% MC.....	42
<b>Figure 17:</b> Regression analysis between NDVI and emissivity .....	43
<b>Figure 18:</b> NDVI for Molopo Site (a.) May Survey and (b.) December Peat Survey .....	44
<b>Figure 19:</b> NDVI for Molemane Site (a.) May Survey and (b.) December Peat Survey .....	44
<b>Figure 20:</b> PSMI distribution of predicted peat moisture in the peat field at Molopo. Survey of May (a.) and of December (b.).....	45
<b>Figure 21:</b> PSMI distribution of predicted peat moisture in the peat field at Molemane. Survey of May (a.) and of December (b.).....	45
<b>Figure 22:</b> TVDI distribution in Molopo, a. May Survey and December Survey .....	46
<b>Figure 23:</b> TVDI distribution in Molemane, a. May Survey and December Survey .....	46
<b>Figure 24:</b> Linear regression for soil moisture field measurements and predicted soil moisture from TIR and NIR bands .....	47
<b>Figure 25:</b> Linear relationship between ground measured soil moisture and TVDI values.....	47
<b>Figure A 1:</b> The outline of the main objectives of the project .....	63
<b>Figure A 2:</b> Model developed to establish indices calculation and soil moisture index .....	63
<b>Figure A 3:</b> Steps for laboratory research performed a.) weighing the samples b.) Samples drying at 70 ° C, for 1 to 3 days, c.)Ceramic heater coil and d.) set up the experiment about the fire; e.) peat rewetting samples; f.), soil moisture calculation using Theta Probe; g.), peat fire burning / smouldering peat surface and h.) peat ash after peat burning.....	64
<b>Figure A 4:</b> Correlation between theta (moisture content) and other variables .....	65

<b>Figure A 5:</b> The relationship between front movement, soil moisture, and temperature during peat ignition for Molemane samples; (a.) 130%MC, (b.) 90%MC, (c.) 56%MC, (d.) 30%MC and (e.)120%MC.....	66
<b>Figure A 6:</b> Green- NDVI for Molopo (a) and Molemane (b).....	67
<b>Figure A 7:</b> NDWI images for Molopo (a.) and Molemane (b.) peat sites .....	67
<b>Figure A 8:</b> Red Edge NDVI for Molopo (a.) and Molemane (b.) peat site .....	68
<b>Figure A 9:</b> Natural Colour Composite [RGB: 3, 2, 1] for Molopo (a.) and Molemane (b.) peat site	68
<b>Figure A 10:</b> Pseudo-infrared composite [RGB: 5, 3, 2] for Molopo (a.) and Molemane (b.) peat site .....	69
<b>Figure A 11:</b> High-resolution multispectral image for Molopo (a.) and Molemane (b.) peat site with RGB: 3, 4, 2 (left) and RGB: 4, 3, 2(right) .....	69
<b>Figure A 12:</b> Thermal images, May survey for peat sites Molopo (a.) and Molemane (b.) (RGB: 3, 2, 1) and December survey, Molopo (c.) and Molemane (d.) peat sites (RGB: 3, 2, 1.....	70
<b>Figure A 13:</b> Molopo peat site Di distribution.....	70
<b>Figure A 14:</b> Molemane Peat site Di distribution .....	71
<b>Figure A 15:</b> Linear regression for soil moisture field measurements and predicted soil moisture from TIR and NIR bands for Molopo site (a.) and Molomane (b.) .....	71
<b>Figure A 16:</b> The relationship between Red and NIR band.....	72

## List of Tables

<b>Table 1:</b> Summary description of various soil moisture indices .....	16
<b>Table 2:</b> Review of laboratory experiment for peat fire analysis .....	18
<b>Table 3:</b> Sensors mounted on UAVs and their potential uses (Tmusic <i>et al.</i> , 2020) .....	20
<b>Table 4:</b> Examples of common UAVs used for field monitoring, including their primary description, features, and cost (Yang <i>et al.</i> , 2017) .....	20
<b>Table 5:</b> Satellite Sensors commonly used in detecting and monitoring forest fires .....	22
<b>Table 6:</b> Peat moisture and thermal characteristics at Molopo and Molemane sites .....	29
<b>Table 7:</b> Examples of elements to consider before launching a drone (Process. St, 2021; DroneDeploy, 2021) .....	32
<b>Table 8:</b> Slantrange® multispectral camera specification .....	33
<b>Table 9:</b> FLIR® Vue Pro R thermal camera specification .....	33
<b>Table 10:</b> Indicators of soil moisture and thermal properties used in the study .....	36
<b>Table 11:</b> Laboratory measurements for both sites .....	39
<b>Table 12:</b> Description statistics of ground measurements for both sites .....	39
<b>Table 13:</b> Correlation matrix for laboratory measurements indicating the thermal properties and moisture measurements.....	40
<b>Table 14:</b> A generalized correlation matrix for ground measurements of both peat sites indicating the thermal properties and moisture measurements .....	40

## List of Acronyms

<b>ATSR</b>	Air Route Surveillance Radar
<b>AVHRR</b>	Advanced High-Resolution Radiometer
<b>ETM</b>	Enhanced Thematic Mapper
<b>LST</b>	Land Surface Temperature
<b>MC</b>	Moisture Content
<b>MODIS</b>	Moderate Resolution Imaging Spectroradiometer
<b>MPDI</b>	Modified Perpendicular Drought Index
<b>MSAVI</b>	Modified Soil Adjusted Vegetation Index
<b>MWIR</b>	Mid-Wave Infrared
<b>NIR</b>	Near-Infrared
<b>NDVI</b>	Normalized Vegetation Index
<b>NBR</b>	Normalized Burn Ratio
<b>PDI</b>	Perpendicular Drought Index
<b>PSMI</b>	Perpendicular Soil Moisture Index
<b>PVI</b>	Perpendicular Vegetation Index
<b>RGB</b>	Red, Green, Blue
<b>REDNDVI</b>	Red Edge Normalized Index
<b>SAVI</b>	Soil Adjusted Vegetation Index
<b>SWIR</b>	Shortwave infrared
<b>SWCI</b>	Surface Water Content Index
<b>SWCTI</b>	Surface Water Content Temperature Index
<b>TDR</b>	Time Domain Reflectometry
<b>TIR</b>	Thermal Infrared
<b>TSAVI</b>	Transformed Soil Adjusted Index
<b>TVDI</b>	Temperature Vegetation Dryness Index
<b>TVMDI</b>	Temperature-Vegetation-soil Moisture Dryness Index
<b>UAVs/ UASs</b>	Unmanned Aerial Vehicles/ Unmanned Aerial Systems

<b>VIR</b>	Visible and Infrared
<b>VSWI</b>	Vegetation Supply Water Index
<b>VNIR</b>	Visible and Near-Infrared
<b>WC</b>	Water Content
<b>WSN</b>	Wireless Sensor Network

## Examiner's Corrections Highlighter Colour

Examiner 1	
Examiner 2	

# CHAPTER ONE: INTRODUCTION

## 1. General Introduction

### 1.1. Peatland functions and characteristics

Peatlands are globally essential ecosystems with a significant role of serving as water and carbon reservoirs (Bispo *et al.*, 2016). They are defined as deposits formed by slightly decomposing plant material accumulating in a water-saturated surrounding (Bonnett *et al.*, 2009). These systems cover about 3 percent of the Earth's landscape, store about 10 percent of the world's fresh water and approximately 500 billion tonnes of the global carbon (Bourgeau-Chavez *et al.*, 2018).

Peatlands are influenced by topography, hydrology, and vegetation (Bourgeau-Chavez *et al.*, 2018), and they occur as fens and bogs, each with its own climatic and topographic characteristics (Vitt, 2013). Ombrotrophic wetlands receive all their water from precipitation, while minerotrophic fens receive water from rainfall mixed with mineral substrates (Biancalani and Avagyan, 2014; Bourgeau-Chavez *et al.*, 2018). These systems play a significant role in biodiversity, especially in semi-arid countries such as South Africa (Biancalani and Avagyan, 2014). They assist in reducing the likelihood of floods and drought by controlling water flows and preventing saltwater intrusion (Minayeva and Sirin, 2012; Biancalani and Avagyan, 2014).

Southern Africa's peatlands are at risk because of factors such as growing population demand to pump underground water, peat mining, invasion of infrastructure and species, and agricultural use (Bonnett *et al.*, 2009; Faul *et al.*, 2016; Gabriel *et al.*, 2018). Thus, it is vital to protect peatlands due to their limited extent, size, and threats posed to them because of population pressure and development (Grundling and Grobler, 2005).

Human-induced activities (such as forest removal, extraction, and fuel-burning) and climate change are major threats to peatland ecosystems (Bourgeau-Chavez *et al.*, 2018). Approximately 15 percent of the world's peatlands are either drained or significantly damaged due to fire (Biancalani and Avagyan, 2014). Peatland degradation occurs because of the water table drainage, drought conditions, and agricultural practices that expose the top peat layer (Gabriel *et al.*, 2018). The dryness of peatlands is influenced by groundwater levels, which increases the risk of peat fires (Gumbricht *et al.*, 2002).

Across different landscapes, the cause of peat fires is mainly agricultural activities such as the processing of ash as fertiliser or land clearing (Minasny *et al.*, 2019). Peatland fires are mostly anthropogenic and can be started by farming communities, land clearing activities, and private firms while preparing to establish planting (Uda *et al.*, 2010).

Peat fires are spontaneous ground fires that occur on the floor of a forest that produce much heat without flames (Chowdary and Gupta, 2018). According to Prat-Guitart *et al.* (2016), peat fires can spread in-depth and on the surface. This results in a full cover vegetation surface but continuous smouldering underneath the vegetated surface (Prat-Guitart *et al.*, 2016).

Physical disturbances such as drainage, surface fires on peatlands release massive amounts of carbon and nitrogen, contributing to the movement of atmospheric greenhouse gases and nitrates to the surface water systems (Bispo *et al.*, 2016; Faul *et al.*, 2016). According to Biancalani and Avagyan (2014), about 70 percent of global emissions are due to drained organic peat soil. The emission is still unevenly distributed globally due to geographic extent and climatic region (Biancalani and Avagyan, 2014).

Uda *et al.*, 2010 demonstrated that multiple toxic gases from peatland fires lead to pollution, human respiratory diseases (such as chronic respiratory, cardiovascular disease, and lung cancer), and environmental issues. Peatland fires contribute significantly to the emission of air pollution pollutants containing a mixture of particulate matter or raw materials and various harmful and non-toxic gases due to incomplete burning (Uda *et al.*, 2010).

Gabriel *et al.* (2018) stated that there is little knowledge about the effects of peatland degradation in South Africa and limited monitoring methods. Peatland degradation is defined as a process whereby peat undergoes rapid subsidence due to land clearing, drainage, and burning (Agus, 2015). The research wants to establish procedures associated with peat fires using peatland dryness as an indicator and determine the application of low altitude remote sensing technologies to monitor peat degradation due to spontaneous underground fires.

## **1.2. The rationale for the study**

Peatlands are characterised as groundwater-dependent ecosystems that occur in the eastern and southern regions of South Africa (Grundling and Grobler, 2005). Numerous peat fire incidents have been reported across the Southern African region over the past two decades (Strydom and Savage, 2016). A degraded peatland is vulnerable to peat fires, which occur during extreme drought conditions or after the groundwater level has been artificially lowered/drained (Teguh *et al.*, 2012). Peat fires result from water removal directly for agricultural or industrial purposes

(Gabriel *et al.*, 2017). Based on particular studies, peat fires in Southern Africa caused by peat dryness happened in the Okavango Delta in Botswana (Gumbricht *et al.*, 2002) and at Bodibe in the North West of South Africa (Grundling and Grobler, 2005). Gumbricht *et al.* (2002) detected burning peat surface fires/fire hotspots using remote sensing data (thermal data) and algorithms. Remote sensing of peatlands can help understand peatland risks and treatments to manage them sustainably (Atwood *et al.*, 2016).

Remote sensing methods can be used to determine the extent of the effects of fire on peatland ecosystems and the atmosphere (smoke affecting air quality) (Atwood *et al.*, 2016). A variety of spectral indices have been created due to the observation of broad-spectrum alterations caused by burning, including NDVI and NBR (Lentile *et al.*, 2006).

According to Atwood *et al.* (2016), remote sensing techniques based on spectral bands in the visible, near-infrared (VNIR) and shortwave infrared (SWIR) are limited by smoke and haze coverage while fires are burning. Therefore, nowadays, sensors based on mid-wave and thermal infrared (MWIR & TIR) are used to detect active fires (Gumbricht *et al.*, 2002; Atwood *et al.*, 2016; Sofan *et al.*, 2019).

Gumbricht *et al.* (2002) used Landsat ETM, MODIS, ATSR, and AVHRR to investigate peat fire occurrences in the Okavango Delta. The authors discovered that satellite data could detect only intense surface fires but not underground or subsurface fires (Gumbricht *et al.*, 2002). Thus, Gumbricht *et al.* (2002) recommended that peat detection be done using mid to thermal infrared data acquired at night because peat fires have a lower brightness temperature, have no smoke, and only show scars. Moreover, in the absence of multiple spectral bands, it is impossible to detect smouldering and flaming fires, which establish the location of peat fire occurrence (Atwood *et al.*, 2016; Sofan *et al.*, 2019).

The project focuses on assessing the effects of degradation and peat fires, using low altitude remote sensing technologies such as unmanned aerial vehicles (UAVs) in South African peatlands. Studies show that unmanned aerial vehicles (UAVs) can detect and diagnose peat fire distribution at a lower level (Prat-Guitart *et al.*, 2016; Burke *et al.*, 2019) and provide high-resolution imagery (Casbeer *et al.*, 2006; Raeva *et al.*, 2019). Knoth *et al.* (2013) observed that the UAV is a tool with the potential for ecological monitoring that can significantly reduce time-consuming and tedious field surveys.

Nowadays, most researchers rely on high-resolution data, which UAVs and multispectral sensors provide (Shin *et al.*, 2019). This is because they are less impacted by atmospheric conditions;

even if the location and timing of a forest fire cannot be predicted, UAVs can generally collect images immediately after a forest fire (Hamilton *et al.*, 2017; Shin *et al.*, 2019). Unmanned Aerial Systems (UAS) and sensor downsizing, according to Hamilton *et al.* (2017), offer a new approach by providing an affordable, safe, and responsive on-demand device for monitoring fire impacts at a much finer spatial resolution than is currently possible with existing technologies.

### 1.3. Problem Statement

South African peatland have a history of burning, which results in a significant volume of ash covering the majority of the peatland region (Grundling *et al.*, 2017). According to Grundling *et al.* (2017), peatland loss has a noticeable and direct impact on the integrity of aquatic ecosystems downstream of peatlands. Fire influences a wide range of temporal and geographical dimensions, making it difficult to identify causal factors, fire impacts, and ecosystem reactions (Lentile *et al.*, 2006). Remote sensing data has become a vital and often utilized resource for fire science and management because of these scale issues, as well as the size and inaccessibility of many wildfires (Lentile *et al.*, 2006).

Peatland remote sensing can offer data to aid in the development of a better knowledge of peatland risks and treatments for long-term management (Atwood *et al.*, 2016). Therefore, the project employs low-altitude remote sensing technology to examine peat dryness and moisture consequences in North West Province peatlands.

Since multispectral UAV images have very high spatial resolution and multispectral bands that may be utilized as training samples for classification utilizing high-resolution satellite images and deep learning algorithms, UAV has a lot of potential in identifying subsurface fires and burn intensity (Shin *et al.*, 2019). Ruwaimana *et al.* (2018) published research examining the benefits of drones over satellite images to survey mangrove ecosystems. Drone photography has been discovered to have the ability to map mangrove species, and it opens up a whole new set of possibilities for clearly identifying and distinguishing mangrove genera and species (Ruwaimana *et al.*, 2018). The better quality of drone photography and its potential application in studies that do not intend to map but rather to target individuals of interest, such as ecological deterioration or quantifying biomass loss due to tree fall or lightning strikes, demonstrate this (Salami *et al.*, 2014; Ruwaimana *et al.*, 2018).

This research will investigate the innovative form of data gathering using Unmanned Aerial Vehicles (UAVs), which lower the cost of aerial photography and equipment. In addition to better spatial resolution, consecutive drone images can give point-cloud 3D views to estimate tree height and crown diameter (Salami *et al.*, 2014; Ruwaimana *et al.*, 2018).

#### **1.4. Aims and objectives**

The research project aims to detect the extent of peatland degradation due to underground fires using low altitude remote sensing techniques [such as handheld sensors and Unmanned Aerial Systems (UASs)] in semi-arid areas of North West Province (South Africa).

The main objectives of the project are to;

1. Identify peat properties (thermal and moisture content) that will establish peat fires at the laboratory experiment scale.
  - a. Peat moisture acquired using ASD4 Field Spectroradiometer
  - b. Peat thermal properties acquired using KD2 Pro Thermal Properties Analyser
2. Estimate peat moisture using thermal infrared (TIR) and near-infrared (NIR) datasets acquired from ground and UAV platforms.
3. Determine the extent of peat fire and peat moisture by integrating multispectral data (RGB, NIR, TIR) and thermal anomalies.

#### **1.5. Research Questions**

- i. Which peat characteristics, when tested in a laboratory, can be recognized as triggering peat fires?
- ii. How can thermal infrared (TIR) and near-infrared (NIR) data from ground and UAV platforms be used to measure peat moisture?
- iii. Is it possible to predict peat moisture and fire using multispectral data and thermal anomalies?

#### **1.6. Research report outlines**

This study seeks to understand the peat's thermal and peat moisture properties, divided into six chapters (Figure 1). Chapter one consists of the general introduction to the study and the associated aims and objectives. A review of previous studies is outlined in Chapter two. Chapter three describes the study area of interest and outlines the methodology applied in the study. The results obtained in the study are presented in Chapter four and further discussed in Chapter five in comparison to similar studies done previously.

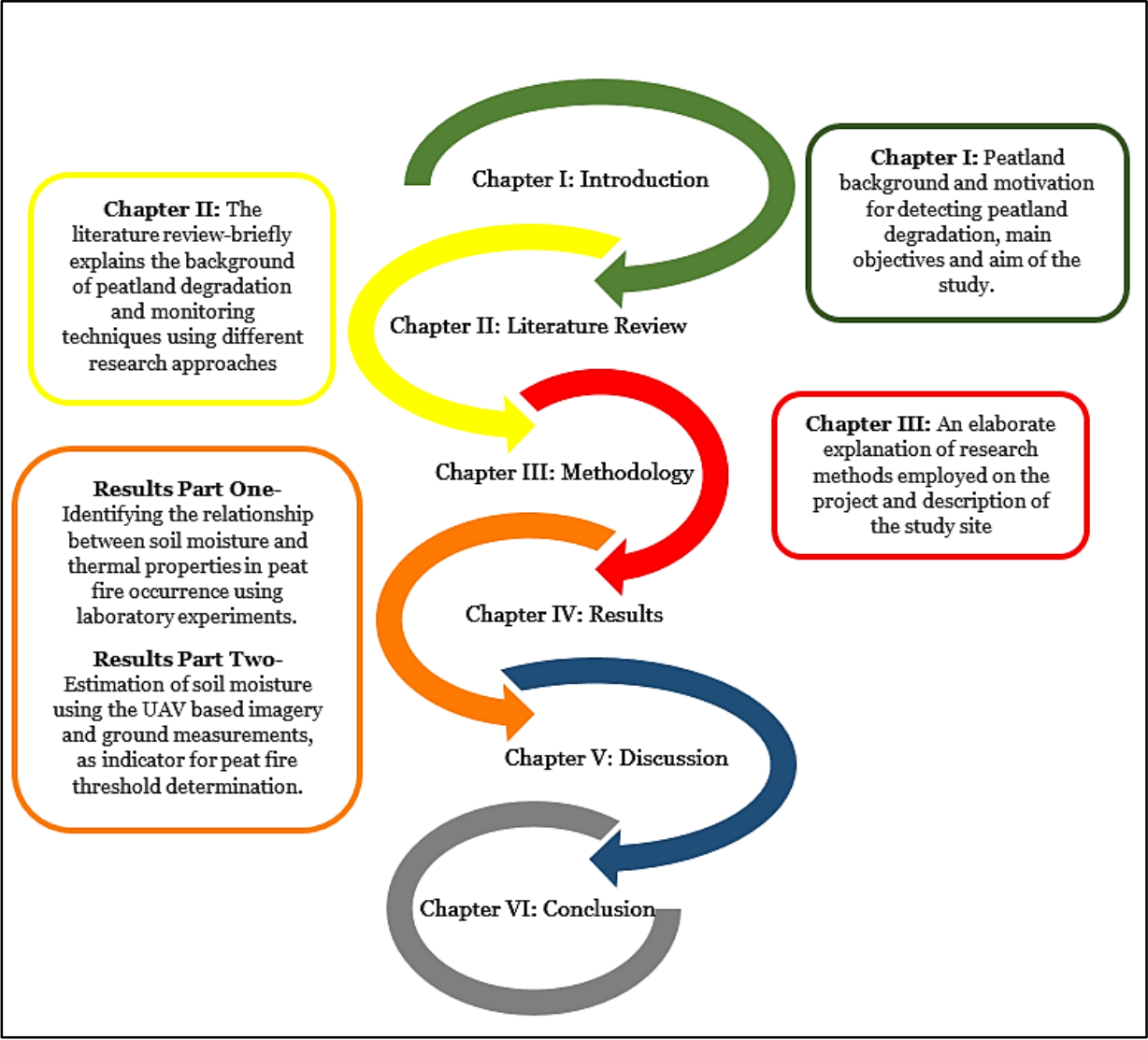


**Figure 1:** Brief explanation of the chapters

## CHAPTER TWO: LITERATURE REVIEW

### 2. General Overview of Peatland Systems

A peatland is delineated as an environment with or without vegetation, a naturally deposited peat layer on the surface (Minasny *et al.*, 2019). Peatlands are described based on their environmental and hydrological settings (Biancalani and Avagyan, 2014). Peat is described as deposits made of slightly decomposing plant material accumulating in a water-saturated environment (Bonnett *et al.*, 2009). These systems occupy about 3 percent of the Earth's surface and are good for preserving carbon and water (Filkov *et al.*, 2015).

Peatlands are threatened by climate change and are a focal point for various global environmental events (Biancalani and Avagyan, 2014). Such structures are important in the environment's resources because they store freshwater, protect wildlife, and provide carbon sequestration for longer periods (Biancalani and Avagyan, 2014). Any disturbance to peatlands causes significant carbon emissions and contribute to global warming (Minasny *et al.*, 2019).

According to Grundling *et al.* (2017), a region must have a minimum thickness depth of 30 cm to 40 cm to be classified as peat (Figure 2). Peatland degrades primarily because of human activities, such as land clearing or drainage, which causes rapid peat surface subsidence (Agus, 2015). Any damage or destruction to these structures could have long-term environmental, social, and economic consequences.



**Figure 2:** Rietvlei Reserve peatland, indicating peat thickness (Grundling *et al.*, 2017, 4)

Peatland degradation is one of the issues mainly raised in global environment headlines because of its importance in multiple ecosystem services (Parish *et al.*, 2008). In South Africa, Peatlands are at risk due to factors such as peat mining, invasion of infrastructure and species, and agricultural use (Bonnett *et al.*, 2009; Faul *et al.*, 2016).

## 2.1. Distribution of Peatland Systems in South Africa

Peatlands are widely spread worldwide, but their high prevalence in the northern hemisphere is attributed to their water-saturated regions. (Parish *et al.*, 2008; Grundling *et al.*, 2017). They can mainly be rain-fed and low nutrient content areas known as bogs or groundwater-dependent and nutrient-rich areas known as fens (Parish *et al.*, 2008; Holden *et al.*, 2010). Climate influences water conditions, vegetation production, and the pace at which dead organic material decomposes; therefore, peatland distribution, peat formation, and storage are largely consequences (Parish *et al.*, 2008; Millard *et al.*, 2018). Grundling *et al.* (2013) indicated that groundwater runoff sufficiently elevates the water level in a valley floor, resulting in permanently wet conditions that favourably impact peat's deposition.

Climate is the primary influence on peatlands distribution since it determines water conditions, vegetation productivity, and peat decomposition (Parish *et al.*, 2008). The peatlands in South Africa vary from the bottom of the tropical coastal valley to a mountainous environment (Figure 3).

Peatlands account for almost half of wetlands globally; however, only 1 percent of wetlands in South Africa are peatlands, compared with about 50 percent of global wetlands representing peatlands (Grundling *et al.*, 2017). Peatlands in South Africa are mostly groundwater-dependent ecosystems that occur in the country's wet eastern and southern parts (Gabriel *et al.*, 2018). High fertility makes peatlands more suitable for cultivation, and the carbon stocks in the peat make them more valuable (Grundling and Grobler, 2005).

Peatlands in South Africa are mainly found in the KwaZulu-Natal Province high rainfall areas, primarily in coastal plains. Though some are in semi-arid regions (such as the North West), they are dependent on groundwater (Grundling and Grobler, 2005; Grundling *et al.*, 2017). Any interference that may affect hydrological processes can contribute to peatland depletion (Grundling *et al.*, 2017). South African peatlands, during low rainfall and evapotranspiration, are primarily influenced by seasons.

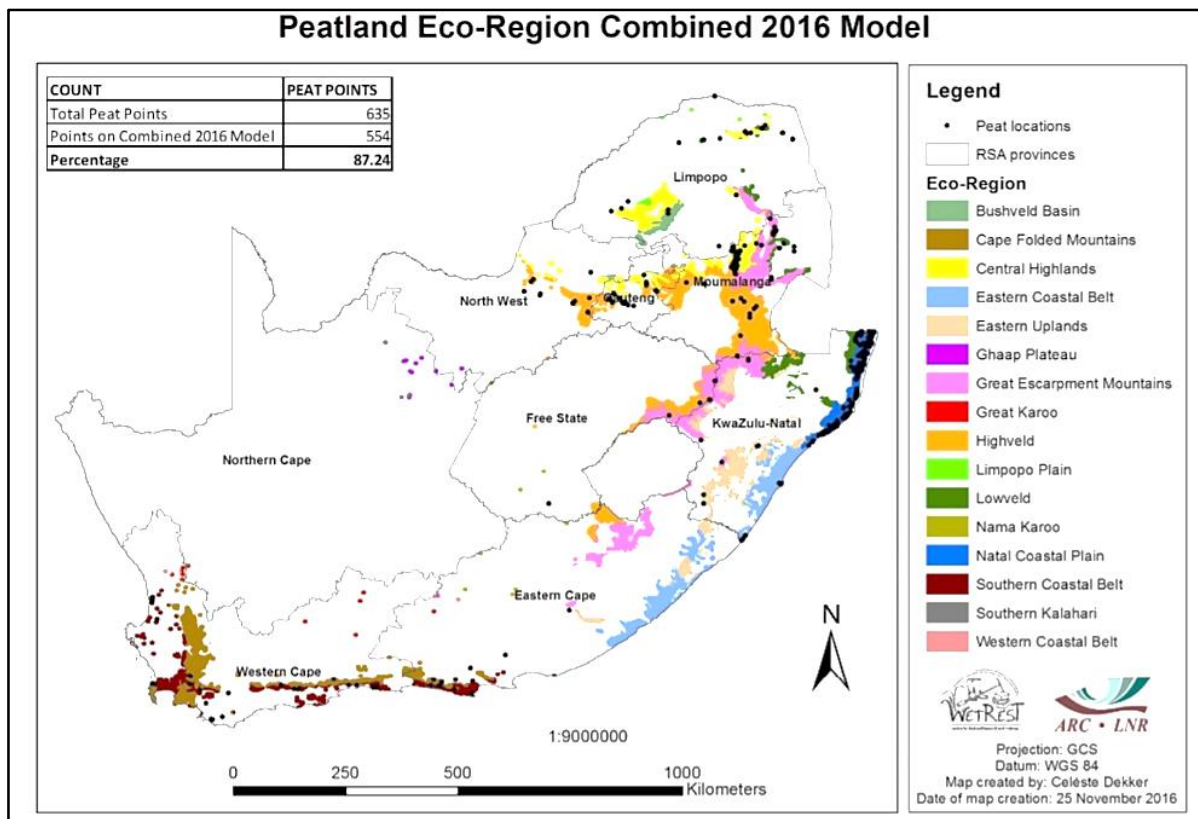


**Figure 3:** The spatial distribution of the peatland in South Africa (Grundling *et al.*, 2017)

## 2.2. Importance of Peatland Systems

Peatlands provide significant soil carbon atmospheric methane sources and act as carbon sinks and atmospheric methane sources (Faul *et al.*, 2016). They also serve as water regulators in renewing groundwater, reducing flooding, and preserving low flow during dry periods (Bispo *et al.*, 2016).

### 2.2.1. Peatland and peat fire functions and characteristics

There are multiple uses of peats, and peatland plays a significant role in geological and human climates. Because they act as water controllers by recharging groundwater, flooding is reduced, and low flow is maintained during dry times (Grundling and Grobler, 2005; Faul *et al.*, 2016). Peats are particularly susceptible to hydrological changes due to land use or climate change (Holden *et al.*, 2010). The water table position shifts impact peat deposition, decomposition, and stabilisation (Holden *et al.*, 2010; Prat-Guitart *et al.*, 2016).

Peatland systems are often immersed with water that prevents them from the destruction caused by anthropogenic activities. Natural impacts such as drought and lightning strikes increase the risk of burning peatlands (Faul *et al.*, 2016; Hu *et al.*, 2018). Several reasons contribute to the

spread of peat fires in South Africa and other countries, including agricultural activities, such as ash production for fertiliser or ground clearing, and other geological elements such as topographic features, as illustrated in Figure 4. Peat fires are vulnerable to changing climate and weather patterns, such as El Nino type events that reduce rainfall, affecting water table functionality, making them sensitive to fire (Parish *et al.*, 2008). For example, during the 1997 El Nino outbreak in Indonesia, a major peatland fire broke out on the islands, caused by slash and land clearing burning operations on farms (Hu *et al.*, 2018).

Peat fires are an environmental threat and have a profound impact on humanity (loss of life and property), the environment (fuel), climate (water quality), and the atmosphere (Bonnett *et al.*, 2009). Nevertheless, they are essential in the functioning of specific habitats and are governed by water distribution changes and water distribution improvements in particular habitats, such as catchments or deltas (Gumbrecht *et al.*, 2002).

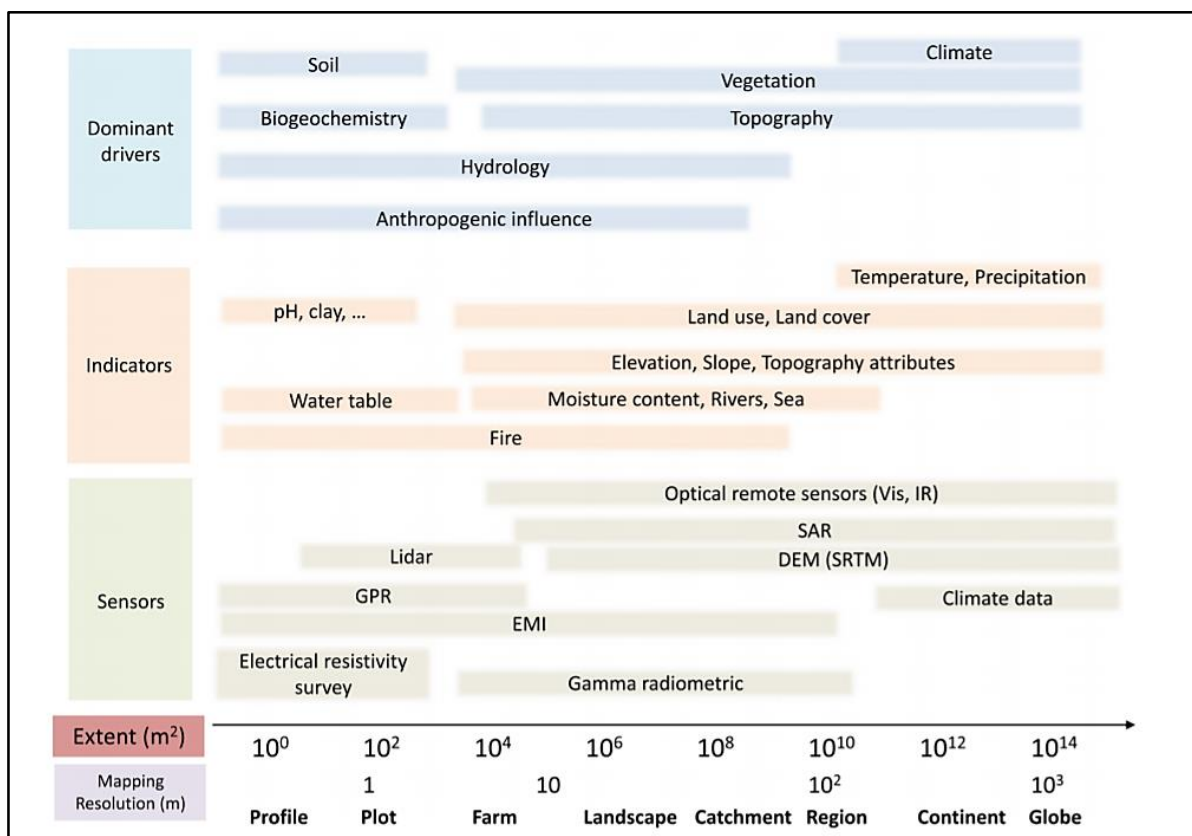


**Figure 4:** Peat formation factors/ indicators, and sensors that can assess the indicators as a function of spatial scale (after Minasny *et al.*, 2019)

### 2.3. Soil Moisture and Thermal Indices

Hydrology is an important component in peatland resilience since high and stable water levels are associated with healthy peatlands, but persistent drought can cause deterioration and long-term harm (Millard *et al.*, 2018; Lees *et al.*, 2021). Soil moisture is an essential factor in landscape hydrology. It is widely recognised as a critical parameter in the mass and energy equilibrium between the ground surface and the atmosphere (Lakshmi, 2013). Soil moisture is a major factor in determining the possibility of peat ignition, as well as the depth and breadth of the fire (Nelson *et al.*, 2021).

Localized warming/drying of peatland soils enhances water table variation and soil moisture variation (Nelson *et al.*, 2021). For example, Millard *et al.* (2018) utilized empirical models to monitor the temporal dynamics of soil moisture in a peatland using remotely sensed images. The study evaluated soil moisture's geographical and temporal variability, the prediction accuracy of empirical soil moisture recovery, and its potential for peatland hydrology monitoring (Millard *et al.*, 2018). The researchers discovered that using empirical models (Linear Mixed Effects) provides a more precise characterisation of soil moisture as a function of peatland classifications (Millard *et al.*, 2018).

Several methods for estimating soil moisture have been developed during the last several decades, including field measurement techniques and remote sensing approaches based on visible (VIR), near-infrared (NIR), shortwave infrared (SWIR) reflectance, thermal infrared (TIR) emittance, and microwave emissions (Lakshmi, 2013; Malik and Shukla, 2014; Elvidge *et al.*, 2015; Hong *et al.*, 2018). Remote sensing techniques offer a cost-effective and time-efficient way to monitor soil moisture at higher temporal and spatial resolutions (Hong *et al.*, 2018). Thermal Infrared (TIR), microwave, and optical spectrums can estimate soil moisture because these bands provide data about emission (Lakshmi, 2013; Malik and Shukla, 2014).

TIR is a good indicator of soil wetness and surface temperature detection (Kaleita *et al.*, 2005; Lakshmi, 2013; Malik and Shukla, 2014). Optical (V, NIR) and thermal infrared spectrums are normally combined to measure soil moisture content (Kaleita *et al.*, 2005). In comparison, the passive and active microwave spectrum is described to detect more specific soil properties such as temperature brightness, soil temperature, and dielectric properties (Malik and Shukla, 2014).

Hong *et al.* (2018) evaluated surface soil moisture using the water content temperature index called Surface Water Content Temperature Index (SWCTI). The authors indicated that soil

moisture could be assessed with MODIS-derived data, using microwave soil moisture monitoring to ensure accurate soil moisture predictions (Hong *et al.*, 2018). SWCTI was calculated using a combination of SWCI and LST. The Surface Water Content Index (SWCI) is more sensitive to surface moisture content than the NDVI (Zhang *et al.*, 2008; Hong *et al.*, 2018). SWCI directly reflects vegetation water content, whereas NDVI reflects vegetation water content based on chlorophyll properties that significantly absorb red light and reflect NIR (Hong *et al.*, 2018). The study suggested that SWCTI in bare to low vegetated areas is the best technique associated with surface soil moisture (Hong *et al.*, 2018).

The study by Hong *et al.* (2018) noted out that other indices may be used to track different types of land cover, such as the Perpendicular Drought Index (PDI), which is based on the spatial characteristics of the NIR–red soil moisture distribution and can be used to track bare land (Amani *et al.*, 2017). There's also the Modified Perpendicular Drought Index (MPDI) for densely vegetated regions, which considers soil moisture and vegetation growth (Ghulam *et al.*, 2007; Hong *et al.*, 2018).

Shafian and Maas (2015) evaluated the relationship between the Perpendicular Soil Moisture Index (PSMI) and soil moisture. The PSMI is a soil moisture index used to estimate soil moisture using ground cover/vegetation cover (NIR, RED band) and TIR band (see formula on Table 1). The results of the study indicated that the PSMI index has a strong correlation with ground-measured soil moisture. According to the research, the PSMI map created from Landsat imagery demonstrated that it could depict the relative spatial distribution of soil moisture across an area. As a result, PSMI is a good proxy for estimating soil moisture using a remote sensing dataset.

Peatland surface moisture characteristics can also be determined by the temperature vegetation dryness index (TVDI), based on the relationship between the vegetation index and land surface temperature (Meng *et al.*, 2010; Chen *et al.*, 2015; Schirmbeck *et al.*, 2017). Holidi *et al.* (2019) found that TVDI (see formula on Table 1) correlates strongly with surface soil moisture, and they assessed the correlation between TVDI values and soil moisture. The study aimed to characterise peatland based on the temperature vegetation dryness index (TVDI) and found a strong relationship between soil moisture at different depths of the peatland and TVDI values (Holidi *et al.*, 2019). Table 1 presents dryness and soil moisture indices, which assess land surface temperature (LST), vegetation indices, and other soil moisture indicators.

**Table 1:** Summary description of various soil moisture indices

Indices	Indices Formula	Description	References
<b>SAVI</b> -Soil-Adjusted Vegetation Index	$SAVI = ((NIR - Red) / (NIR + Red + L)) \times (1 + L)$	Assesses the difference between soil and vegetation. The index minimises soil influence on vegetation canopy by including the constant L on the NDVI equation's denominator.	Huete, 1988
<b>MSAVI</b> -Modified Soil Adjusted Vegetation Index	$MSAVI2 = (1/2) \times (2(NIR + 1) - \sqrt{(2 \times NIR + 1)^2 - 8(NIR - Red)})$	It reduces the impacts of bare soil on the Soil-Adjusted Vegetation Index.	Huete, 1988
<b>TSAVI</b> -Transformed Soil-Adjusted Vegetation Index	$TSAVI = (s(NIR - s \times Red - a)) / (a \times NIR + Red - a \times s + X \times (1 + s^2))$	Utilises slope attribute and intercept to reduce soil brightness.	Baret and Guyot, 1991
<b>PSMI</b> -Perpendicular Soil Moisture Index	$PSMI_i = D_i / (1 + NDVI_{norm})$ $D_i = (TIR_{norm} + NDVI_{norm}) / \sqrt{2}$	Estimating soil moisture, which applies to various vegetation conditions.	Shafian and Mass, 2015
<b>VSWI</b> -Vegetation Supply Water Index	$VSWI = NDVI / LST$	It is a useful metric estimating soil moisture in areas with moderate to dense vegetation cover.	Hong <i>et al.</i> , 2018
<b>SWCI</b> -Surface Water Content Index	$SWCI = \frac{B_6 - B_7}{B_6 + B_7}$	Based on bands derived from MODIS, it evaluates soil moisture.	Hong <i>et al.</i> , 2018
<b>SWCTI</b> -Surface Water Content Temperature Index	$SWCTI = \frac{SWCI}{LST - C}$	It provides a more accurate estimation of surface soil moisture than NDVI.	Hong <i>et al.</i> , 2018

<b>PDI-</b> Perpendicular Drought Index	$PDI = \frac{1}{\sqrt{M^2 + 1}} (\rho_{RED} + M\rho_{NIR})$	Indicates soil moisture status in bare land to low vegetated areas. It is based on the spatial characteristics of the soil moisture distribution in NIR–red space.	Amani <i>et al.</i> , 2017; Hong <i>et al.</i> , 2018
<b>PVI-</b> Perpendicular Vegetation Index.	$PVI = \frac{(NIR - a \times Red - b)}{(\sqrt{(1 + a^2)})}$	Determines the differences in vegetation reflectance but is sensitive to atmospheric changes.	Shafian and Mass, 2015
<b>TVDI-</b> Temperature Vegetation Dryness Index	$TVDI = \frac{T_s - T_{smin}}{T_{smax} - T_{smin}}$ $T_{smax} = a + b(NDVI)$	Estimates soil moisture, using the relation between LST and vegetation status.	Chen <i>et al.</i> , 2015 ; Meng <i>et al.</i> , 2010 ; Amani <i>et al.</i> , 2017 ; Holidi <i>et al.</i> , 2019
<b>TVMDI-</b> Temperature- Vegetation-Soil Moisture Dryness Index	$TVMDI = \sqrt{LST^2 + SM^2 + \left(\frac{\sqrt{3}}{3} - PVI\right)^2}$ $SM = \frac{\rho_{NIR} + \frac{\rho_{red}}{M} - b}{\sqrt{1 - \frac{1}{M^2}}}$	Indicates the temporal and spatial variation of dryness values for medium spatial resolution images.	Chen <i>et al.</i> , 2015 ; Amani <i>et al.</i> , 2017;

## 2.4. Mapping and monitoring peatland degradation

### 2.4.1. Ground-Based Peatland Degradation Monitoring

Multiple studies use ground monitoring methods to validate ground-level peat degradation (Agus, 2015; Pastor *et al.*, 2018). An understanding of the stages and processes of peatland degradation is vital to control peat fires. Gabriel *et al.* (2018) stated that knowledge of the effects of degradation in South African peatlands is limited. The authors described peat degradation using peat properties such as organic matter content, degree of decomposition, bulk density, and hydrophobicity (Gabriel *et al.*, 2018).

Due to runoff, the study found that wood peatland degradation progresses faster than radical (root fragments) peat, causing spontaneous underground fires (Gabriel *et al.*, 2018). The critical concern is the increased likelihood of peat fires occurring with increasing runoff and dryness on the peatlands. Peat moisture and groundwater level are closely linked to peat fire spread and

combustion (Prat-Guitart *et al.*, 2016). Many studies focused on analysing the factors influencing the ignition of smouldering and extinguishing factors, which play a role in preserving the spread of peat fire, as seen in Table 2.

**Table 2:** Review of laboratory experiment for peat fire analysis

<b>Experiment</b>	<b>Method</b>	<b>Results</b>	<b>Reference</b>
<p><b>Burn experiment</b></p> <p>The laboratory experiment was designed to contribute to the heat flow. Develop to evaluate the heat flow response from porous smouldering fuel to the significant fuel parameters depth, organic bulk density, and moisture and inorganic content.</p>	<p>A box of 18 cm X 28 cm X 12.5 cm. Twelve samples were taken randomly from the 18 bags to determine the inorganic content. Samples were dried overnight and sieved through a 6 mm mesh opening; ashing was done in a furnace at 600 °C. Stepwise multiple linear regressions analysed data.</p>	<p>It was observed that heat load through the heat content is directly related. Measured heat loads were within the range of 10 to 100MJ m<sup>-2</sup>. The heat load increased nonlinearly with increasing inorganic ratio and decreased linearly with increasing moisture ratio. The heat load is linear with depth, holding the organic bulk density and constant moisture and inorganic rates.</p>	<p>Frandsen, 1998</p>
<p><b>Smouldering tests/ experiment</b></p> <p>Experiment to detect smouldering fire signatures and how they can reconstruct past environments.</p>	<p>A 10 cm X 10 cm X 26 cm open-top column ignition is activated using an electric heated coil buried in a 5cm top free surface and providing 100 W of energy for 30 min.</p>	<p>Depth of Burn experiment decreases with moisture content. A high N and reduce the C/N ratio.</p>	<p>Zacone <i>et al.</i>, 2014</p>
<p><b>Estimated Smouldering Probability (ESP) model</b></p> <p>A predictive tool is used to reflect the chance of smoking to continue after a successful ground ignition and when smouldering becomes dependent on soil moisture and soil properties (bulk density, mineral content).</p>	<p>Comparison of root mat soil and muck soil using a smouldering test of whether the smouldering front will self-sustain throughout different soil types and varying soil properties (moisture content and mineral content).</p>	<p>The experiment indicated that the root mat soil's ESP is related to moisture content and soil mineral content. While the muck soils' ESP is also related to moisture content, it is not sensitive to mineral content.</p>	<p>Reardon and Curcio, 2011</p>

<p><b>Peat fire suppression experiment-</b></p> <p>To determine which foam layer can suppress peat fire. Assessment of the smouldering front dynamics from the igniter to the other end of the reactor, where the different thicknesses of foam poured on top of the peat to explore the effect of varying thickness on peat fire suppression.</p>	<p>An average amount of 3.8L of foam per kilogram of peat was needed to extinguish a peat fire. The peat sample was put in a 10x10x10 cm<sup>3</sup> reactor, where a coil heater was turned on at 80 - 100W for 30 minutes to generate a smouldering front. K-type thermocouples and infrared thermography were used to explore the suppression mechanism.</p>	<p>From multiple experiments, a correlation was observed between the thickness of the foam layer and the suppression of peat fires.</p>	<p>Ratnasari <i>et al.</i>, 2018</p>
--	---	---	--------------------------------------

#### 2.4.2. Low Altitude Level Monitoring for Underground Fire Detection

It has been reported that evaluating ground fire capacity methods is limited when examining organic soils (Burke *et al.*, 2019; Knoth *et al.*, 2013). Usage of unmanned aerial vehicles (UAVs) is useful for identifying and treating underground fires (Casbeer *et al.*, 2006; Burke *et al.*, 2019). Low altitude sensors are high-resolution photogrammetric devices with great accuracy that can reach X, Y, and Z directions of 0.053m, 0.070m, and 0.061m, respectively, in regions with unusual terrain (Carvajal-Ramírez *et al.*, 2019). For example, Fraser *et al.* (2017) utilized an RGB sensor mounted on a UAV to correlate two fire severity indices acquired from an RGB sensor mounted on a UAV with two additional traditional indices gathered from a Landsat satellite to calibrate satellite data on a regional scale.






Sensor downsizing has allowed for installing thermal, multispectral, and hyperspectral cameras (primarily in the VIS-NIR range) on small UAS, allowing for a substantial expansion in the variety of potential applications (Table 3). A study by Teguh *et al.* (2012) integrated a wireless sensor network (WSN) with a UAV in Central Kalimantan, Indonesia, for real-time monitoring and detection of size, distribution, and location of peat fires. The authors observed that UAVs could effectively detect and monitor peat fires' sites and the spread of smouldering (Teguh *et al.*, 2012). Unmanned aerial vehicles can be utilised at the operational level for high-resolution detection whenever the satellite shows suspected fire spots (Burke *et al.*, 2019; Shin *et al.*, 2019).

**Table 3: Sensors mounted on UAVs and their potential uses (Tmusic *et al.*, 2020)**

Sensor Type	Specifics	Main Applications
RGB	Optical	aerial photogrammetry, SfM-based 3D modeling, change detection, fluid flow tracking
Multispectral (<10-20 bands)	Multiple wavelengths	vegetation mapping, water quality, classification studies
Hyperspectral overlapping contiguous bands	Analyzing the shape of spectrum	vegetation mapping, plant physiology, plant phenotyping studies, water quality, minerals mapping, pest-detection
Thermal	Brightness surface temperature	thermography, plant stress, thermal inertia, soil water content, urban heat island mapping, water temperature, animal detection.
LiDAR (Light Detection and Ranging)	Surface structure	3D reconstruction, digital terrain mapping, canopy height models, plant structure, erosion studies

Due to their diverse capabilities and uses, several researchers have used various UAVs (Table 4) for monitoring. In comparison to satellite-based systems, UAVs have the potential to improve image resolution and update rates; nevertheless, UAVs are thought to have a restricted communication and sensing range (Casbeer *et al.*, 2006). Casbeer *et al.*, 2006, for example, tested whether UAVs can monitor and track the growth and direction of major forest fires using an algorithm for tracking the extent of flames with an onboard infrared sensor.

**Table 4: Examples of common UAVs used for field monitoring, including their primary description, features, and cost (Yang *et al.*, 2017)**

Specification	Description				
	Multi-rotor	Helicopter	Fixed-wing	Blimps	Flying wing
					
Model	DJIS1000+	AXH-E230	Bat-3	CB3000	Pathfinder-Plus
Manufacturer	DJI technology	AVIX	MLB Co.	Beijing CSCA Co.	AeroVironment
Materials	Carbon fiber, High strength performance engineered plastics	Carbon fiber, aluminum alloy	Carbon fiber, engineered plastics	Kevlar fibers, fiber optic, electrical cores	Carbon fiber, Nomex, Kevlar, plastic sheeting, plastic foam
Cost	Low	Medium	Medium	High	very high
Power/Motors	Eight electric, 0.5 kw max each	One BLDC motors	Two-stroke engine	One oil engine	Eight (8) solar-electric, 1.5 kW max each
Gross weight/kg <sup>a</sup>	6	15	56	300	318
Payload capacity/kg <sup>b</sup>	7	15	9	10	67.5
Speed/m s <sup>-1</sup>	12	23	33	15	14
Endurance/h <sup>c</sup>	0.25	0.8	6	12	15
Altitude ceiling/m	500 <sup>d</sup>	3,000	3,000	120	25,000

<sup>a</sup>Total weight with a battery; <sup>b</sup>The payload including battery; <sup>c</sup>Endurance with maximum payload; <sup>d</sup>The maximum flight height in China (the flight control system was restricted by the national regulations to set the flight height lower than 500 m).

UAVs are valuable ground sensing instruments that can carry visual and infrared cameras and transmit data to a ground-based base station (Teguh *et al.*, 2012; Beyer *et al.*, 2019). According to Teguh *et al.* (2012), UAV and WSN have effectively identified and diagnosed peat fires, enabling better and more accurate detection of their size, distribution, and location. UAVs can

fly for around "45 minutes" on a single battery and require relatively steady weather conditions (i.e., mostly sunny) to operate (Knoth *et al.*, 2013; Yuan *et al.*, 2015).

Knoth *et al.* (2013) discovered that a UAV equipped with NIR can monitor the restoration of cut-over bogs and significantly decrease tedious work. Raeva *et al.* (2019) used UAVs with fixed-wing platforms mounted with multispectral and thermal cameras for agricultural purposes such as yield estimation and plant disease detection. It was discovered that they could provide farmers with harvesting goal achievements.

#### **2.4.3. Satellite-Based Monitoring Research Approach for Underground Fire Detection and Peatland Degradation**

It is desirable to use remote satellite sensing because it offers comprehensive landscape coverage, quantitative earth surface measurements, low cost, easily accessible, and time or periodic coverage (Gumbricht *et al.*, 2002). Satellite imagery can be used to estimate correct surface temperature and emissivity, i.e., using thermal bands (Gumbricht *et al.*, 2002). Some researchers focused on remotely sensed data for tracking biomass burning, with several studies measuring surface fires instead of underground fires (Gumbricht *et al.*, 2002). Several studies indicated that thermal data could detect actively burning surface fires using certain algorithms, thus enabling the identification of surface fire hotspots. However, this approach cannot determine the spatial distribution of fires due to prevailing clouds and sensor overpass timing during fires (Gumbricht *et al.*, 2002). Monitoring based on satellite imagery can be utilised as a continuous and low-cost source of information (Table 5).

Extensive work has been carried out on remote sensing technology to track peat fires. For example, Gumbricht *et al.* (2002) assessed the probability of detecting peat fires and their scars using various remote sensing systems (i.e., ATSR, AVHRR, MODIS, and Landsat ETM). During that analysis, it was found that only extreme surface fires were detected by MODIS Airborne Simulator, ATSR, and AVHRR and that Landsat ETM could not detect the fires (Gumbricht *et al.*, 2002). Consequently, Gumbricht *et al.* (2002) proposed using night-time imagery to detect peat fires' smouldering impact as they occurred underneath the surface soil layer.

**Table 5:** Satellite Sensors commonly used in detecting and monitoring forest fires

	<b>Spectral Bands</b>	<b>Spatial Resolution</b>	<b>Temporal Frequency</b>	<b>Applications</b>	<b>References</b>
<b>Landsat-TM</b>	RGB, NIR, SWIR, thermal, panchromatic bands	30m(multispectral) 15m (panchromatic)	~16 days	Detection and mapping of burn scars; vegetation classification and mapping.	Liew, 2001; Liu and Zhang <i>et al.</i> , 2011
<b>SPOT</b>	Green, red, NIR, SWIR, panchromatic Bands.	20m (multispectral); 10m (panchromatic)	~Daily	Detecting active fires, accurate fire location, detecting and mapping burn scars, vegetation classification, and mapping.	Liew, 2001
<b>NOAA-AVHRR</b>	Red, NIR, MWIR, thermal bands	1km	~Daily	Detection of thermal emissions from active fires (hot spots).	Liew, 2001
<b>DMSP-OLS</b>	RGB, thermal bands	2.7km	~Daily	Detection of light emission from night-time fires.	Liew, 2001
<b>MODIS</b>	36 bands-visible, NIR, SWIR, MWIR, thermal IR bands	250m for two bands, and 500m in RGB, NIR, SWIR; 1km on MWIR and thermal IR	~Daily	Detection of thermal emissions from active fires; burn scars mapping; vegetation/land cover mapping.	Liew, 2001

## 2.5. Conclusion of the Literature Review

In conclusion, peatlands play an important role in both the physical and human environment. They are a significant soil carbon store and act as water regulators. Peatlands are rare and unique in South Africa and occur in patches and stripes at the bottom of valleys. Therefore, they are mostly found in the country's wet eastern and southern regions and are highly characterized as an ecosystem rich in nutrients and dependent on ground conditions.

Detecting peat fires is difficult because they occur underground. There is little information about the evaluation of peat fires using remote sensing technologies at low altitudes. It is essential to understand the peat fires and develop techniques for monitoring them (Figure 5).

Unmanned aerial vehicles have many benefits but drawbacks because they can increase the image size or capture images at high resolution. They can detect and diagnose low-level peat fire distribution. The key disadvantages of UAVs are that many factors affect accuracy, including camera efficiency, camera calibration, the number and position of ground control points, and software processing preference.

The depth and width of the fire (Figure 5), as well as the likelihood of peat igniting, were discovered to be all determined by soil moisture throughout the literature review. The highly concentrated warming or drying of peatland soils increases the water table and increases soil moisture variability.

Remote sensing approaches for estimating soil moisture have revealed that several VIR, NIR, SWIR, and TIR data indices can identify soil moisture distribution in diverse land covers (i.e. bare land or dense vegetation). It was found that the integration of thermal and vegetation indices is useful in precise soil moisture estimation (Kaleita *et al.*, 2005).

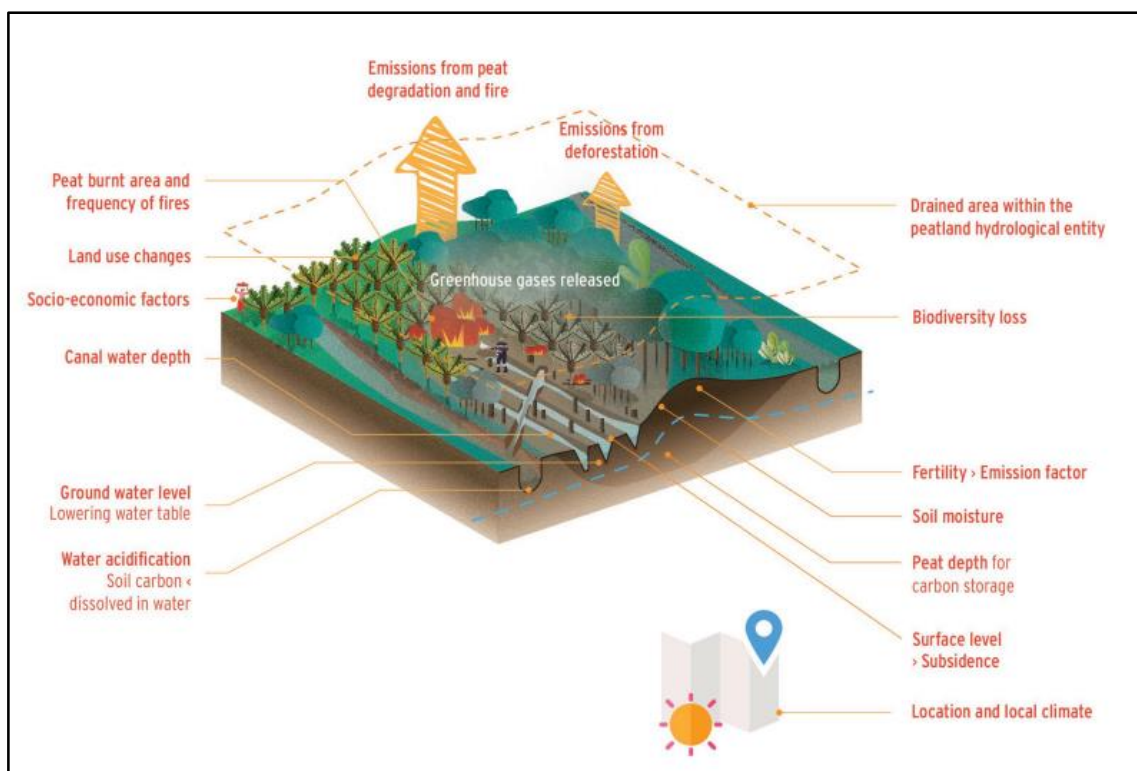


**Figure 5:** In a summary, the data required for peatland monitoring (FAO, 2020)

In South Africa, there is limited knowledge about peatland systems, resulting in policy and decision making not focused on a good knowledge base and thus may accidentally lead to extreme damage of these important ecosystems. Therefore, there is a need to effectively

manage peatland ecosystems by gathering precise scientific information about peatland and peat fire characteristics.

Peatland mapping provides the foundation for effective monitoring systems. Monitoring changes in peatland ecosystems, whether natural, degraded, or in the process of restoration, is critical for preserving the water, species richness, and carbon content of peatlands (FAO, 2020). Effective mapping techniques provide a reliable baseline for monitoring and aid in establishing management goals for specific peatland regions (FAO, 2020).

A study by Grundling *et al.* (2017) introduced a model to characterize, identify and classify peatland systems in South Africa. According to Grundling *et al.* (2017), it is necessary to implement recovery measures on degraded peatland systems to reduce their risk of depletion, such as re-establishing the hydrological function of the peatland system; rewetting dried-up or drained areas; and gaining a better understanding of the groundwater balance and its functions.

## CHAPTER THREE: RESEARCH METHODOLOGY

### 3. Materials and Methods

#### 3.1. Study Site

The study focused on two proximal peat sites in North West Province to assess the extent of peatland degradation, namely Moloopo and Molemane. Consequently, peat fire affects all of them at various rates, and this is due to the amount of peat moisture in each area.

In addition, the source (dolomitic eye) that supplied water to it has dried up. The study sites (Moloopo and Molemane) are located within the hydrological karst belt zone, making them susceptible to degradation when disturbed by economic activities such as natural resource mining (Ndou *et al.*, 2018).

The research focused on two peatland systems in North West Province, South Africa; the Molemane and the Moloopo. Molemane peat (25.8144 ° S, 26.0774 ° E) is peat that has not been significantly altered by cultivation/drainage degradation and the adjacent land cover that is cultivated (Figure 6).

Moloopo (25.7271 ° S; 24.2764 ° E) is peat devastated by a recent forest fire, is cultivated, and the surrounding land/land use is residential. Moreover, the significant impact on these peats (e.g., Moloopo peat) is water abstraction, donga erosion, road construction, and urbanisation (Grundling and Grobler, 2005; Grundling *et al.*, 2017; Ndou *et al.*, 2018).

The peatlands were chosen to compare the level between wet peatland and dry peatland when underground/spontaneous fires occur. In doing so, the analysis must set the threshold at which pristine or dry peatland responds to the fire events by analysing the peat's soil moisture and thermal conductivity.

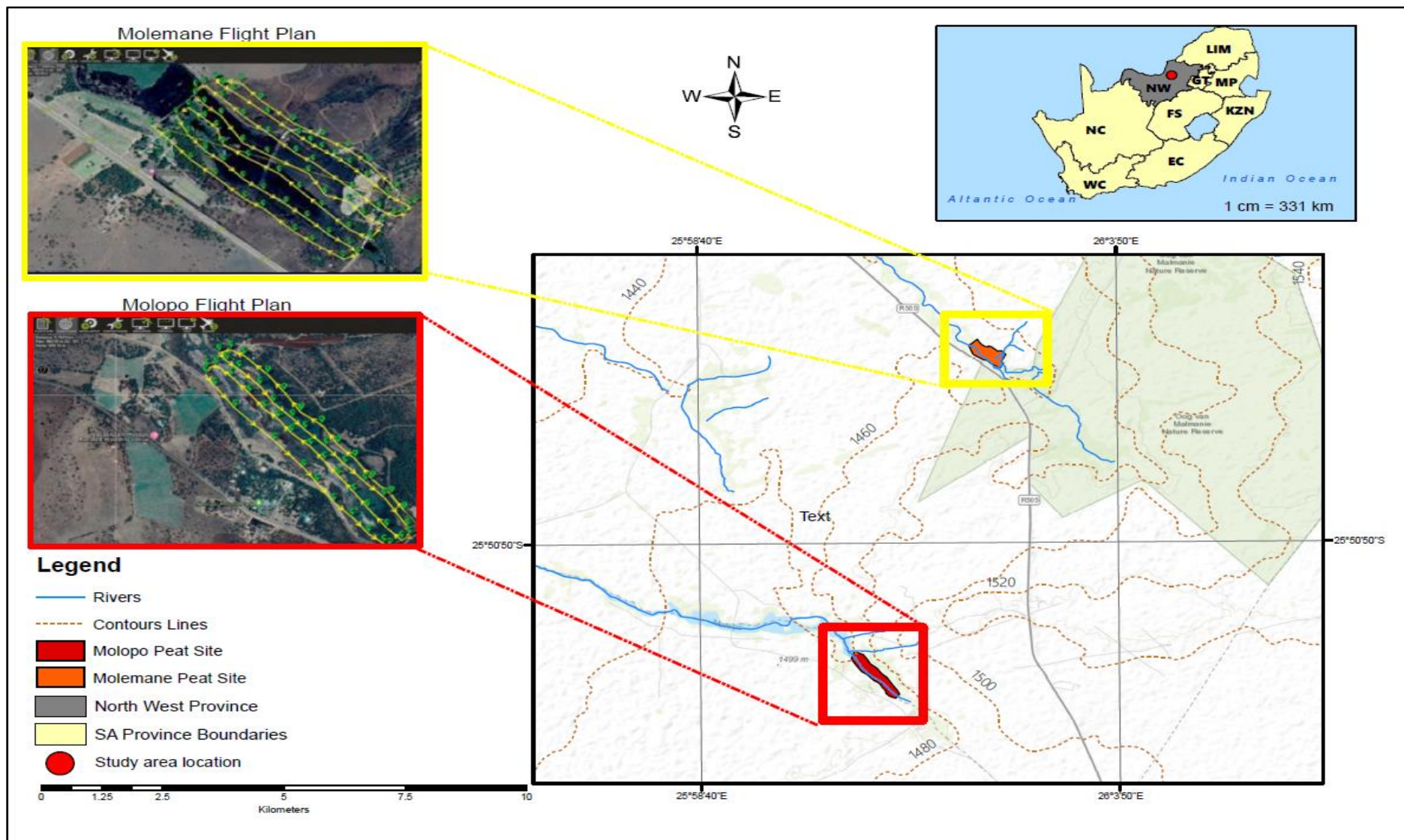


**Figure 6:** Map depicting the study area of interest and the two peatlands selected for the study

The North West Province is part of the Highveld eco-region comprising about 17.5 percent of South African peatlands as a whole (Grundling and Grobler, 2005). The peatlands are valley bottom fens with reeds and *Carex* species prevalent in the vegetation (Grundling and Grobler, 2005). It is located in Rocky Highveld Grassland and Dry Sandy Highveld at Grassland Biome (Figure 7). This region has dry conditions with a mean annual rainfall of 500–600 mm and frequent droughts (Thomas *et al.*, 2007).

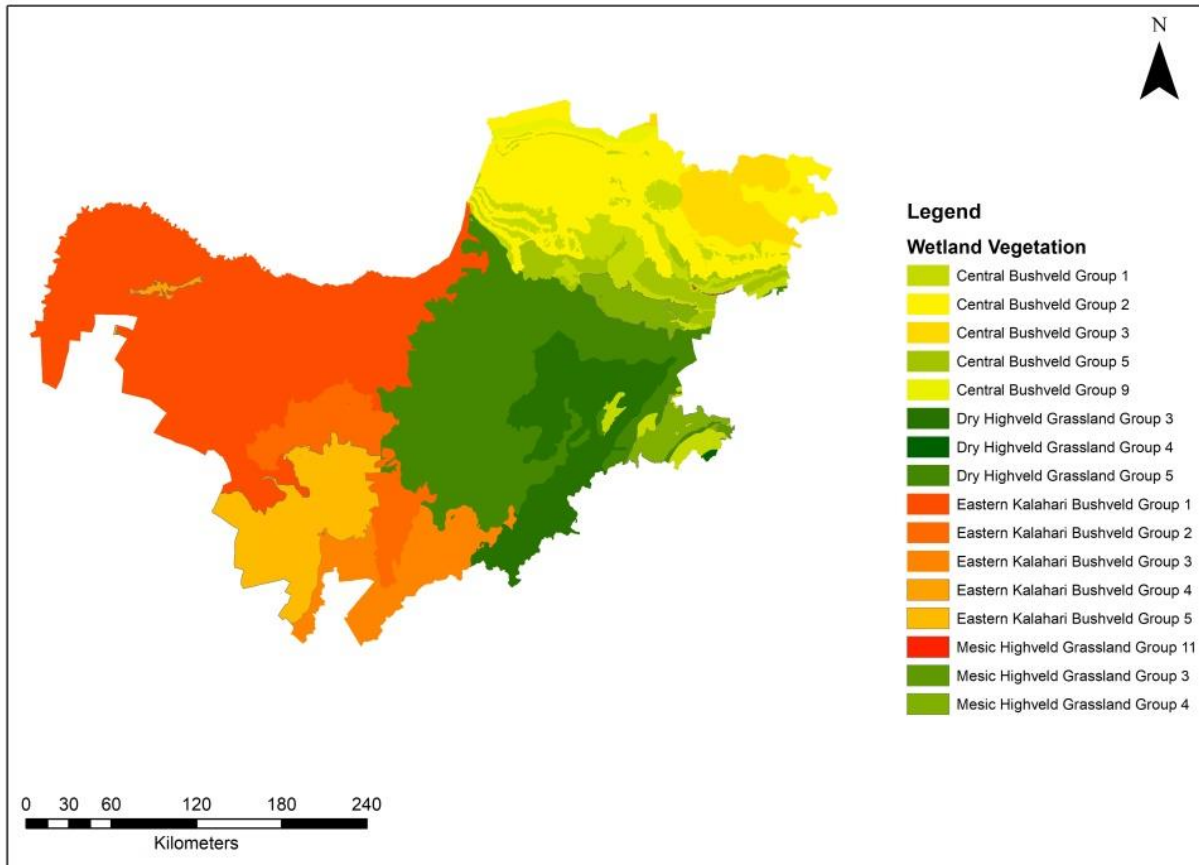


**Figure 7:** Wetland Vegetation distribution of North West Province, South Africa

### 3.2. Ground data measurements

Ground data was also collected, including surface spectral signatures with an ASD4 field Spectroradiometer, soil moisture was collected using a dielectric sensor, and soil thermal properties were ascertained a KD2 Pro Thermal Properties Analyser (Figure 8).

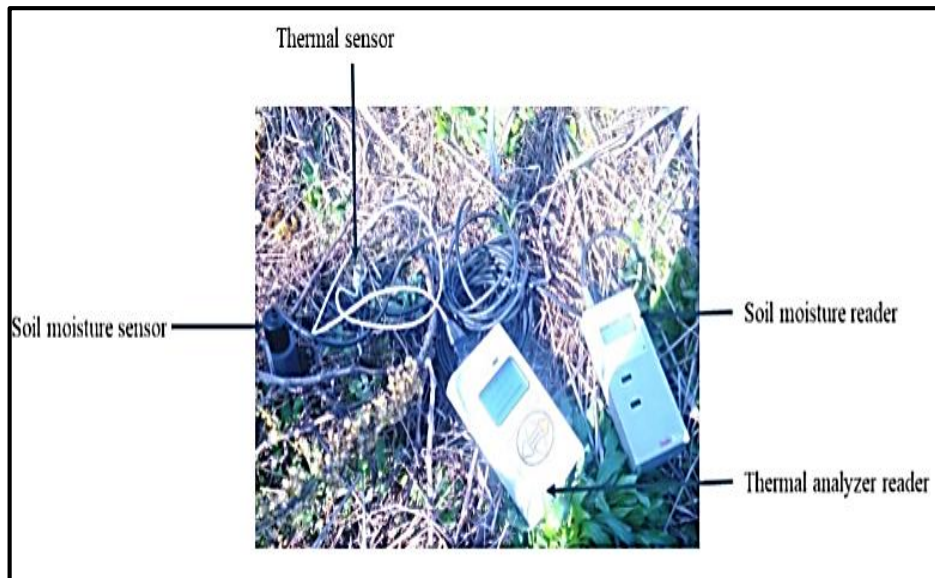


**Figure 8:** Ground measurements tools

The study determined the peat moisture content under wet and dry peat conditions and peat fire location during peatland survey (using UAV) after the rainy season and before the end of the dry season. Two planned surveys were done for the UAV flight and ground measurements, which took place in May 2019 (dry season) and December 2019 (wet season). In Molopo, about 18 samples were taken, and in Molemane, about 19 samples were taken (Table 6).

**Table 6:** Peat moisture and thermal characteristics at Molopo and Molemame sites

MOLOPO PEAT								
ID	Theta	mv	Rho	T	K	C	D	Attribute s
001	0.26	0.518	198.1	9.94	0.505	1.872	0.27	Clear area
002	0.226	0.455	351.9	9.38	0.284	1.442	0.197	Clear area
003	0.2	0.408	177.8	7.39	0.563	2.012	0.28	Reeds
004	0.088	0.201	459	8.41	0.218	1.07	0.204	Ash
005	0.088	0.202	779.1	11.25	0.128	0.666	0.193	Red Plants
006	0.109	0.239	331.9	11.05	0.301	1.225	0.246	Red Plants
007	0.121	0.263	327.1	9.53	0.306	1.561	0.196	Short Grass
008	0.057	0.145	783.3	23.44	0.128	0.94	0.136	Short Grass
009	0.151	0.317	127.1	11.81	0.787	1.681	0.468	Grass
010	0.065	0.16	710.6	13.32	0.141	0.947	0.149	Tall Grass
011	0.129	0.277	449.5	12.43	0.222	1.259	0.177	Reeds
012	0.133	0.285	321.9	16.06	0.321	1.331	0.241	Open area Bare
013	0.243	0.487	372.4	14.89	0.269	1.491	0.18	Dead grass
014	0.207	0.42	296.3	11.65	0.338	1.753	0.192	Reeds
015	0.124	0.267	409.9	11.75	0.244	1.452	0.168	Reeds
016	0.077	0.179	586	9.51	0.171	0.981	0.174	Reeds
017	0.106	0.234	307.3	8.6	0.325	1.725	0.189	Reeds/wet
018	0.083	0.266	295	7.85	0.339	1.432	0.237	Bare Soil Up
MOLEMAME PEAT								
ID	Theta	mv	Rho	T	K	C	D	Attribute s
019	0.524	1.003	183.6	19.61	0.545	2.825	0.193	Grass
020	0.569	1.089	148	13.12	0.676	3.946	0.171	Reeds
021	0.496	0.953	86.72	14.43	1.153	3.089	0.373	Grass/reeds
022	0.192	0.392	392	19.7	0.255	0.508	0.502	Grass short
023	0.452	0.872	316.6	28.31	0.316	0.347	0.91	Short Reed New
024	0.57	1.089	145.7	19.1	0.686	1.327	0.517	Short Reeds, fiber
025	0.023	0.139	321.8	30.35	0.311	1.54	0.202	mixed/Grass/Rocks
026	0.329	0.783	238	19.1	0.42	1.696	0.248	Grass
027	0.046	0.125	748	22.83	0.134	0.0.668	0.2	Reeds/Rocks
028	0.115	0.331	99.11	16.11	1.009	1.193	0.846	Grass/mineral
029	0.569	1.087	79.94	13.35	1.251	3.276	0.382	Wet Grass peat
030	0.478	0.921	73.78	17.64	1.355	3.621	0.374	Reeds/Grass
031	0.505	0.969	110.2	15.62	0.907	2.807	0.323	Reeds Wet Peat
032	0.508	0.974	165.4	15.19	0.605	2.873	0.21	Peat Reeds Fiber
033	0.471	0.907	103.6	13.85	0.965	2.613	0.369	Grass/ Peat
034	0.482	0.926	107.6	16.21	0.93	2.867	0.324	Grass/ Peat
035	0.502	0.963	101	13.08	0.99	2.943	0.336	Grass/Peat/wet
036	0.52	0.996	112.1	14.81	0.992	2.981	0.299	Grass/Peat
037	0.512	0.981	104.8	14.9	0.955	2.746	0.348	Grass/Peat

### 3.3. Laboratory experiment setup

Peat properties such as peat soil moisture, volume, and bulk density were measured using KD2 Pro sensor and soil moisture reader during laboratory experiments. These properties are known to be the key factors affecting the ignition rate and spread of underground fires (Prat-Guitart *et al.*, 2013; Prat-Guitart *et al.*, 2015). The use of optical and thermal remote sensing together will provide various indications linked to peat surface moisture. Peat samples were obtained from both sites (collected during the May 2019 survey) and processed for two weeks in August 2019 at the ARC-SCW laboratories.

The characteristics of peat thermal and soil moisture are essential aspects for the peat degradation evaluation. The peat sample was oven-dried for +/- 48 hours at 60 ° C-70 ° C and some sample trays were perforated, and then peat samples were rewetted to achieve saturation moisture level. Figure A 3 on the appendix sheet displays the methods used to determine the peat samples' moisture and thermal properties. For the burning experiment preparation, an open-top box of 20 cm x 20 cm (Figure 9) with the same thermal conductivity as peat (0.07-0.11 W m<sup>-1</sup>K<sup>-1</sup>) with a depth of 5 cm was used. The moisture content of peat is the key limiting factor of ignition; the experiment used dry (< 25% Moisture Content) and wet (> 100% Moisture Content) peat soil to determine the ignition (burning) and heat spread rate through different wetting conditions.

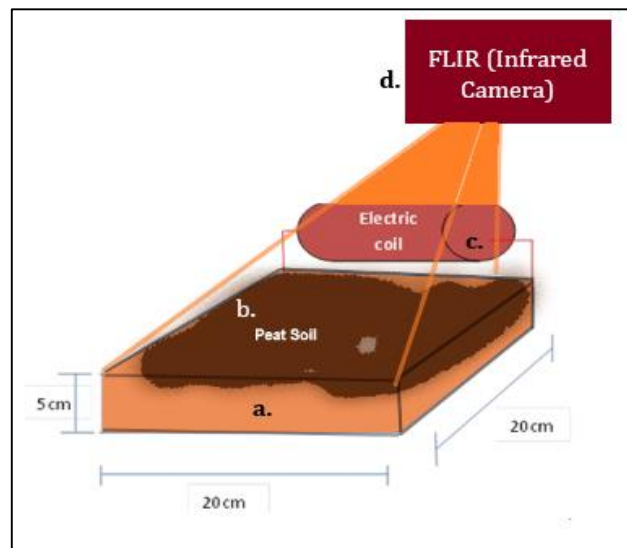


**Figure 9:** Schematic diagram of the peat burn experiment, a. 20cm x 20cm x 5cm open-top box; b. Peat soil (wet/dry soil moisture); c. Electrical heating coil; d. infrared camera and a thermal camera (FLIR Systems)

The ignitor generated approximately 100 W for 5 min and switched off to calculate the heat distribution across the peat sample, using transects to determine the ignitor's distance. The peat sample was dried for +/- 48 hrs at 60 ° C-70 ° C, and some samples were perforated to allow free drainage. Then they were saturated for 24 hrs using an identical metal tray filled with tap water, and then removed from the water and left for 12 hrs to drain the water. Figure 10 indicates the equipment used to determine the moisture and thermal characteristics of the peat samples.

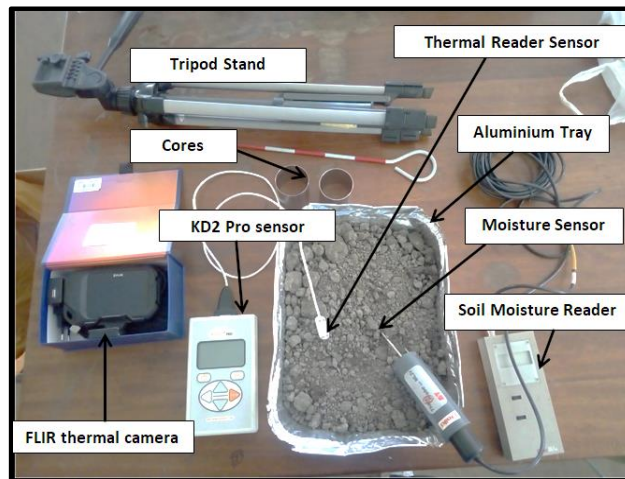


**Figure 10:** Equipment for performing laboratory experiments

### **3.4. Unmanned Aerial Vehicle (UAV) monitoring system**

#### *3.4.1. UAV Image acquisition*

The study examined the ability of remote sensing instruments at low altitudes in detecting peat fires on the peat sites of Molopo and Molemane. Molopo and Molemane were the two sites considered for UAV application to detect thermal anomalies and moisture levels. Early morning, thermal data was collected to eliminate the sun's heat and track any underground thermal emissions. In the middle of the day, the multispectral data was collected. Pre-flight calibration was performed to ensure that the drone was set and secure for the survey; the components tested before the flight are listed below (Table 7).

**Table 7:** Examples of elements to consider before launching a drone (Process. St, 2021; DroneDeploy, 2021)

Pre-Flight Checklist	Checked	Description
<b>The Drone's Operation</b>	✓	Before heading out in the field, inspect the DJI Matrice 600 Drone for damage to confirm it was ready and safe to fly.
<b>Charged remote controller, mobile device with DJI Apps and Batteries.</b>	✓	Ascertain that all batteries are fully charged for a successful payload.
<b>Assure that there is enough space on the SD card for the images and enough propellers for the drone.</b>	✓	Make sure the SD card has adequate space.
<b>Before taking off, check or analyse the weather conditions.</b>	✓	Make sure the weather is acceptable for the flight.
<b>Check and update firmware, and adjust antennas for best signal reception.</b>	✓	Check that the firmware and controller were both up to date. Ensure that the antennas are properly positioned for the greatest possible signal reception.
<b>Set the maximum flying height and calibrate the Global Positioning System (GPS) and Inertial Measurement Unit (IMU).</b>	✓	Reset the GPS coordinates and double-check that they are all correct. The IMU was calibrated by verifying the drone's battery and stability.

The multispectral and thermal sensors installed on a DJI Matrice 600 Drone were used to monitor both sites (Figure 11). The drone weighs 350g and has a high-resolution RGB camera and a multispectral camera array covering the Blue, Green, Red, Red Edge, and Near-Infrared bands. Slanrange ® 4P multispectral sensor with four bands in the 410-950 nm range was utilized to acquire pictures (Table 8). The drone's battery has a maximum flight period of 27 minutes, and the ground resolution was 4.0 cm at a flying height of 100 meters. The thermal sensor was Flir ® Vue Pro R with the lens 13 mm and the sensor resolution 640 x 512 (Table 9).

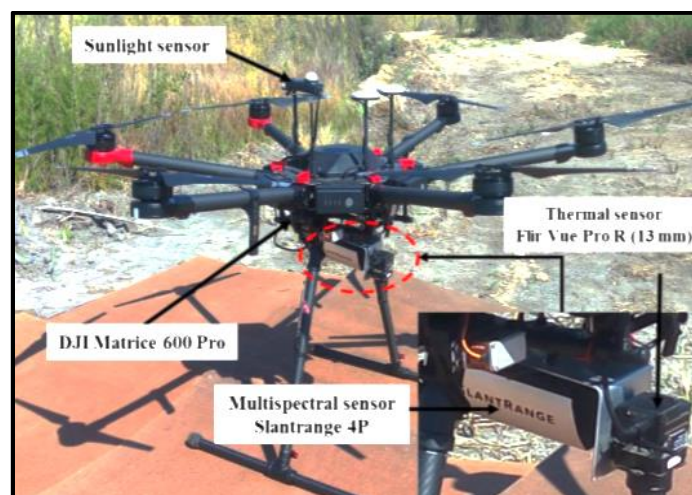


**Figure 11:** Unmanned Aerial Vehicle (UAV) with available sensors utilised to monitor the peat conditions

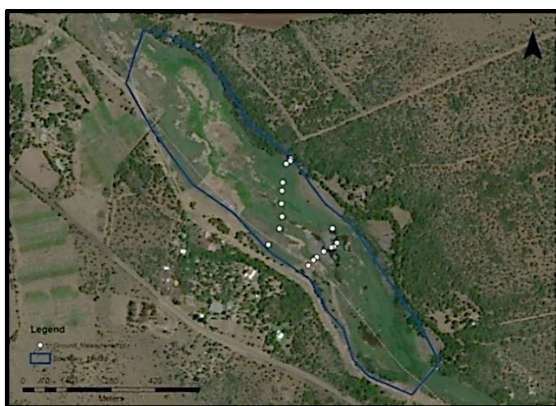
**Table 8: Slanrange® multispectral camera specification**

Characteristics	Specification
Spatial Resolution (GSD @ 100 m AGL)	4.0 cm
Spectral Channels	6
Available Spectral Range	410 – 950 nm*
Recommended Image Overlap	20%
Output Formats	KML, SHP, GeoTIFF
Size	14.6 x 6.9 x 5.7 cm
Weight	350 g
Power	12 W @ 9.0 – 28.0 VDC

**Table 9: FLIR® Vue Pro R thermal camera specification**

Characteristics	Specification
Size	2.26" x 1.75" (including lens)
Spectral Band	7.5 - 13.5 $\mu\text{m}$
Thermal Imager	Uncooled VOx Microbolometer
Weight	3.25 - 4 oz (Configuration Dependant)
Lens Options	13 mm
Scene Presets & Image Processing	Yes - Adjustable in App
Sensor Resolution	640 x 512

The thermal data was calibrated using the temperature data from the ground control point. To allow for various analysis methodologies and peatland indicators, the thermal images were resampled to 0.08 m pixel size for a coarser resolution. Figure 12 displays the UAV flight plan (Figure 12 c, d) and the location of the peat field measurements being taken (Figure 12 a, b). In order to detect any thermal irregularities, the thermal properties of the peat were tested in the morning. The average temperature was 11.57 degrees Celsius. The lowest temperature measured at bare surface areas was 7.8 °C. The average surface temperature at Molemane peatland, on the other hand, was 17.75 °C, as measured during a drone flight (UAV) around mid-day.



(a.)



(b.)



**Figure 12:** Ground Measurements and Flying Area for Molopo (a.) and Molemane peat sites (b.); Flight Plan for Molopo (c.) and Molemane peat sites (d.)

### 3.4.2. Pre-Processing of the UAV Images

The pre-processing of UAV-based multispectral sensors is a necessary and vital factor affecting spectral accuracy and quantitative analysis, according to Jiang *et al.* (2019). The crucial initial steps required to extract geometrically compatible sensor data from raw data are sensor corrections (Figure 13). Noise correction, vignette, and lens distortion correction are part of this portion of the measurement process (Jiang *et al.*, 2019). Image noise refers to any unwanted signal created by the sensor, while the purpose of the noise correction is to eliminate structural errors in the multispectral sensor (Jiang *et al.*, 2019).

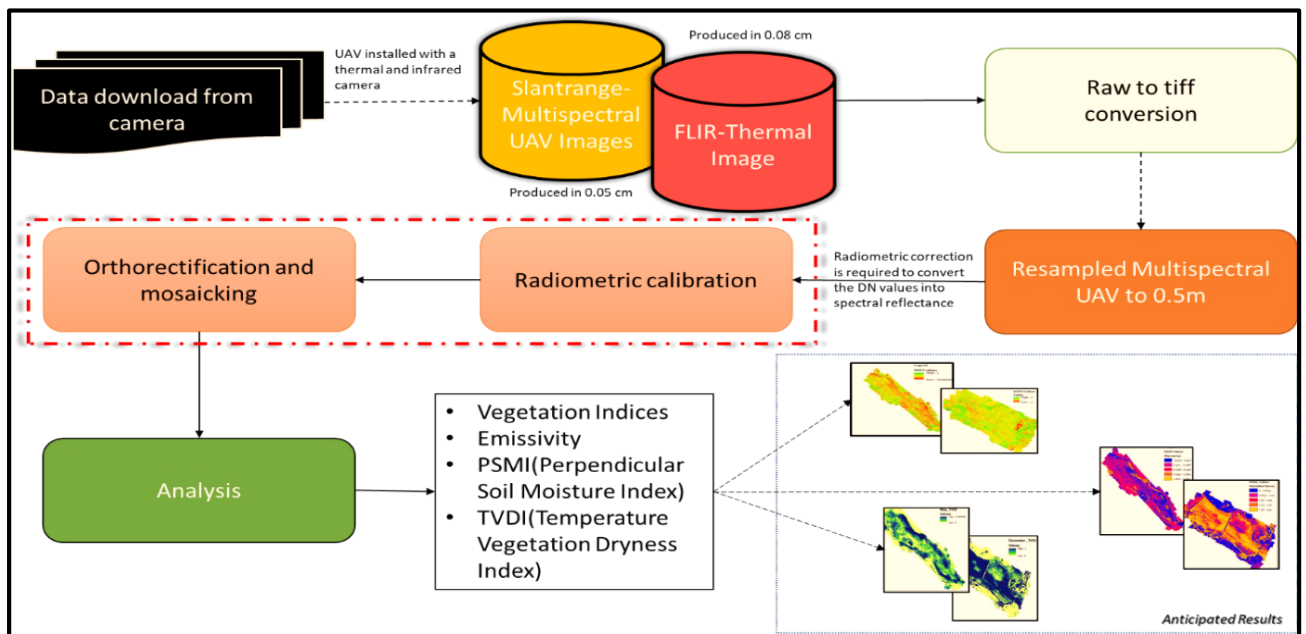


**Figure 13:** Brief process followed from data acquisition to data analysis

#### **3.4.2.1. Radiometric calibration**

Data from unmanned aerial vehicles are seldom calibrated in the same way that images from space platforms are; because UAV data is less affected by atmospheric influences, a thorough atmospheric correction is not required (Moravec *et al.*, 2021). To get the radiated energy flux estimates, the images were corrected for the angles of the infrared and webcam cameras and analysed at the pixel scale. The multispectral images were adjusted using the ENVI 5.4 (ENVI/IDL) platform to convert DN values to spectral reflectance. When images are acquired with an RGB camera, spectral reflectance is critical for recognizing different types of surfaces such as vegetation, wet regions, bare ground, etc. (Bhatnagar *et al.*, 2021).

#### **3.4.2.2. Image geo-referencing and orthomosaic**

At the exploratory and investigation phases, processing UAV images resolution were a time-consuming and memory-intensive operation. As a result, ERDAS IMAGINE 2020 was utilized to resample the images and reduce the processing time. Using ArcGIS Pro, an orthomosaic workspace was created to achieve a smooth mosaic dataset, the geometric distortion was corrected, and the images were colour balanced. Multispectral and thermal images were produced with a 0.05cm and 0.08cm resolution, respectively, after a peat survey using a UAV installed with a thermal and infrared camera. For analysis purposes and applying various indicators, the UAV images were resampled to a coarser resolution of 0.5m. The mosaicked multispectral images were orthorectified and resampled to 0.5 m resolution on ERDAS IMAGINE 2020.

#### **3.4.3. Post Processing of the UAV images**

The spectral index is where different waveband compositions can be used to assess the relationship between spectral data and specific targets such as soil moisture to measure hyperspectral details quantitatively (Ge *et al.*, 2019). Table 10 indicates some of the indices to be used to assess how the peat site has deteriorated, such as using vegetation indices (NDVI) to assess plant health and soil moisture. Determining the extent of a peat dryness by integrating multispectral data (RGB, NIR, and TIR) and thermal anomalies with UAV (120m). Soil moisture was predicted using the equation in Table 10 Perpendicular Soil Moisture Index (PSMI), which is derived from NDVI (Table 10) and normalised TIR (Table 10) following a study by Shafian and Maas (2015).

**Table 10: Indicators of soil moisture and thermal properties used in the study**

Index	Name	Formula	Brief Description	References
<b>NDVI</b>	Normalised Difference vegetation index	$NDVI = \frac{NIR - Red}{NIR + Red}$	The NDVI explains the variation in plant reflectance between visible and near-infrared wavelengths.	Tran <i>et al.</i> , 2018; Ge <i>et al.</i> , 2019
<b>PSMI</b>	Perpendicular Soil Moisture Index	$PSMI = Di / (1 + NDVI_{norm})$ $Di = (TIR_{norm} + NDVI_{norm}) / \sqrt{2}$	PSMI is a simple remote sensing-based technique for estimating soil moisture, which applies to various vegetation conditions	Shafian and Mass, 2015
<b>TVDI</b>	Temperature Vegetation Dryness Index	$TVDI = \frac{T_s - T_{smin}}{T_{smax} - T_{smin}}$	The moisture stress indicator (TVDI) introduced from NDVI-Ts feature space that reflects well the surface soil moisture, particularly in large areas of vegetation cover, is often used to assess the drought condition locally.	Meng <i>et al.</i> , 2010; Chen <i>et al.</i> , 2015; Schirmbeck <i>et al.</i> , 2017

### 3.5. Statistical Analysis

#### 3.5.1. Correlation matrix for thermal and moisture measurements obtained in the laboratory and field

A correlation matrix is nothing more than a table that displays the correlation coefficients for various variables (CFI, 2015). The matrix illustrates the relationship between all possible pairs of values in a table. It is a strong tool for summarizing a large dataset and identifying and visualizing trends in the data (CFI, 2015). SAS Enterprise Guide 9.4 was used to compute the correlation matrix for the field and laboratory measurements of the thermal and moisture properties. The assumption underlying assessing the significance of the relationship between thermal properties and moisture content is that the variables have a linear relationship. For example, consider the following hypothesis requirements for this investigation, which relate to thermal conductivity and moisture content:

**Null Hypothesis:**  $H_0 =$  There is no significant correlation between Thermal Conductivity ( $K$ ) and Moisture Content ( $\theta$ ) in the population (i.e.  $\rho > 0.05$ )

**Alternative Hypothesis:**  $H_a =$  There is a significant correlation between Thermal Conductivity ( $K$ ) and Moisture Content ( $\theta$ ) in the population (i.e.  $\rho < 0.05$ )

3.5.2. Linear Regression of PSMI and TVDI

To statistically explain or comprehend the link between estimated soil moisture and ground measured soil moisture using the applicable indices (PSMI/TVDI). Linear regression applies to two or more variables (Maulud and Abdulazeez, 2020). Thus, the relationship between peat moisture measured on the field and predicted peat moisture (PSMI/TVDI) is validated. Linear regression assumes a relationship between observed peat moisture on the ground and calculated/predicted peat moisture. The simple linear regression model (Maulud and Abdulazeez, 2020):

$$Y_i = \beta_0 + \beta_1 x + \varepsilon \dots\dots\dots (1)$$

Where  $Y_i$  = “expected value of”;  $\beta_0$ = intercept parameter and  $\beta_1 x$ = slope parameter.

In this case, the linear regression for PSMI:

$$Y_i = \beta_0 + \beta_1 PSMI \dots\dots\dots (2)$$

Where  $Y_i$  = expected value of predicted soil moisture;  $\beta_0$ = intercept parameter and  $\beta_1 PSMI=PSMI$

In this case, the linear regression for TVDI:

$$Y_i = \beta_0 + \beta_1 TVDI \dots\dots\dots (3)$$

Where  $Y_i$  = expected value of predicted soil moisture;  $\beta_0$ = intercept parameter and  $\beta_1 TVDI=TVDI$ .

## CHAPTER FOUR: RESULTS

### 4. Peat properties at the laboratory experiment scale

#### 4.1. Peat soil moisture and thermal properties

##### 4.1.1. Relationship between Bulk Density and Peat Moisture

Molemane samples have a moisture content ranging from 70 percent MC to 177 percent MC, and Molopo has a moisture content ranging from 45 percent MC to 97 percent MC. The bulk density graph (Figure 14) shows the bulk density for Molemane and Molopo wet and dry samples. The graph indicates that Molemane has high bulk density for both wet and dry samples compared with Molopo samples. The findings demonstrate that the bulk density of wet peat is greater than that of dry peat, suggesting that bulk density is considered as the mass of dry peat material per unit volume.

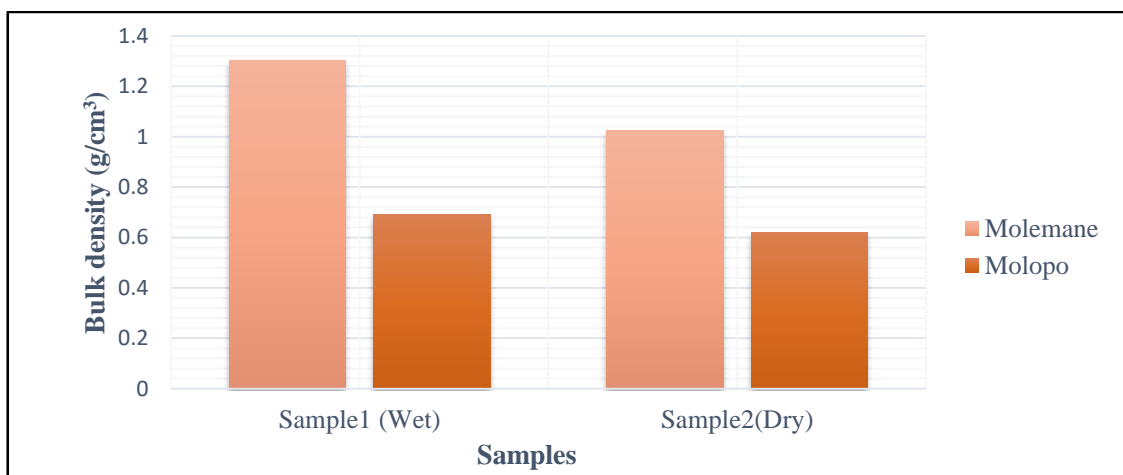


**Figure 14:** Bulk density for Molopo and Molemane wet and dry samples( $g/cm^3$ )

##### 4.1.2. Peat thermal and moisture properties were measured in the laboratory and compared to measurements taken on the field

Table 11 displays the statistics of the two sites derived during the laboratory test. The average moisture content of the Molopo site is 0.04075, with a minimum of 0.004 and a maximum of 0.119, while the average peat moisture content of Molemane is roughly 0.31933. The ground measurements (Table 12) still provide comparable findings to the laboratory results. An average ground measured peat moisture in Molopo site moisture content of 0.141, a minimum of 0.06, and a maximum of 0.26. The average peat moisture in Molemane is around 0.426, with a maximum of 0.57 and a minimum of 0.023.

**Table 11:** Laboratory measurements for both sites

<b>Molopo samples</b>					
<b>Variable</b>	<b>Mean</b>	<b>Std Dev</b>	<b>Sum</b>	<b>Minimum</b>	<b>Maximum</b>
<b>Theta</b>	0.04075	0.05302	0.16300	0.00400	0.11900
<b>K(W/(m·K)</b>	0.53225	0.48427	2.12900	0.10300	0.98200
<b>C(MJ/m<sup>3</sup>·K)</b>	10.71500	12.21229	42.86000	0.12500	21.51000
<b>D(mm<sup>2</sup>/s)</b>	0.51025	0.41939	2.04100	0.12800	0.91300
<b>RHO (cm·°C /W)</b>	360.51500	420.90811	1442	0.12400	798.30000
<b>MV</b>	0.10100	0.07080	0.40400	0.04700	0.20400
<b>Molemane samples</b>					
<b>Variable</b>	<b>Mean</b>	<b>Std Dev</b>	<b>Sum</b>	<b>Minimum</b>	<b>Maximum</b>
<b>Theta</b>	0.31933	0.21638	1.91600	0.02800	0.53500
<b>K(W/(m·K)</b>	0.48833	0.28962	2.93000	0.10500	0.87700
<b>C(MJ/m<sup>3</sup>·K)</b>	1.65983	0.68795	9.95900	0.84800	2.43200
<b>D(mm<sup>2</sup>/s)</b>	0.27417	0.09581	1.64500	0.12300	0.37800
<b>RHO (cm·°C /W)</b>	340.51667	321.41982	2043	114.00000	955.90000
<b>MV</b>	0.62683	0.39799	3.76100	0.09100	1.02300

**Table 12:** Description statistics of ground measurements for both sites

<b>Molopo</b>					
<b>Variable</b>	<b>Mean</b>	<b>Std Dev</b>	<b>Sum</b>	<b>Minimum</b>	<b>Maximum</b>
<b>Theta</b>	0.14129	0.06275	2.40200	0.05700	0.26000
<b>mv</b>	0.30371	0.11268	5.16300	0.14500	0.51800
<b>Rho(cm·°C /W)</b>	11.46706	3.86558	194.94000	7.39000	23.44000
<b>T</b>	0.32053	0.16550	5.44900	0.12800	0.78700
<b>K(W/(m·K)</b>	1.40547	0.35670	23.89300	0.66600	2.01200
<b>C(MJ/m<sup>3</sup>·K)</b>	0.22047	0.07423	3.74800	0.13600	0.46800
<b>Molemane</b>					
<b>Variable</b>	<b>Mean</b>	<b>Std Dev</b>	<b>Sum</b>	<b>Minimum</b>	<b>Maximum</b>
<b>Theta</b>	0.42617	0.17700	7.67100	0.02300	0.57000
<b>mv</b>	0.83933	0.30705	15.10800	0.12500	1.08900
<b>Rho(cm·°C /W)</b>	17.64500	4.99855	317.61000	13.08000	30.35000
<b>T</b>	0.78889	0.34495	14.20000	0.13400	1.35500
<b>K(W/(m·K)</b>	2.37538	1.09006	42.75680	0.06680	3.94600
<b>C(MJ/m<sup>3</sup>·K)</b>	0.36806	0.20572	6.62500	0.17100	0.91000

The correlation coefficient between the thermal properties and peat moisture measured in the laboratory is shown in Table 13. The results indicate that thermal resistivity negatively correlates with mvolt and theta (with a p-value greater than  $\alpha=0.05$ ). In contrast, thermal diffusivity, conductivity and temperature positively correlate with mvolt and theta (with a p-value greater than  $\alpha=0.05$ ). This may indicate that there is no significant linear correlation

between thermal properties and moisture content measurements. However, the correlation matrix (Table 14) of the ground measured thermal, and moisture properties, thermal conductivity and thermal diffusivity have a strong positive correlation with mvolt and theta, and the p-value is less than  $\alpha=0.05$ . This indicates that there is a linear relationship between thermal conductivity/diffusivity and moisture content. The correlation findings suggest that dielectric sensors could be used for continuous peat dryness measurement, which could be used to measure degradation, depending on various organic and mineral content proportions.

**Table 13:** Correlation matrix for laboratory measurements indicating the thermal properties and moisture measurements

	MV	Theta	K	C	D	rho
MV	1	0.99911 <.0001	0.58257 0.0772	0.55215 0.0979	0.45384 0.1877	-0.34835 0.3239
Theta		1	0.57496 0.0821	0.54579 0.1027	0.44383 0.1988	-0.33850 0.3387
K			1	0.95918 <.0001	0.89619 0.0004	-0.90455 0.0003
C				1	0.75959 0.0108	-0.85112 0.0018
D					1	-0.93384 <.0001
rho						1
Moisture Measurements			Thermal Measurements			

(Theta-organic moisture content, mv-mvolt, D-thermal diffusivity, Rho-thermal resistivity, K-Thermal conductivity, C-temperature in °C)

**Table 14:** A generalized correlation matrix for ground measurements of both peat sites indicating the thermal properties and moisture measurements

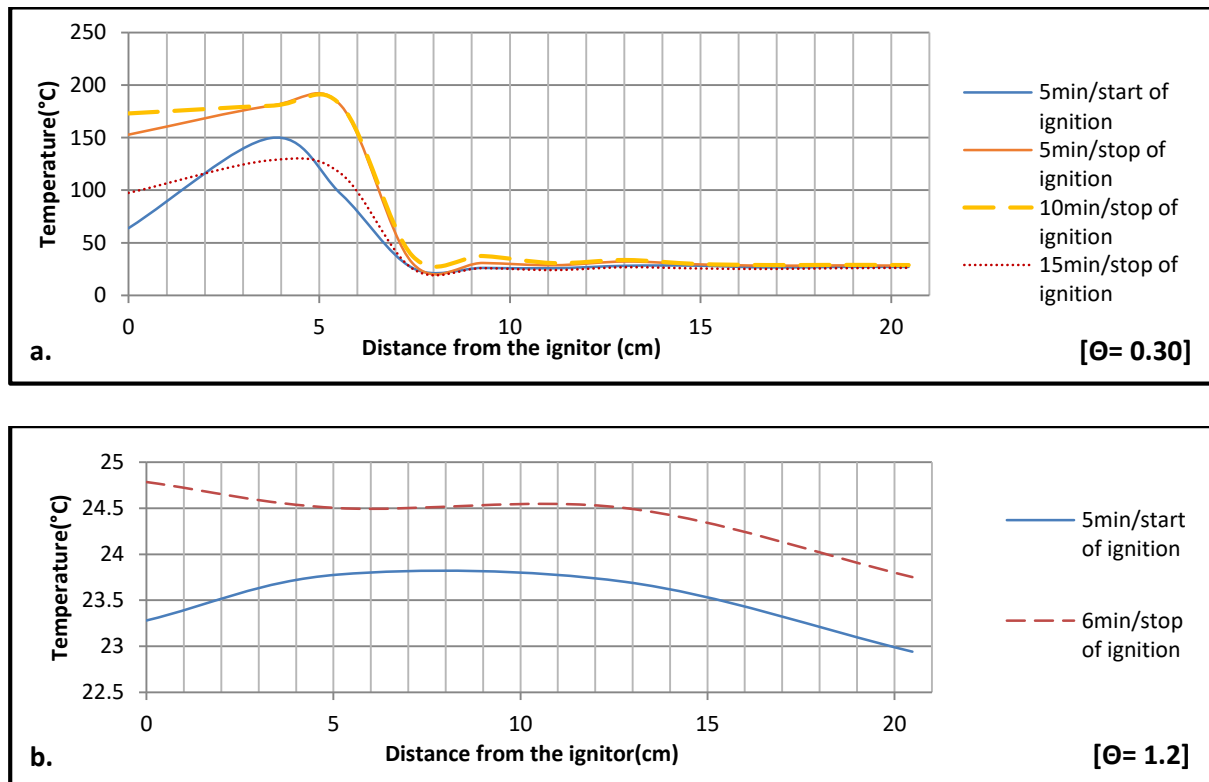
	Theta	MV	D	Rho	K	C
Theta	1	0.99656 <.0001	0.73837 <.0001	0.15883 0.3621	0.77086 <.0001	0.29963 0.0803
MV		1	0.74455 <.0001	0.17857 0.3047	0.76844 <.0001	0.31684 0.0637
D			1	0.01521 0.9309	0.78877 <.0001	0.44107 0.0080
Rho				1	-0.12634 0.4695	0.32958 0.0532
K					1	-0.05986 0.7327
C						1
Moisture Measurements			Thermal Measurements			

(Theta-organic moisture content, mv-mvolt, D-thermal diffusivity, Rho-thermal resistivity, K-Thermal conductivity, C-temperature in °C)

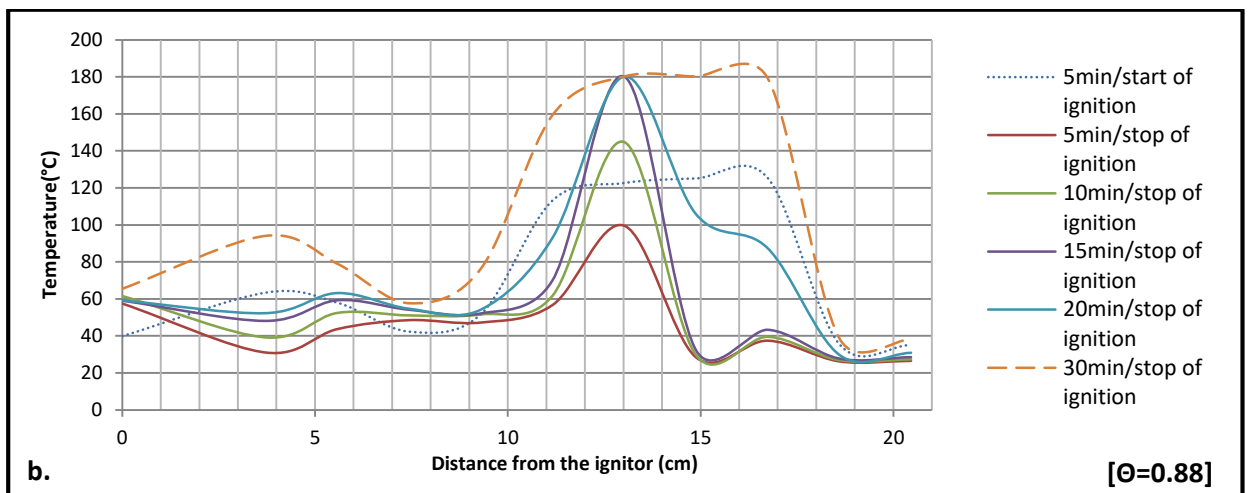
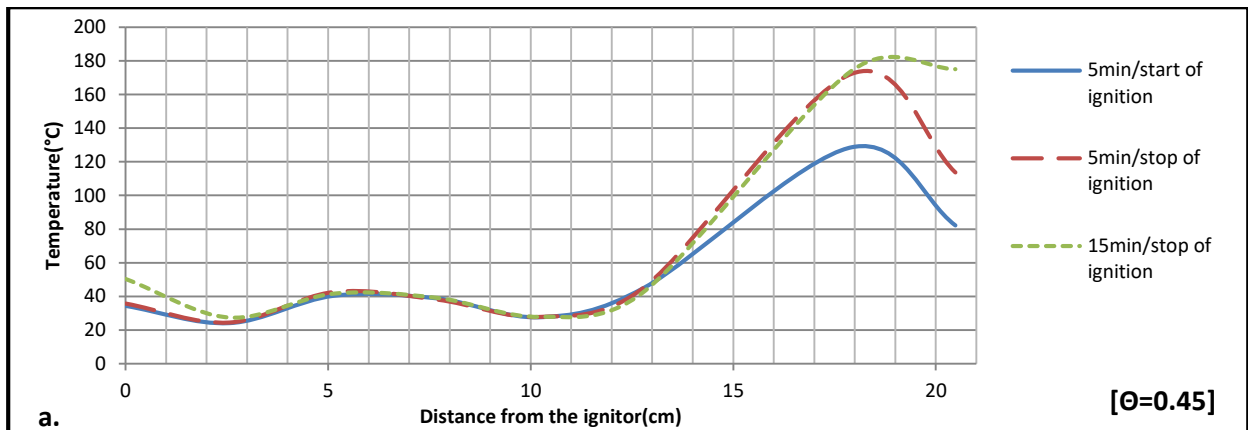
#### 4.2. The behaviour of ignition front or front movement in peat samples

Figure 15 and 16 show the simulation of peat fire distribution in peat with different moisture contents. Calculations were done using the gravimetric equation (equation 4), which shows that this equation's soil water content is represented by a unit mass of oven-dried soil. The overall results show that peat fire spread slowly under the wet peat surface due to the typical moisture content. For all the samples, the temperature of the peat fire begins to decrease after ignition. Low-moisture samples have a high heat spread to the maximum tray span (about 20.5cm), and a high moisture content suppresses the heat from 10cm down to 15cm. Temperatures were higher in samples with low moisture content than those with high moisture content. The findings in Figure 15 show that Molemane is pristine peat because when the moisture content of the peat is high (120% MC), the temperature ranges from 22.5 to 24.7 ° C, meaning that the moisture content suppressed the heat. At the same time, Figure 16 indicates that ignition stops at high temperatures and takes longer to stop than the Molopo peat samples when recovering peat.

$$\text{Gravimetric soil water content (\%)} = \left[ \frac{\text{mass of moist soil (g)} - \text{mass of oven-dried soil (g)}}{\text{mass of oven-dried soil (g)}} \right] \times 100 \dots \dots \dots (4)$$



**Figure 15:** The relationship between front movement, soil moisture, and temperature during peat ignition for Molemane sample with a gravimetric moisture content of (a.) 30% and (b.).130% MC



**Figure 16:** Molopo samples indicating the relationship between temperature and distance from the ignitor with a gravimetric moisture content of (a) 45% MC and (b) 88% MC

## 5. Soil moisture estimates using thermal infrared (TIR) and near-infrared (NIR)

### 5.1. Relationship between vegetation and TIR

A check to assess the association between emissivity and NDVI: The findings indicate a clear positive relationship between the two factors, NDVI and Emissivity (equation 5). Many derived values are at the emissivity value of 1 (Figure 17), implying that little to moderate vegetation will shield more radiation. Thermal emissivity was positively related to NDVI after applying the logarithmic transformation, with a correlation coefficient of  $R=0.98077$ .

$$Emissivity = 0.8979 - 0.1782(NDVI) \dots\dots\dots (5)$$

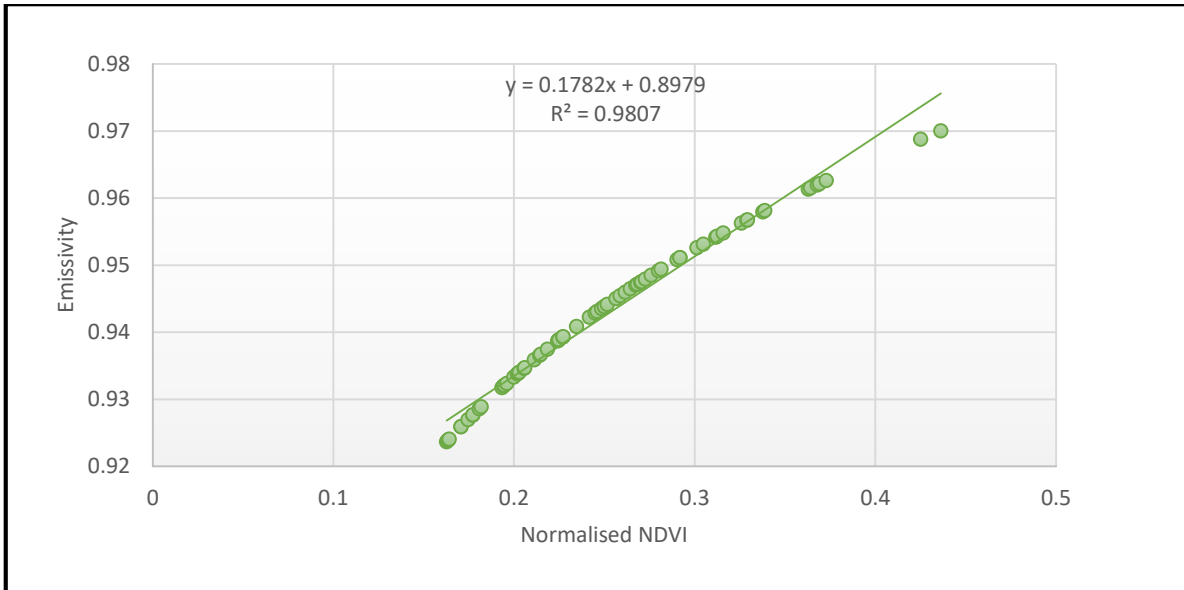


**Figure 17:** Regression analysis between NDVI and emissivity

NDVI values of 0.1 or less are considered unhealthy or low NDVI values, whereas values of 0.2 to 0.5 are considered moderate NDVI values, and values of 0.6 to 1 are considered high NDVI values or healthy vegetation (Zhang *et al.*, 2019). According to the NDVI readings from the May survey, Molopo is characterized by low vegetation density (with NDVI values ranging from -0.69 to 0.89), and Molemane is dominated by moderate vegetation density (with NDVI values ranging between -1 and 1).

NDVI data from the May survey indicate a high density of unhealthy vegetation on the Molopo peat site, indicating burned regions and barren fields. According to the May study, Molemane is more vegetated and healthier than Molopo. In contrast to the December survey, Molemane's NDVI demonstrates a low to medium vegetation density with values ranging from -1 to 0.494253 (Figure 19), while Molopo's NDVI shows a moderate vegetation density with values ranging from -0.38983 to 0.58159 (Figure 18).

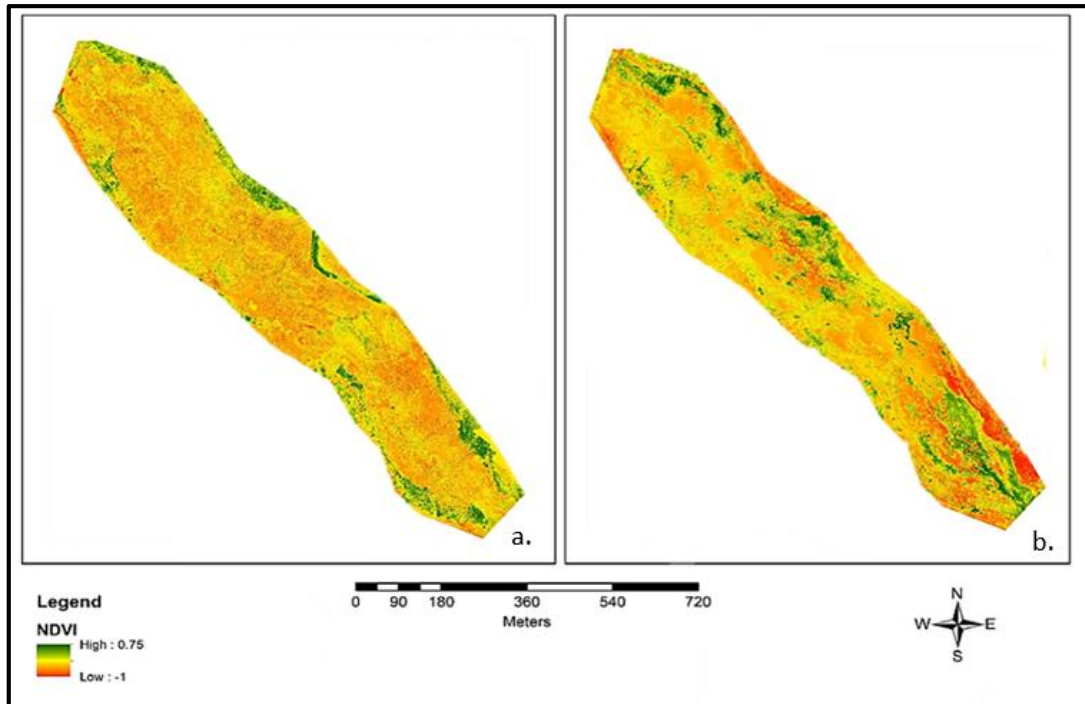


**Figure 18:** NDVI for Molopo Site (a.) May Survey and (b.) December Peat Survey

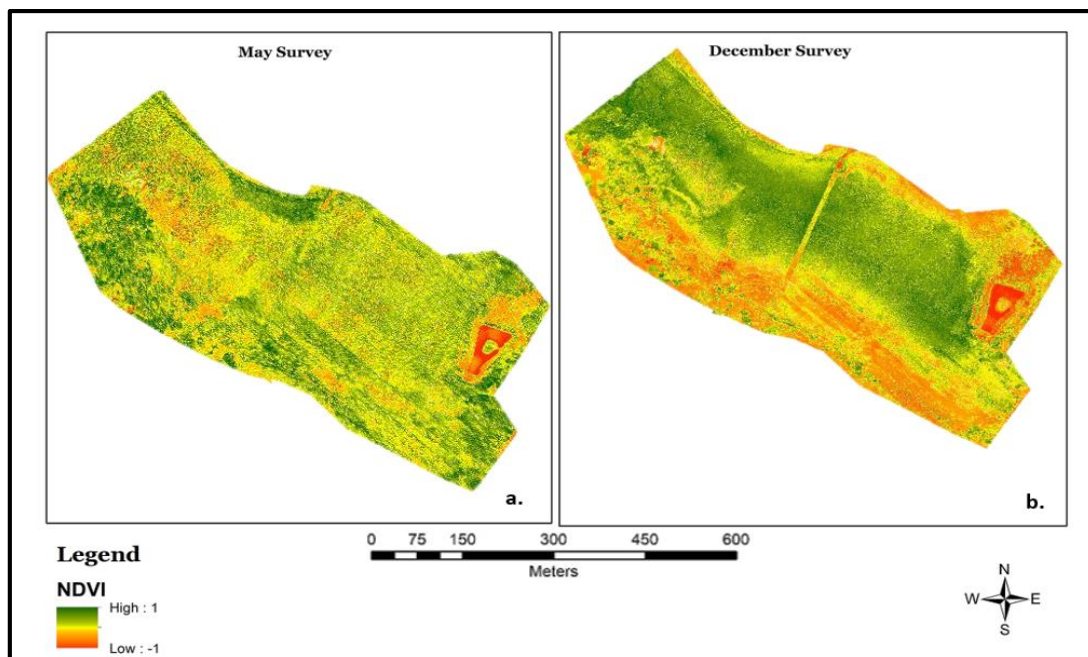


**Figure 19:** NDVI for Molemane Site (a.) May Survey and (b.) December Peat Survey

## 5.2. Comparison between PSMI and TVDI

Two soil moisture indexes (PSMI and TVDI) are used to assess the peat sites' soil moisture content to provide detailed indicators and prove the effectiveness of monitoring soil moisture. Both indices use variables of surface temperature and vegetation. The UAV images were used to determine the PSMI and TVDI index, monitoring and sustaining management purposes. As shown in Figure 20 and 21, the soil moisture index determines both sites' moisture content,

indicating Molopo PSMI classified values with a maximum value of 0.78 and a maximum of 0.71 PSMI Molemane. Therefore, it reveals that the Molemane peat is more pristine or healthier than Molopo.

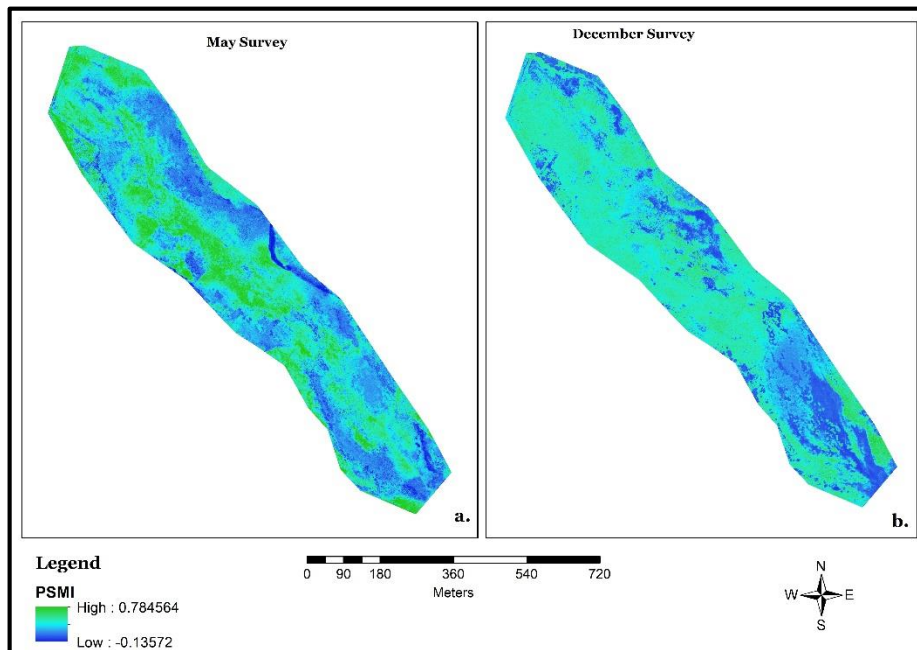


**Figure 20:** PSMI distribution of predicted peat moisture in the peat field at Molopo. Survey of May (a.) and of December (b.)

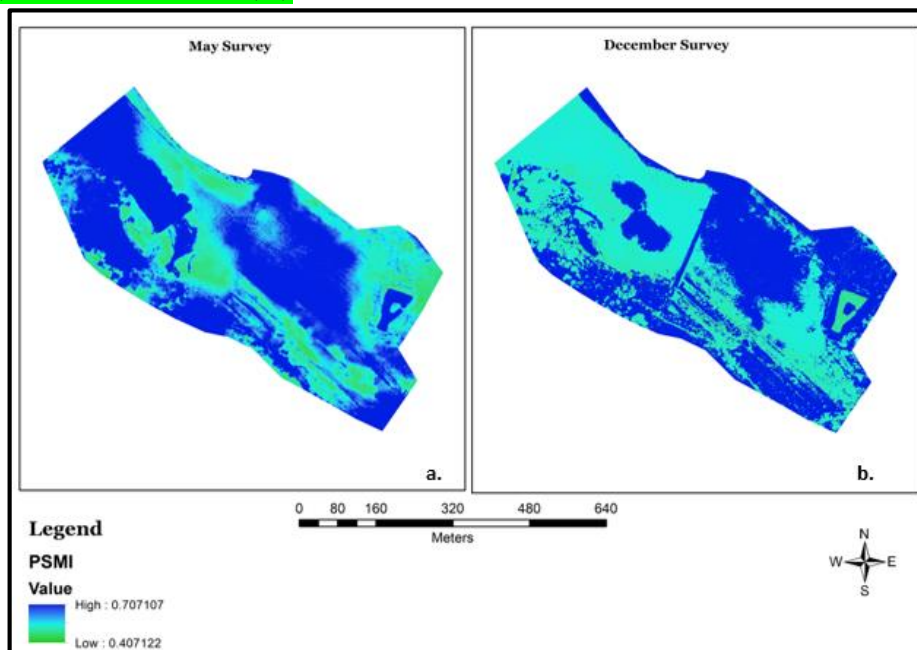


**Figure 21:** PSMI distribution of predicted peat moisture in the peat field at Molemane. Survey of May (a.) and of December (b.)

The following figures (Figure 22 and 23) indicate a Temperature-Vegetation Dryness Index (TVDI) derived from the combination of vegetation indices and surface temperature. There is an inverse relationship between soil moisture and TVDI values, where the high TVDI is the

low content of soil moisture. TVDI's spatial distribution analysis has shown that regions with high and low index values occur in all images of both peat sites. In this case, Molopo peat has a higher TVDI value (0.61) than Molemane (0.51).

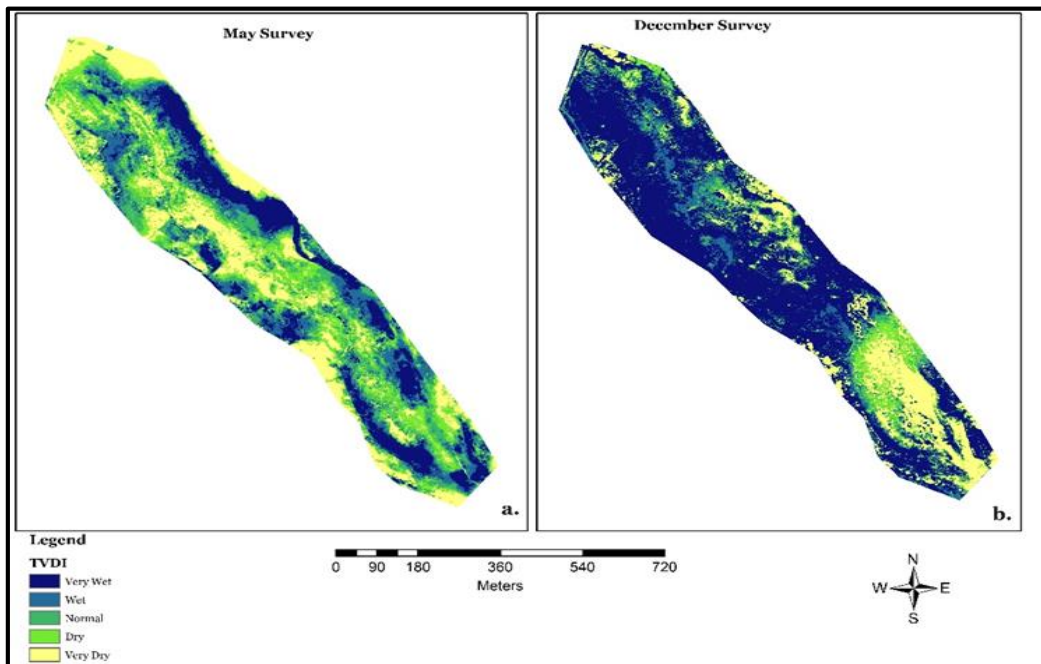


**Figure 22:** TVDI distribution in Molopo, a. May Survey and December Survey

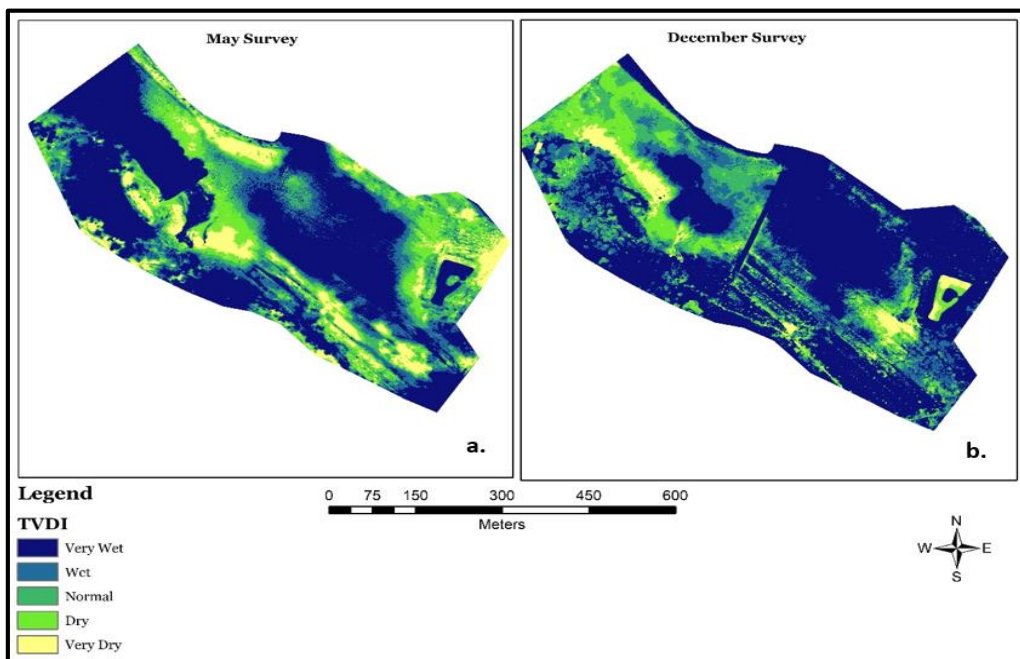


**Figure 23:** TVDI distribution in Molemane, a. May Survey and December Survey

### 5.3. Validation of imagery derived soil moisture data with ground measured soil moisture content

The linear regression analysis is predicated on the assumption that a relationship exists between projected soil moisture and measured soil moisture on the ground. Figure 24 depicts a strong negative correlation between the soil moisture measured on the field and the predicted soil moisture (PSMI). R2 for Figure 24 equals 0.67, which means that the linear model explains about 67 percent of the data variation and 33 percent of the variation is not defined. Whilst Figure 25 and Equation 7 demonstrate that soil moisture is related to TVDI, with greater TVDI values correlating to lower soil moisture levels. R2 for Figure 25 equals 0.64, which means that the linear model explains about 64 percent of the data variation and 36 percent of the variation is not defined. Equations 2 and 3 were used to produce Equations 6 and 7. The hypothesis states a relationship between observed peat moisture on the ground and calculated/predicted peat moisture.

$$WC = 0.8898 - 0.2253(PSMI) \dots\dots\dots (6)$$

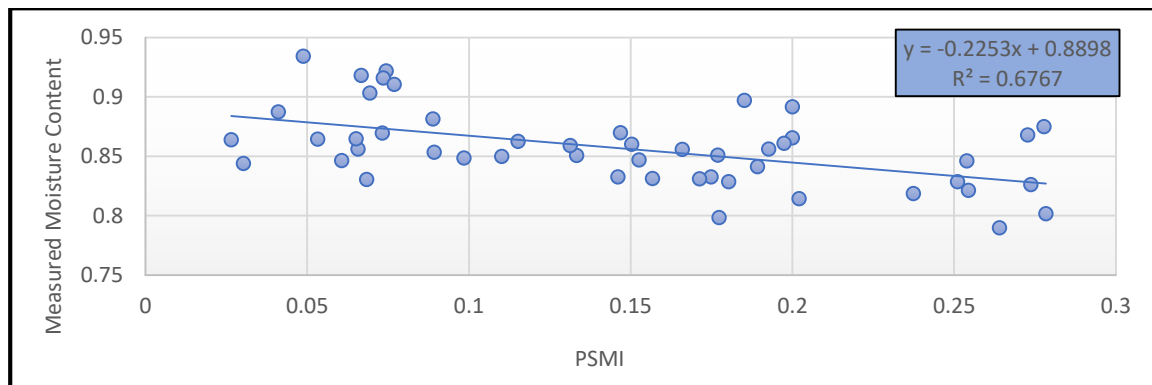


**Figure 24:** Linear regression for soil moisture field measurements and predicted soil moisture from TIR and NIR bands

$$WC = 1.2206 - 0.6445(TVDI) \dots\dots\dots (7)$$

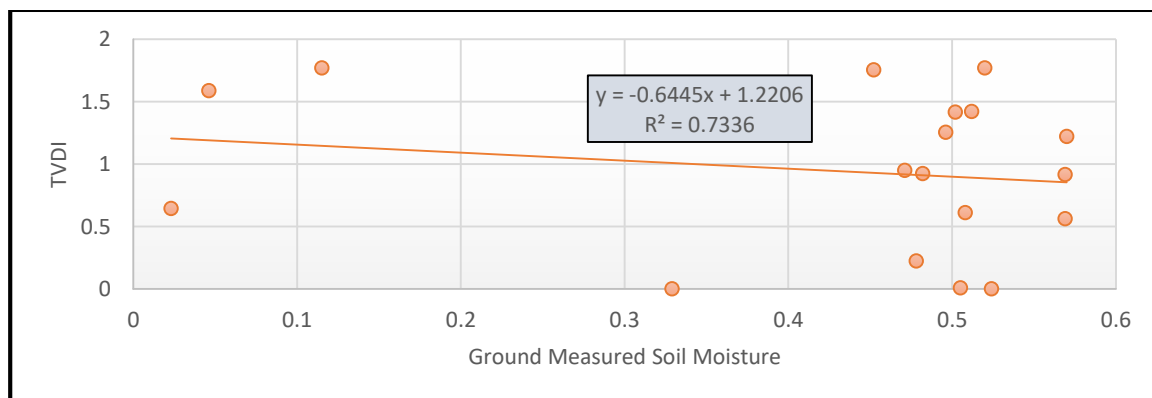


**Figure 25:** Linear relationship between ground measured soil moisture and TVDI values

## CHAPTER FIVE: DISCUSSION

### 6.1. Laboratory Experiment

#### 6.1.1. Peat moisture estimation (Laboratory-Based)

During the laboratory experiment, the weight of the samples before and after drying was utilized to quantify moisture content and bulk density. Figure 14 shows that wet samples have a higher bulk density than dry samples, suggesting that bulk density is defined as the mass of dry peat material per unit volume. According to Huang and Rein (2017), the likelihood of peat igniting may be calculated based on moisture, inorganic content, and bulk density, with the probability of sustained ignition decreasing as any of the factors increases. The above means that the high bulk density observed on Molemane (Figure 14), along with the fact that it is pristine peat (high moisture content), has the ability to reduce the risk of peat fires. This is in agreement with the predictions of Haung *et al.* (2016), who reported that wet peat density increases with moisture content, whereas dry peat density decreases with moisture content.

Although the research did not examine bulk density changes due to peat ignition or smouldering, other studies show that increased wet bulk density reduces peat fire spread. In experimental and computational research, Huang and Rein (2017) studied the vertical downward propagation of smoldering fire in moss peat under varying moisture content (MC) and bulk density. The observed downward spread rate decreased with depth and wet bulk density (Huang and Rein, 2017).

#### 6.1.2. Peat moisture and thermal characteristics (Ground-based and laboratory-based)

Table 14 shows the field measurement of peat moisture and thermal properties; the findings show thermal conductivity strongly correlates with moisture content, while thermal resistivity and moisture content have a low correlation coefficient. Similar to the laboratory results (Table 13), thermal conductivity and moisture content have a positive correlation coefficient; however, the p-value indicates that the correlation is insignificant.

To demonstrate that thermal conductivity is a suitable indicator for monitoring peat dryness. In interior Alaskan black spruce environments, O'Donnell *et al.* (2009) studied the relationship between thermal conductivity and soil moisture for different moss and organic horizon formations. Thermal conductivity was calculated using a transient line heat source system over a range of moisture contents (O'Donnell *et al.*, 2009). The findings revealed a significant

positive correlation between thermal conductivity and volumetric water content (O'Donnell *et al.*, 2009), which is similar to current study findings.

According to the findings, thermal conductivity and moisture content have a linear relationship, i.e. the thermal conductivity decreases as moisture content decreases. This implies that dielectric sensors can be employed to monitor peat dryness based on organic and mineral content proportions.

These findings highlight the significance of dielectric sensor calibration before using it to test peat moisture. The research, however, did not examine the specifics of how soil moisture sensors are calibrated. The use of Time Domain Reflectometry (TDR) to properly measure soil moisture content was investigated by Oleszczuk *et al.* (2004), who concluded that determining soil moisture content using TDR required knowledge of the apparent dielectric constant and volumetric moisture content. The calibration method used undisturbed soil samples, and the volumetric moisture content and dielectric constant were determined concurrently (Oleszczuk *et al.*, 2004). According to the findings, bulk density significantly impacts the relationship between the dielectric constant and moisture content in peat soils (Oleszczuk *et al.*, 2004).

### 6.1.3. Spread of peat fire under different moisture

The overall findings indicated that the peat fire spread steadily under saturated peat soil due to the normal moisture content. Under dry peat conditions (moisture content of 30%), the temperature was comparatively high and distributed at a very slow rate, while high moisture content peat samples suppressed the heat spread. However, in both cases, the peat fire did not spread as far as predicted; it can be due to the low oxygen level within the peat tray.

To understand more about the causes of peat fire spread concerning different moisture content. In a laboratory-scale study, Prat-Guitart *et al.* (2016) investigated the influence of peat moisture content and bulk density on the horizontal propagation of smouldering fire. According to a linear model, increasing moisture content and bulk density substantially reduced the median fire spread rate (Prat-Guitart *et al.*, 2016). The influence of moisture content on the spread rate was greater than the effect of bulk density (Prat-Guitart *et al.*, 2016). The research discovered that spatial gradients in moisture content have significant local effects on the horizontal distribution and should be considered in field and modelling studies (Prat-Guitart *et al.*, 2016).

While the study did not look into the dynamics of peat fire distributions, previous research suggests that monitoring and understanding smouldering propagation directions are necessary. Huang and Rein (2017) study was the first to look at peat fire's upward expansion. The modelling findings demonstrate that oxygen diffusion controls the whole uphill-to-downward growth of a peat fire; peat oxidation supports the first stage of upward spread, while char oxidation supports the second stage of downward spread (Huang and Rein, 2017). These kinds of studies aid in gaining a better understanding of the peat fire's persistence and help focus fire prevention and management strategies.

Molopo samples were rewetted during the study to assess the spread of peat fire. It was discovered that the rewetted samples continued to burn even after the ignition was turned off 30 minutes later. Dianti *et al.* (2018) investigated the characteristics of rewetting peat smouldering combustion in a research. At 80 mm intervals, a thermocouple collection was utilized to evaluate the horizontal spread rate (Dianti *et al.*, 2018). In experiments with rewetting peat, the authors discovered that the chance of peat fire is greater than that of natural combustion (Dianti *et al.*, 2018). This is comparable with the findings of the current study, which show that after rewetting peat, the smouldering spread rate is high.

## **6.2. UAV Application**

### **6.2.1. UAV images for peatland monitoring**

Molopo and Molemane were the two sites considered for UAV application to detect thermal anomalies and moisture levels. Monitoring of both sites was performed using the multispectral and thermal sensors mounted on a drone. The combination of thermal and vegetation indices aids in accurate soil moisture measurement (Kaleita *et al.*, 2005). Mustaffa *et al.* (2020) discovered that the physical properties of peat soil are associated with the healthiness index of pineapple crops. The index is dependent on visible spectral wavelengths of Red, Blue, Green (RGB), and Near Infrared (NIR) captured by a multispectral camera mounted on the drone (Mustaffa *et al.*, 2020).

As a result, the study proved that using multispectral images from a drone would compare the healthiness of pineapple crops with the physical properties of the soil (Mustaffa *et al.*, 2020). UAV can successfully detect and monitor peatland degradation, can be used for ground verification of satellite data in large peatland areas (Teguh *et al.*, 2012). UAVs are applicable in detecting and diagnosing peat dryness for better and accurate detection of underground fires'

size, distribution, and location (Teguh *et al.*, 2012). UAVs with NIR can monitor the restoration of cut-over bogs and can reduce tedious work significantly (Knoth *et al.*, 2012).

Bhatnagar *et al.* (2021) study expands the potential of remote sensing-based wetlands monitoring by integrating RGB image processing, machine learning algorithms, and satellite data analysis to establish seasonal maps of vegetation communities within the wetlands. This approach decreases the number of field surveys that are usually needed to determine the long term ecological change of certain wetland ecosystems (Bhatnagar *et al.*, 2021). The proposed method's success demonstrates a reliable, simple, and cost-effective method for mapping wetland environments seasonally and investigating their eco-hydrological synergies (Bhatnagar *et al.*, 2021).

### 6.2.2. Estimation of peat moisture using UAV data

To track soil moisture efficiently in an appropriate manner, TVDI and PSMI were used to predict peatland moisture content. The study demonstrates a strong negative correlation between PSMI and ground measured peat moisture (Figure 24). These results concur with Shafian and Maas (2015) study, which concluded that PSMI is inversely proportional to ground measured soil moisture due to variation in thermal emittance and vegetation cover. According to Shafian and Maas (2015), the theoretical calculation of PSMI is controlled by soil moisture, which is the critical source of variability for thermal infrared.

On the other hand, a favourable relationship exists between peat moisture measured on the field and TVDI values. Ground soil moisture measurements for each peat site were routinely established to verify the TVDI's effectiveness as an index for assessing soil moisture. According to Zhang *et al.* (2019), the closer TVDI is to 0, the higher the soil moisture and the lower the degree of dryness.

Hypothetically TVDI distribution on the peat sites was supposed to be moderate to high moisture content on the December survey (especially Molemane peat site) than those of the May survey. However, the results indicate that the predicted soil moisture distribution is between low to moderate soil moisture from the December analysis. The Molemane peat site negatively correlates with TVDI and ground measured peat moisture. These findings support existing evidence that the TVDI and ground measured soil moisture has a strong negative relationship (Chen *et al.*, 2015; Bai *et al.*, 2017).

The results contribute a clearer understanding of PSMI as a good proxy to identify peatland dryness compared to TVDI. Ground measured peat moisture had better correlations to PSMI than TVDI, indicating more statistically significant relationships between PSMI and peat moisture. In as much as TVDI has been commonly used because of its ease of use and high monitoring accuracy, it has several shortcomings that restrict its applicability (Bai *et al.*, 2017).

## CHAPTER SIX: CONCLUSION AND RECOMMENDATIONS

### 7.1. Conclusion of the study

Peatland systems are essential ecosystems globally that play a significant role in serving as water and carbon reservoirs (Bispo *et al.*, 2016). They play a significant role in biodiversity as well as semi-arid countries such as South Africa. However, these systems are threatened by improper management and use, such as drainage (Bonnett *et al.*, 2009; Faul *et al.*, 2016; Gabriel *et al.*, 2018). Thus, it is vital to conserve peatland systems due to their limited extent, size, and threats posed to them because of population pressure and development (Grundling and Grobler, 2005).

The research aimed to assess peat soil moisture and thermal properties' effect on peat fires' propagation or occurrence in the semi-arid province in South Africa (North West Province) using multi-platform remote sensing tools for peat fire detection and monitoring project. This project is based on the monitoring of remote sensing at low altitudes. The fundamental goal of the project was to monitor the level of peatland destruction due to underground burning in semi-arid regions of the North West Province, using low-altitude remote sensing techniques [such as handheld sensors and unmanned aerial systems (UASs)] (South Africa).

The goal of the study was to discover peat characteristics (thermal and moisture content) that might cause peat fires in a laboratory setting. It was determined that peat thermal and soil moisture properties are critical characteristics for peat fire suitability. Different peat samples with variable moisture content were analysed. There was a visible relationship between peat soil moisture and thermal properties. Peat moisture, bulk density, and thermal conductivity are significant indicators that influence peat fires' distribution and persistence. Thus, there is a need to preserving peatlands from drying out to reduce peat fires and, consequently, the emission of carbon dioxide.

Thermal infrared (TIR) and near-infrared (NIR) datasets obtained from ground and UAV platforms were used to assess peat moisture. By combining multispectral data with thermal anomalies, the researcher hoped to estimate the amount of peat fire and peat moisture. However, the study did not identify the extent of the peat fire, but peat dryness was identified as a useful proxy for determining how the peat fire can be distributed.

PSMI and TVDI indices were used to estimate peat moisture, which was used to develop maps illustrating the geographical distribution of peat moisture over the Molopo and Molemane peat areas. It was found that high values of PSMI or TVDI indicate low peat moisture content, and low values of the two indices indicate high peat moisture content. The study has also shown the potential of high-resolution (UAV) imagery in extinguishing peat soil moisture and thermal character. The study proved that the Molemane peat site is more pristine or healthier than Molopo, and PSMI is a more reliable peat dryness indicator.

## **7.2. Recommendations and future studies**

The priorities that have been discussed for the whole project are outlined in Figure A1 below, which outlines objectives that have been addressed for the entire project. Based on the research findings, the recommendations are:

- Based on these findings, practitioners should consider changes in soil reflectance under varying moisture conditions because remote sensing provides a broader view of soil and vegetation properties.
- There is insufficient knowledge of peatland systems in South Africa, resulting in policy and decision-making that is not based on a strong information base and can, therefore, unintentionally result in significant harm to these critical ecosystems. Therefore, peatland habitats need to be controlled efficiently by obtaining detailed scientific information on peatland and peat fire characteristics. Peatlands should be surveyed and tracked in order to prevent degradation and to plan recovery successfully.
- Measures such as re-establishing the hydrological function of the peatland system; rewetting dried-up or drained areas; improved the knowledge of the groundwater balance and its processes, discerning the characteristics of the various water sources of the system; and improve the monitoring of peat fires and erosion dynamics.
- Future research should explore the topic of peat fires to understand the effects of these findings further, as no peat fires were observed during the surveys; at the time, dryness hotspots were established.

## REFERENCES

- Agus, F. 2015. Degradation and Sustainable Management of Peat Soils in Indonesia. In *MARCO Symposium Tsukuba International Congress Center Japan*, 7.
- Amani, M., Salehi, B., Mahdavi, S., Masjedi, A. and Dehnavi, S. 2017. Temperature-vegetation-soil moisture dryness index (TVMDI). *Remote sensing of environment*, 197,1-14.
- Atwood, E., Englhart, S., Lorenz, E., Halle, W., Wiedemann, W., and Siegert, F. 2016. Detection and characterization of low-temperature peat fires during the 2015 fire catastrophe in Indonesia using a new high-sensitivity fire monitoring satellite sensor (FireBird). *PLoS ONE*, 11, 1–24.
- Bai, J.J., Yuan, Y.U. and Di, L., 2017. Comparison between TVDI and CWSI for drought monitoring in the Guanzhong Plain, China. *Journal of integrative agriculture*, 16, 389-397.
- Baret, F. and Guyot, G. 1991. Potentials and limits of vegetation indices for LAI and APAR assessment. *Remote Sensing of Environment*, 35, 161–173.
- Beyer, F., Jurasinski, G., Couwenberg, J. and Grenzdörffer, G. 2019. Multisensor data to derive peatland vegetation communities using a fixed-wing unmanned aerial vehicle. *International Journal of Remote Sensing*, 1-23.
- Bhatnagar, S., Gill, L., Regan, S., Waldren, S. and Ghosh, B. 2021. A nested drone-satellite approach to monitoring the ecological conditions of wetlands. *ISPRS Journal of Photogrammetry and Remote Sensing*, 174, 151-165.
- Biancalani, R. and Avagyan, A., 2014. Towards climate-responsible peatlands management. *Mitigation of Climate Change in Agriculture Series (MICCA)*. Available from: <http://www.fao.org/3/a-i4029e.pdf>. Accessed on 23 December 2019.
- Bispo, D.F.A., Silva, A.C., Christofaro, C., Silva, M.L.N., Barbosa, M.S., Silva, B.P.C., Barral, U.M. and Fabris, J.D. 2016. Hydrology and carbon dynamics of tropical peatlands from Southeast Brazil. *Catena*, 143, 18-25.
- Bonnett, S.A.F., Ross, S., Linstead, C. and Maltby, E. 2009. A review of techniques for monitoring the success of peatland restoration. University of Liverpool. *Natural England Commissioned Reports*, Number 086.
- Bourgeau-Chavez, L.L., Endres, S.L., Graham, J.A., Hribljan, J.A., Chimner, R.A., Lillieskov, E.A. and Battaglia, M.J. 2018. Mapping peatlands in boreal and tropical ecoregions. In: *Liang, S., ed. Comprehensive Remote Sensing, vol. 6. Oxford, UK: Elsevier: 24–44.*, 24-44.

- Burke, C., Wich, S., Kusin, K., McAree, O., Harrison, M.E., Ripoll, B., Ermiasi, Y., Mulero-Pázmány, M. and Longmore, S. 2019. Thermal-Drones as a Safe and Reliable Method for Detecting Subterranean Peat Fires. *Drones*, 3,23.
- Casbeer, D.W., Kingston, D.B, Beard, R.W. and McLain, T.W. 2006. Cooperative forest fire surveillance using a team of small unmanned air vehicles. *International Journal of Systems Science*, 37, 351-360.
- Carvajal-Ramírez, F., Marques da Silva, J.R., Agüera-Vega, F., Martínez-Carricondo, P., Serrano, J. and Moral, F.J. 2019. Evaluation of Fire Severity Indices Based on Pre-and Post-Fire Multispectral Imagery Sensed from UAV. *Remote Sensing*, 11(9), 993.
- Chowdary, V. and Gupta, M.K. 2018. Automatic Forest Fire Detection and Monitoring Techniques: A Survey. In: Singh, R., Choudhury, S. and Gehlot, A. (eds.). *Intelligent Communication, Control and Devices, Advances in Intelligent Systems and Computing*, 1111-1117.
- CFI,2015. Correlation Matrix. Available from <https://corporatefinanceinstitute.com/resources/excel/study/correlation-matrix/>. Accessed on 14 September 2021.
- Chen, S., Wen, Z., Jiang, H., Zhao, Q., Zhang, X. and Chen, Y. 2015. Temperature vegetation dryness index estimation of soil moisture under different tree species. *Sustainability*, 7, 11401-11417.
- Dianti, A., Ratnasari, N.G., Palamba, P. and Nugroho, Y. 2018. Effect of rewetting on smouldering combustion of a tropical peat. *In E3S Web of Conferences*,67, 1-6.
- DroneDeploy, 2021. Pre-Flight Checklist. Available from <https://support.dronedeploy.com/docs/pre-flight-checklist>. Accessed on 12 September 2021.
- Elvidge, C.D., Zhizhin, M., Hsu, F.-C., Baugh, K., Khomarudin, M.R., Vetruta, Y., Sofan, P., Suwarsono and Hilman, D. 2015. Long-wave infrared identification of smouldering peat fires in Indonesia with night-time Landsat data. *Environmental Research Letters*, 10(6).
- FAO. 2020. Peatlands Mapping and Monitoring-Recommendations and technical overview. Rome. Available from <http://www.fao.org/3/ca8200en/ca8200en.pdf>. Accessed on 09 September 2021.
- Faul, F., Gabriel, M., Roßkopf, N., Zeitz, J., van Huyssteen, C. W., Pretorius, M.L. and Grundling, P. 2016. Physical and hydrological properties of peatland substrates from different hydrogenetic wetland types on the Maputaland Coastal Plain, South Africa. *South African Journal of Plant and Soil*, 33, 265-278.

- Filkov, A., Leroy-Cancellieri, V., Cancellieri, D., Gladky, D. and Simeoni, A. 2015. Modelling Peat Fire Hazards: From Drying to Smouldering. In: Stracher, G.B., Prakash, A. and Rein, G. (eds.), *Coal and Peat Fires: A Global Perspective*. Elsevier, 89-120.
- Frandsen, W.H. 1998. Heat Flow Measurements from Smouldering Porous Fuel. *International Journal Wildland Fire*, 8, 137-145.
- Fraser, R.H., Van der Sluijs, J. and Hall, R.J. 2017. Calibrating satellite-based indices of burn severity from UAV-derived metrics of a burned boreal forest in NWT, Canada. *Remote Sensing*, 9, 1-17.
- Gabriel, M., Galka, M., Pretorius, M.L. and Zeitz, J. 2017. The development pathways of two peatlands in South Africa over the last 6200 years: Implications for peat formation and palaeo climatic research. *The Holocene*, 1-17.
- Gabriel, M., Toader, C., Faul, F., Roßkopf, N., Grundling, P., van Huyssteen, C.W. and Zeitz, J. 2018. Physical and hydrological properties of peat as proxies for degradation of South African peatlands: Implications for conservation and restoration. *Mires and Peat*, 21, 1-21.
- Gabriel, M., Toader, C., Faul, F., Roßkopf, N., Grundling, P., van Huyssteen, C.W. and Zeitz, J. 2018. Peatland substrates in northern KwaZulu-Natal: a study of the forming environments, properties and an approach towards classification. *South African Journal of Plant and Soil*, 35, 149-160.
- Ge, X., Wang, J., Ding, J., Cao, X., Zhang, Z., Liu, J. and Li, X. 2019. Combining UAV-based hyperspectral imagery and machine learning algorithms for soil moisture content monitoring. *PeerJ*, 7, 6926.
- Ghulam, A., Qin, Q., Teyip, T. and Li, Z.L. 2007. Modified perpendicular drought index (MPDI): a real-time drought monitoring method. *ISPRS journal of photogrammetry and remote sensing*, 62, 150-164.
- Grundling, P.L. and Grobler, R. 2005. Peatlands and Mires of South Africa. *Landesmuseen Neue Serie*, 35, 379-396.
- Grundling, A.T., van den Berg, E.C. and Price, J.S. 2013. Assessing the distribution of wetlands over wet and dry periods and land-use change on the Maputaland Coastal Plain, north-eastern KwaZulu-Natal, South Africa. *South African Journal of Geomatics*, 2, 120-139.
- Grundling, P.L., Grundling, A.T. and Pretorius, L. 2017. South African Peatlands: Ecohydrological Characteristics and Socio-economic Value: Report to the Water Research Commission. Water Research Commission. Available from: <http://www.wrc.org.za/wp-content/uploads/mdocs/2346-1-17.pdf>. Accessed on 19 December 2019.

- Gumbrecht, T., McCarthy, T.S., McCarthy, J., Roy, D, Frost, P.E. and Wessels, K. 2002. Remote sensing to detect subsurface peat fires and peat fire scars in the Okavango Delta, Botswana. *South African Journal of Science*, 98, 351-358.
- Hamilton, D., Bowerman, M., Colwell, J., Donohoe, G. and Myers, B. 2017. Spectroscopic analysis for mapping wildland fire effects from remotely sensed imagery. *Journal of unmanned vehicle systems*, 5, 146-158.
- Holden, Z.A., Morgan, P., Smith, A.M. and Vierling, L. 2010. Beyond Landsat: a comparison of four satellite sensors for detecting burn severity in ponderosa pine forests of the Gila Wilderness, NM, USA. *International Journal of Wildland Fire*, 19, 449-458.
- Holidi, H., Armanto, M., Damiri, N. and Putranto, D.D.A. 2019. Characteristics of Selected Peatland Uses and Soil Moisture Based on TVDI. *Journal of Ecological Engineering*, 20.
- Hong, Z., Zhang, W., Yu, C., Zhang, D., Li, L. and Meng, L. 2018. SWCTI: Surface Water Content Temperature Index for Assessment of Surface Soil Moisture Status. *Sensors*, 18, 2875.
- Hu, Y., Fernandez-Anez, N., Smith, T.E.L. and Rein, G. 2018. Review of emissions from smouldering peat fires and their contribution to regional haze episodes. *International Journal of Wildland Fire*, 27, 293–312.
- Huang, X. and Rein, G. 2017. Downward spread of smouldering peat fire: the role of moisture, density and oxygen supply. *International Journal of Wildland Fire*, 26, 907-918.
- Huete, A.R. 1988. A soil-adjusted vegetation index (SAVI). *Remote sensing of environment*, 3,295-309.
- Jiang, J., Zheng, H., Ji, X., Cheng, T., Tian, Y., Zhu, Y., Cao, W., Ehsani, R. and Yao, X. 2019. Analysis and evaluation of the image preprocessing process of a six-band multispectral camera mounted on an unmanned aerial vehicle for winter wheat monitoring. *Sensors*, 19, 747.
- Kaleita, A.L., Tian, L.F. and Hirschi, M.C. 2005. Relationship between soil moisture content and soil surface reflectance. *Transactions of the ASAE*, 48,1979-1986.
- Knoth, C., Klein, B., Prinz, T. and Kleinebecker, T. 2013. Unmanned aerial vehicles as innovative remote sensing platforms for high-resolution infrared imagery to support restoration monitoring in cut-over bogs. *Applied Vegetation Science*, 16, 509–517.
- Lakshmi, V. 2013. Remote sensing of soil moisture. *ISRN Soil Science*, 1-34.
- Lees, K.J., Artz, R.R.E., Chandler, D., Aspinall, T., Boulton, C.A., Buxton, J., Cowie, N.R. and Lenton, T.M. 2021. Using remote sensing to assess peatland resilience by

- estimating soil surface moisture and drought recovery. *Science of The Total Environment*, 761, 1-38.
- Lentile, L.B., Holden, Z.A., Smith, A.M., Falkowski, M.J., Hudak, A.T., Morgan, P., Lewis, S.A., Gessler, P.E. and Benson, N.C. 2006. Remote sensing techniques to assess active fire characteristics and post-fire effects. *International Journal of Wildland Fire*, 15(3), 319-345.
- Liu, L. and Zhang, Y. 2011. Urban heat island analysis using the Landsat TM data and ASTER data: A case study in Hong Kong. *Remote Sensing*, 3,1535-1552.
- Liew, S.C. 2001. Satellite detection of forest fires and burn scars. In *Workshop on Minimizing the Impact of Forest Fire on Biodiversity in Asean*. Available from [https://www.researchgate.net/publication/228935625\\_6\\_Satellite\\_detection\\_of\\_forest\\_fires\\_and\\_burn\\_scars](https://www.researchgate.net/publication/228935625_6_Satellite_detection_of_forest_fires_and_burn_scars). Accessed on 4 April 2019.
- Malik, M.S. and Shukla, J.P. 2014. Estimation of Soil Moisture by Remote Sensing and Field Methods: A Review. *International Journal of Remote Sensing and Geoscience (IJRSG)*, 3, 21-27.
- Maulud, D. and Abdulazeez, A.M. 2020. A Review on Linear Regression Comprehensive in Machine Learning. *Journal of Applied Science and Technology Trends*, 1(4), 140-147.
- Meng, L., Li, J., Chen, Z., Xi, W., Chen, D. and Duan, H. 2010. The calculation of TVDI based on the composite time of pixel and drought analysis. *The International Archives of the Photogrammetry, Remote Sensing and Spatial Information Sciences*, 38.
- Millard, K., Thompson, D.K., Parisien, M.A. and Richardson, M. 2018. Soil moisture monitoring in a temperate peatland using multi-sensor remote sensing and linear mixed effects. *Remote Sensing*, 10, 1-16.
- Minasny, B., Berglund, Ö., Connolly, J., Hedley, C., de Vries, F., Gimona, A., Kempen, B., Kidd, D., Lilja, H., Malone, B. and McBratney, A. 2019. Digital mapping of peatlands— A critical review. *Earth-Science Reviews*, 196, 1-38.
- Minayeva, T.Y. and Sirin, A.A. 2012. Peatland biodiversity and climate change. *Biology Bulletin Reviews*, 2, 164-175.
- Moravec, D., Komárek, J., López-Cuervo Medina, S. and Molina, I. 2021. Effect of Atmospheric Corrections on NDVI: Intercomparability of Landsat 8, Sentinel-2, and UAV Sensors. *Remote Sensing*, 13, 1-14.
- Mustaffa, A.A., Mukhtar, A.N., Rasib, A.W., Suhandri, H.F. and Bukari, S.M. 2020. Mapping of Peat Soil Physical Properties by Using Drone-Based Multispectral Vegetation Imagery. In *IOP Conference Series: Earth and Environmental Science*, 498, 1-8.

- Nelson, K., Thompson, D., Hopkinson, C., Petrone, R. and Chasmer, L. 2021. Peatland-fire interactions: A review of wildland fire feedbacks and interactions in Canadian boreal peatlands. *Science of the Total Environment*, 769, 1-14.
- Ndou, N.N., Palamuleni, L.G. and Ramoelo, A. 2018. Modelling depth to groundwater level using SEBAL-based dry season potential evapotranspiration in the upper Molopo River Catchment, South Africa. *The Egyptian Journal of Remote Sensing and Space Sciences*, 21, 237-248.
- O'Donnell, J.A., Romanovsky, V.E., Harden, J.W. and McGuire, A.D. 2009. The effect of moisture content on the thermal conductivity of moss and organic soil horizons from black spruce ecosystems in interior Alaska. *Soil Science*, 174, 646-651.
- Oleszczuk, R., Brandyk, T., Gnatowski, T. and Szatyłowicz, J. 2004. Calibration of TDR for moisture determination in peat deposits. *International agrophysics*, 18, 1-7.
- Parish, F., Sirin, A., Charman, D., Joosten, H., Minayeva, T., Silvius, M. and Stringer, L. 2008. *Assessment on Peatlands, Biodiversity and Climate Change: Main Report*. Global Environment Centre, Kuala Lumpur and Wetlands International, Wageningen. Available from: [http://www.imcg.net/media/download\\_gallery/books/assessment\\_peatland.pdf](http://www.imcg.net/media/download_gallery/books/assessment_peatland.pdf). Accessed on 18 February 2019.
- Pastor, E., Oliveras, I., Urquiaga-Flores, E., Quintano-Loayza, J.A., Manta, M.I. and Planas, E. 2018. A new method for performing smouldering combustion field experiments in peatlands and rich-organic soils. *International Journal of Wildland Fire*, 26, 1040-1052.
- Prat-Guitart, N., Belcher, C.M, Hadden, R.M, Rein, G. and Yearsly, J.M. 2013. A laboratory study of the effect of moisture content on the spread of smouldering in peat fires. *FLAMMA*, 6, 35-38.
- Prat-Guitart, N., Hadden, R.M., Belcher, C.M., Rein, G. and Yearsley, J.M. 2015. Infrared Image Analysis as a Tool for Studying the Horizontal Smouldering Propagation of Laboratory Peat Fires. *Coal and Peat Fires: A Global Perspective*, 4, 121-139.
- Prat-Guitart, N., Rein, G., Hadden, R.M., Belcher, C.M and Yearsly, J.M. 2016. Propagation probability and spread rates of self-sustained smouldering fires under controlled moisture content and bulk density conditions. *International Journal of Wildland Fire*, 25, 456–465.
- Process.St. 2021. Drone Preflight Checklist. Available from <https://www.process.st/checklist/drone-pre-flight-checklist/#charge-drone-batteries>. Accessed on 12 September 2021.

- Raeva, P.L., Sedina, J. and Dlesk, A. 2019. Monitoring of crop fields using multispectral and thermal imagery from UAV. *European Journal of Remote Sensing*, 52, 192-201.
- Ratnasari, N.G., Dianti, A., Palamba, P., Ramadhan M.L., Prayogo, G., Pamitran, A.S., Nugroho, Y.S. 2018. Laboratory Scale Experimental Study of Foam Suppression on Smouldering Combustion of a Tropical Peat. IOP Conf. Series: *Journal of Physics: Conference Series*, 1107, 1-6.
- Reardon, J. and Curcio, G. 2011. Estimated Smouldering Probability: A New Tool for Predicting Ground Fire in the Organic Soils on the North Carolina Coastal Plain. *Fire Management Today*, 71, 31-35.
- Ruwaimana, M., Satyanarayana, B., Otero, V., M. Muslim, A., Syafiq A, M., Ibrahim, S., Raymaekers, D., Koedam, N. and Dahdouh-Guebas, F. 2018. The advantages of using drones over space-borne imagery in the mapping of mangrove forests. *PloS one*, 13(7),1-22.
- Salami, E., Barrado, C. and Pastor, E. 2014. UAV flight experiments applied to the remote sensing of vegetated areas. *Remote Sensing*, 6, 11051-11081.
- Sofan, P., Bruce, D., Jones, E. and Marsden, J. 2019. Detection and Validation of Tropical Peatland Flaming and Smouldering Using Landsat-8 SWIR and TIRS Bands. *Remote Sensing*, 11, 1-28.
- Schirmbeck, L.W. 2017. Understanding TVDI as an index that expresses soil moisture. *Journal of Hyperspectral Remote Sensing*, 7, 82-90.
- Shafian, S. and Maas, S.J. 2015. Index of Soil Moisture Using Raw Landsat Image Digital Count Data in Texas High Plains. *Remote Sensing*, 7, 2352-2372.
- Shin, J.I., Seo, W.W., Kim, T., Park, J. and Woo, C.S., 2019. Using UAV Multispectral Images for Classification of Forest Burn Severity-A Case Study of the 2019 Gangneung Forest Fire. *Forests*, 10,1025.
- Strydom, S. and Savage, M.J. 2016. A Spatio-temporal analysis of fires in South Africa. *South African Journal of Science*, 112, 1-8.
- Teguh, R., Honma, T., Usop, A., Shin, H. and Igarashi, H. 2012. Detection and verification of potential peat fire using wireless sensor network and UAV. In *Proceedings of the International Conference Information Technology and Electrical Engineering, Yogyakarta, Indonesia*, 6-10.
- Thomas, D.S., Twyman, C., Osbahr, H. and Hewitson, B. 2007. Adaptation to climate change and variability: farmer responses to intra-seasonal precipitation trends in South Africa. *Climatic change*, 83, 301-322.

- Tmusic, G., Manfreda, S., Aasen, H., James, M.R., Gonçalves, G., Ben-Dor, E., Brook, A., Polinova, M., Arranz, J.J., Mészáros, J. and Zhuang, R. 2020. Current practices in UAS-based environmental monitoring. *Remote Sensing*, 12(6), 1-35.
- Tran, B., Tanase, M., Bennett, L. and Aponte, C. 2018. Evaluation of spectral indices for assessing fire severity in Australian temperate forests. *Remote Sensing*, 10, 1680.
- Uda, S.K., Hein, L. and Atmoko, D. 2010. Assessing the health impacts of peatland fires: a case study for Central Kalimantan, Indonesia. *Environ Sci Pollut Res*, 26, 31315–31327.
- Yang, G., Liu, J., Zhao, C., Li, Z., Huang, Y., Yu, H., Xu, B., Yang, X., Zhu, D., Zhang, X. and Zhang, R. 2017. Unmanned aerial vehicle remote sensing for field-based crop phenotyping: current status and perspectives. *Frontiers in plant science*, 8, 1111.
- Yuan, C., Zhang, Y. and Liu, Z. 2015. A survey on technologies for automatic forest fire monitoring, detection, and fighting using unmanned aerial vehicles and remote sensing techniques. *Canadian journal of forest research*, 46, 783-792.
- Vitt, D.H. 2013. Peatlands. *Encyclopedia of Ecology*, 2, 557-566.
- Zaccone, C., Rein, G., D’Orazio, V., Hadden, R.M., Belcher, C.M. and Miano, T.M. 2014. Smouldering fire signatures in peat and their implications for paleoenvironmental reconstructions. *Geochimica ET Cosmochimica Acta*, 137, 134-146.
- Zhang, H.W., Chen, H.L., Shen, S., Zhou, G. and Yu, W. 2008. Drought remote sensing monitoring based on the surface water content index (SWCI) method. *Remote Sensing Technology and Application*, 23(6), 624-628.
- Zhang, J., Zhang, Q., Bao, A. and Wang, Y. 2019. A New Remote Sensing Dryness Index Based on the Near-Infrared and Red Spectral Space. *Remote Sensing*, 11, 456.
- Zhang, G., Ali, S., Wang, X., Wang, G., Pan, Z. and Zhang, J. 2019. SPI-based drought simulation and prediction using ARMA-GARCH model. *Applied Mathematics and Computation*, 355, 96-107.

# APPENDICES

## Appendix A: Figures

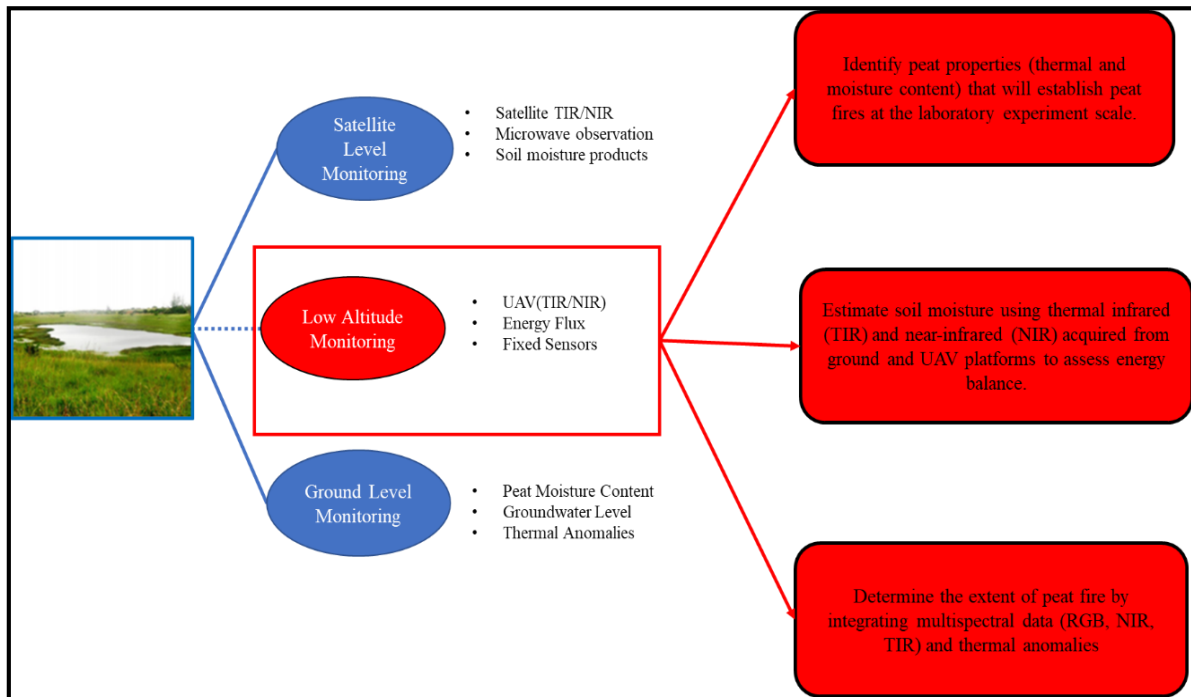


**Figure A 1:** The outline of the main objectives of the project

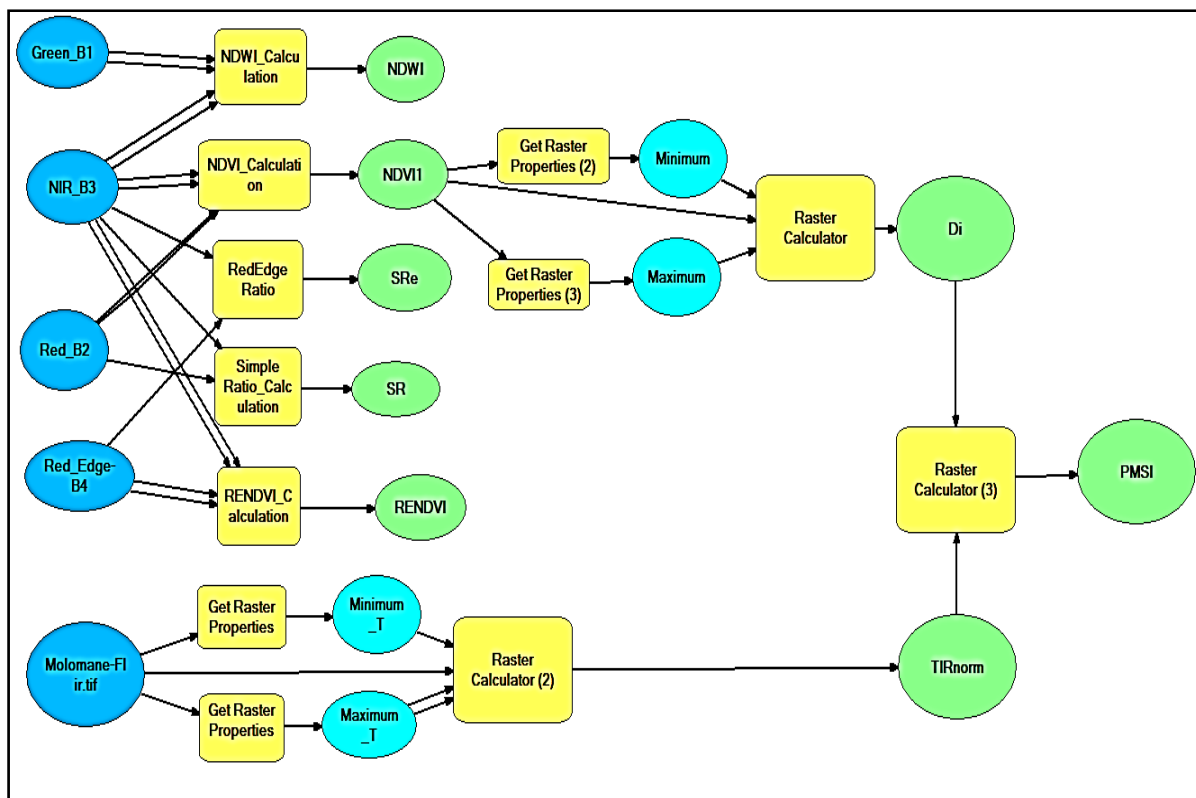


**Figure A 2:** Model developed to establish indices calculation and soil moisture index

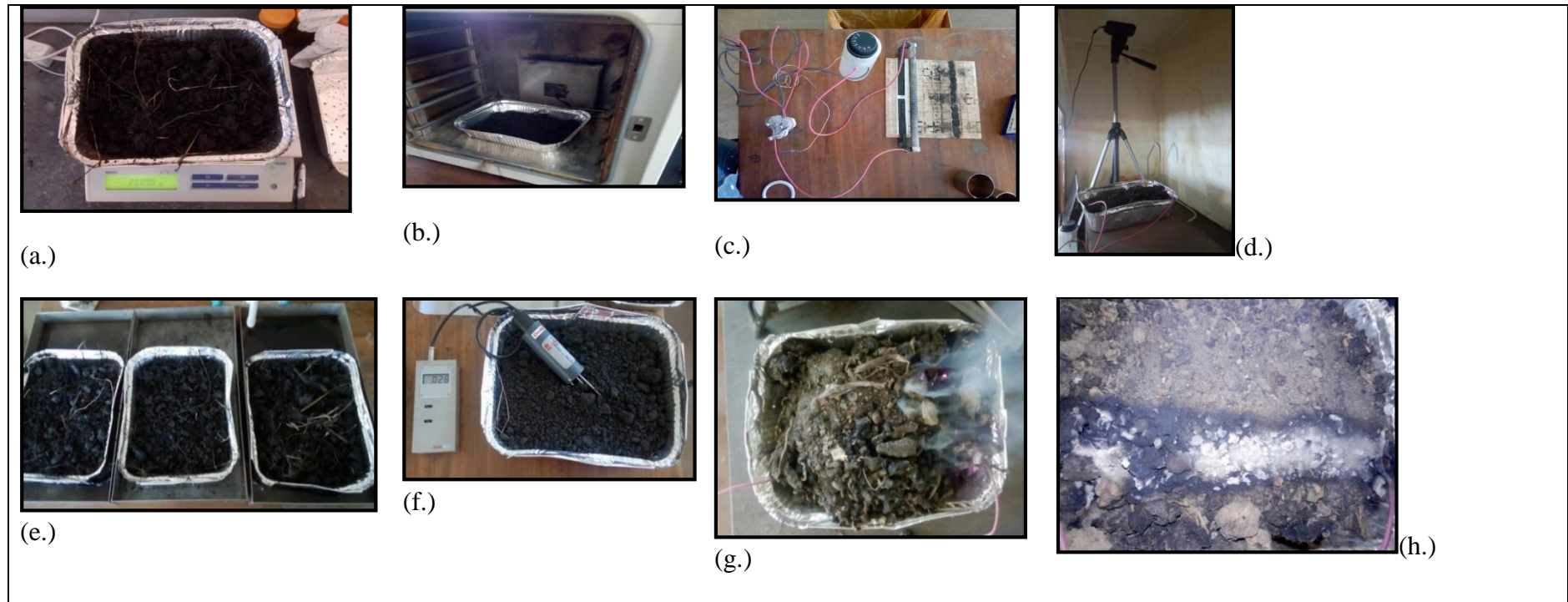


**Figure A 3:** Steps for laboratory research performed a.) weighing the samples b.) Samples drying at 70 ° C, for 1 to 3 days, c.) Ceramic heater coil and d.) set up the experiment about the fire; e.) peat rewetting samples; f.), soil moisture calculation using Theta Probe; g.), peat fire burning / smouldering peat surface and h.) peat ash after peat burning.

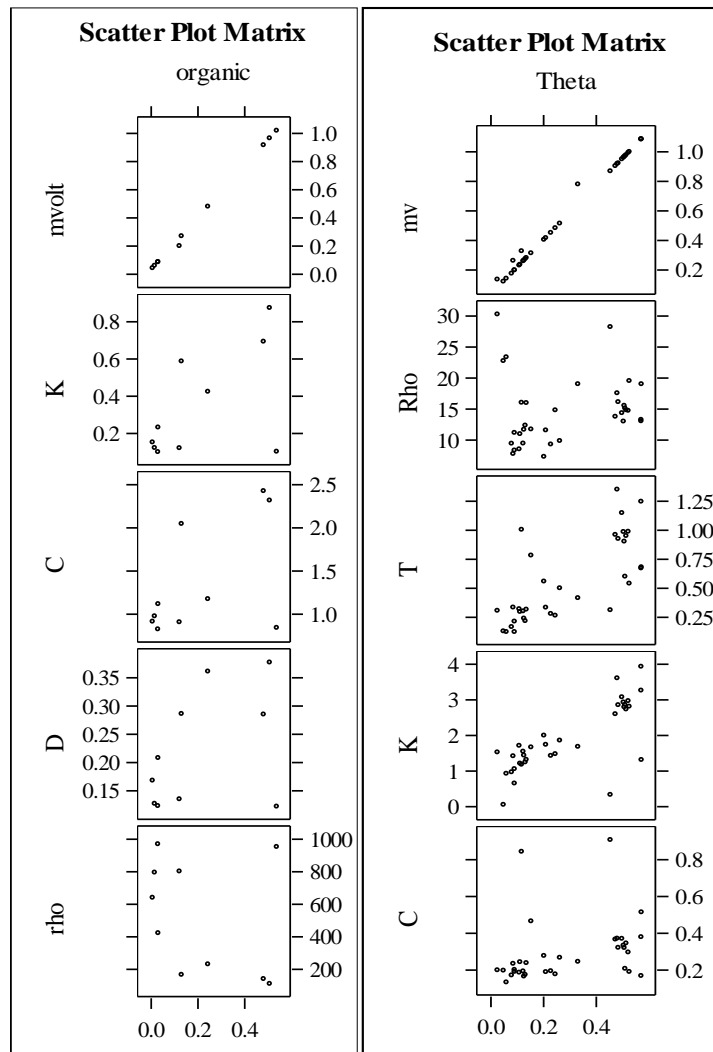
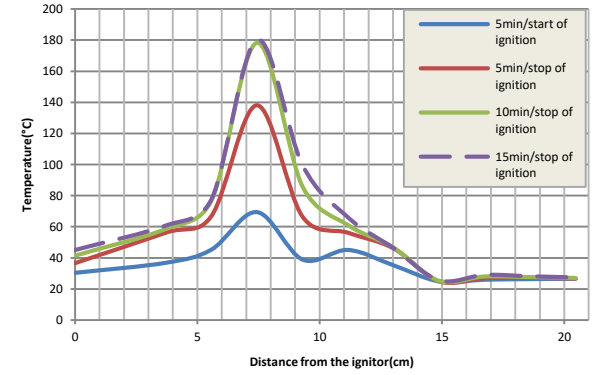
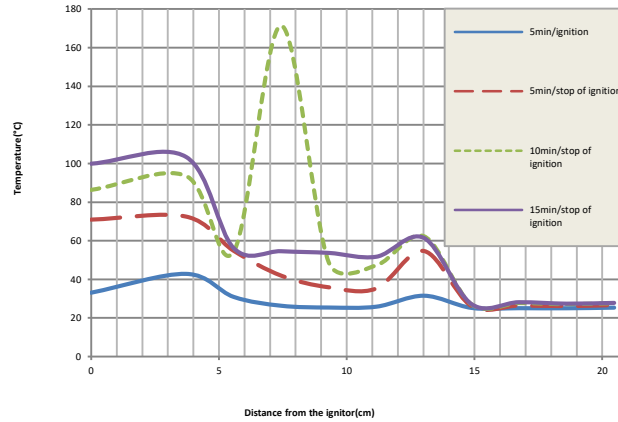
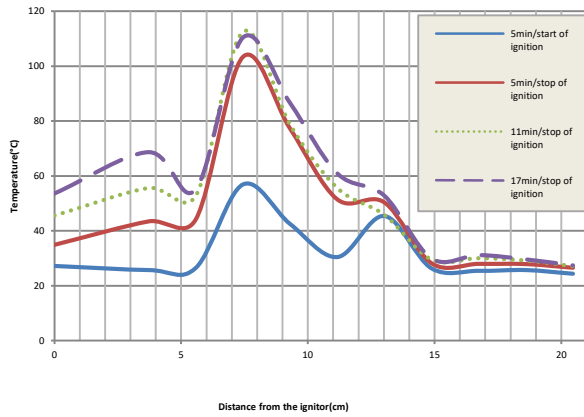


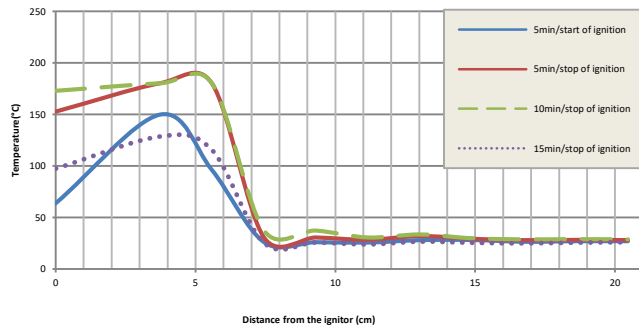
**Figure A 4:** Correlation between theta (moisture content) and other variables



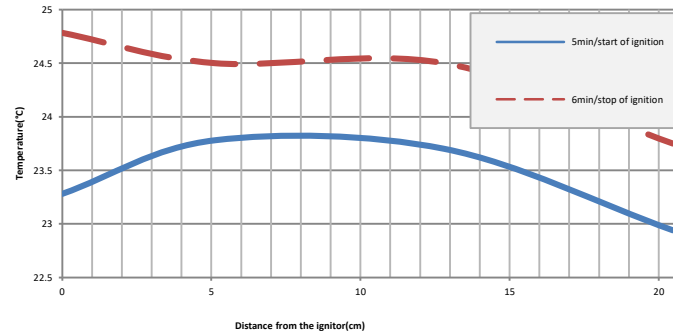
(a.)  $[\theta = 1.30]$

(b.)  $[\theta = 0.9]$

(c.)  $[\theta = 0.56]$



(d.)  $[\theta = 0.3]$



(e.)  $[\theta = 1.2]$

**Figure A 5:** The relationship between front movement, soil moisture, and temperature during peat ignition for Molemane samples; (a.) 130%MC, (b.) 90%MC, (c.) 56%MC, (d.) 30%MC and (e.)120%MC

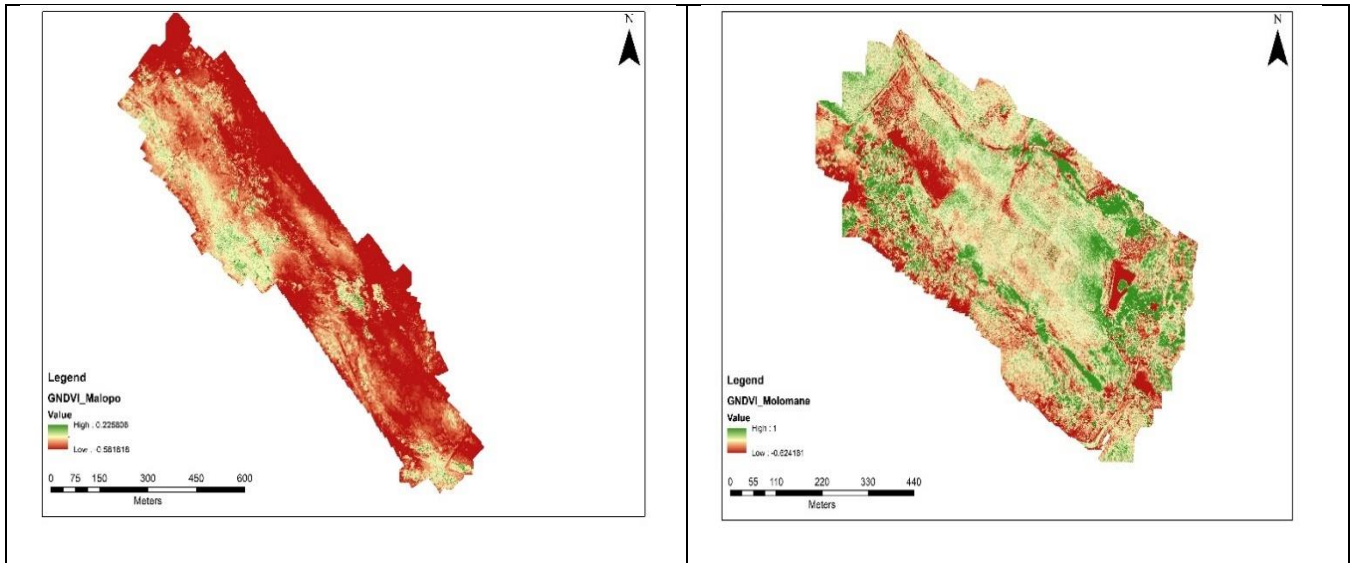


**Figure A 6:** Green- NDVI for Molopo (a) and Molemane (b)

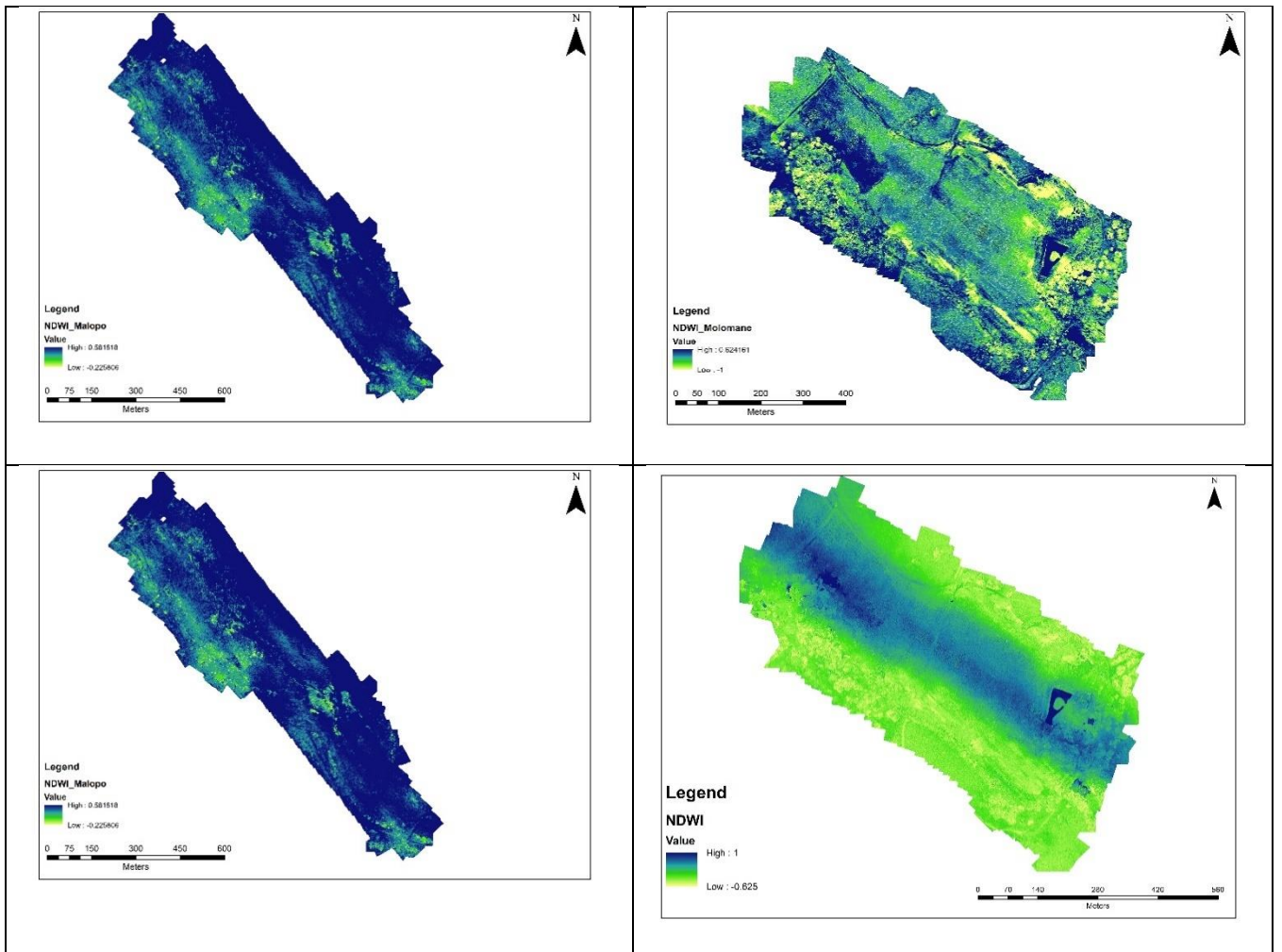


**Figure A 7:** NDWI images for Molopo (a.) and Molemane (b.) peat sites

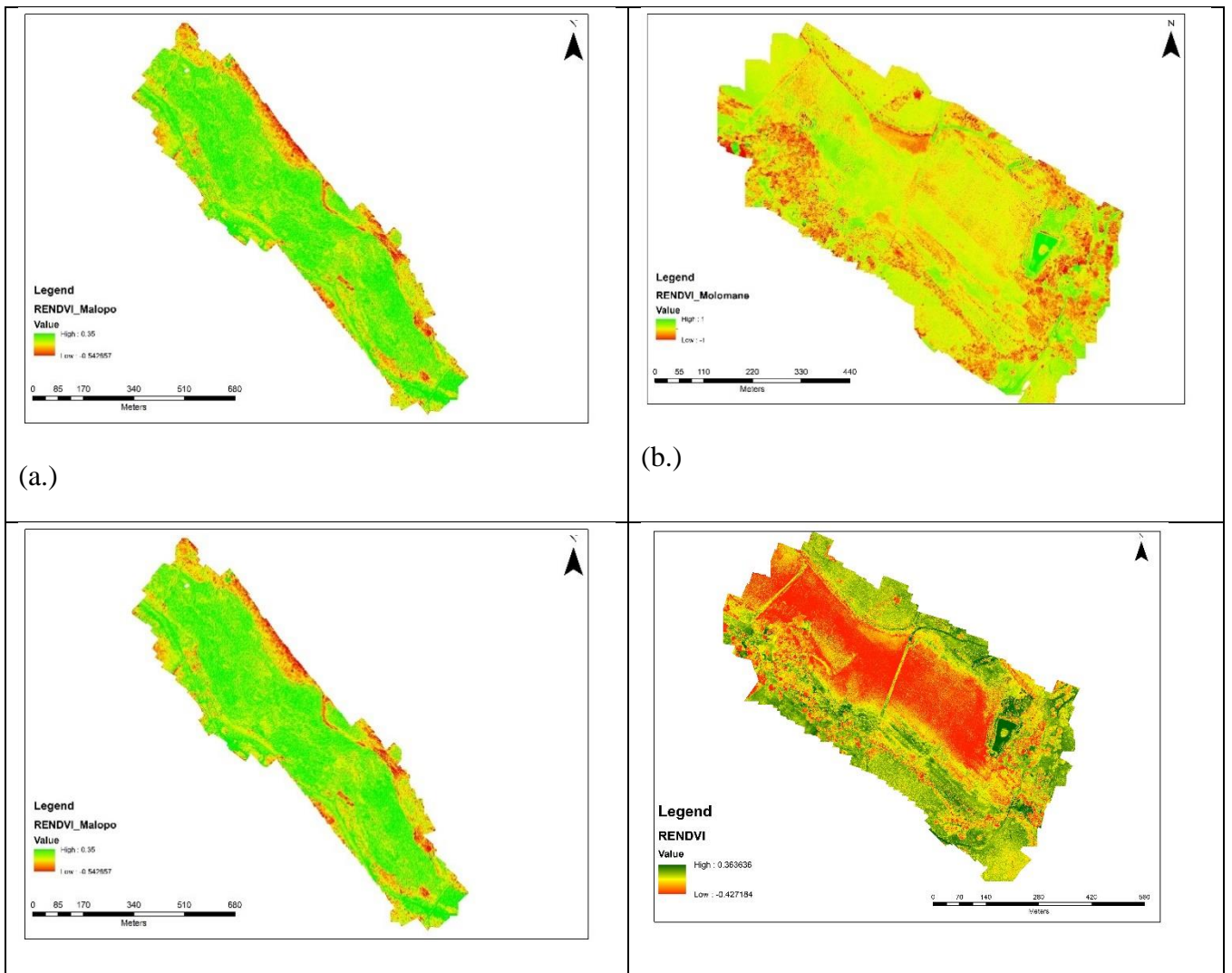


**Figure A 8:** Red Edge NDVI for Molopo (a.) and Molemane (b.) peat site

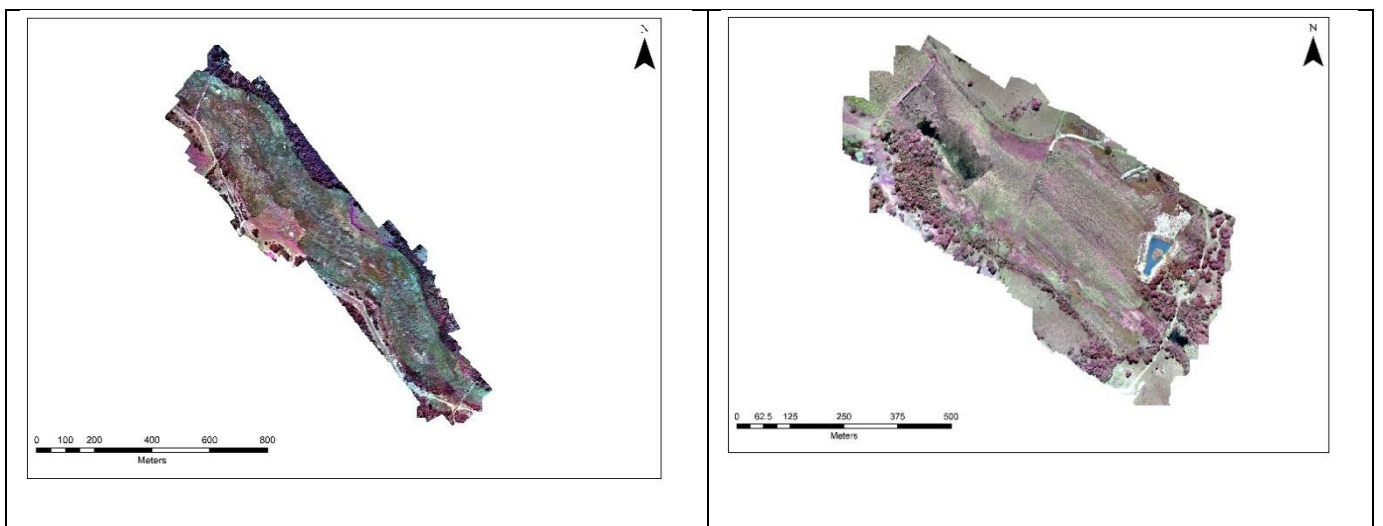


**Figure A 9:** Natural Colour Composite [RGB: 3, 2, 1] for Molopo (a.) and Molemane (b.) peat site

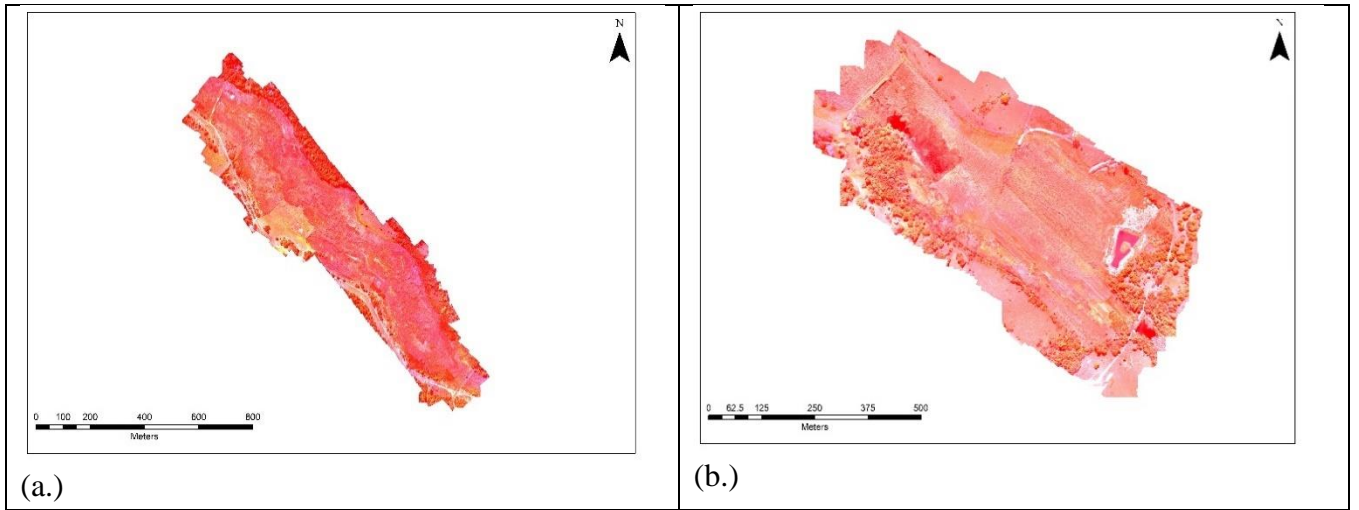


**Figure A 10:** Pseudo-infrared composite [RGB: 5, 3, 2] for Molopo (a.) and Molemane (b.) peat site

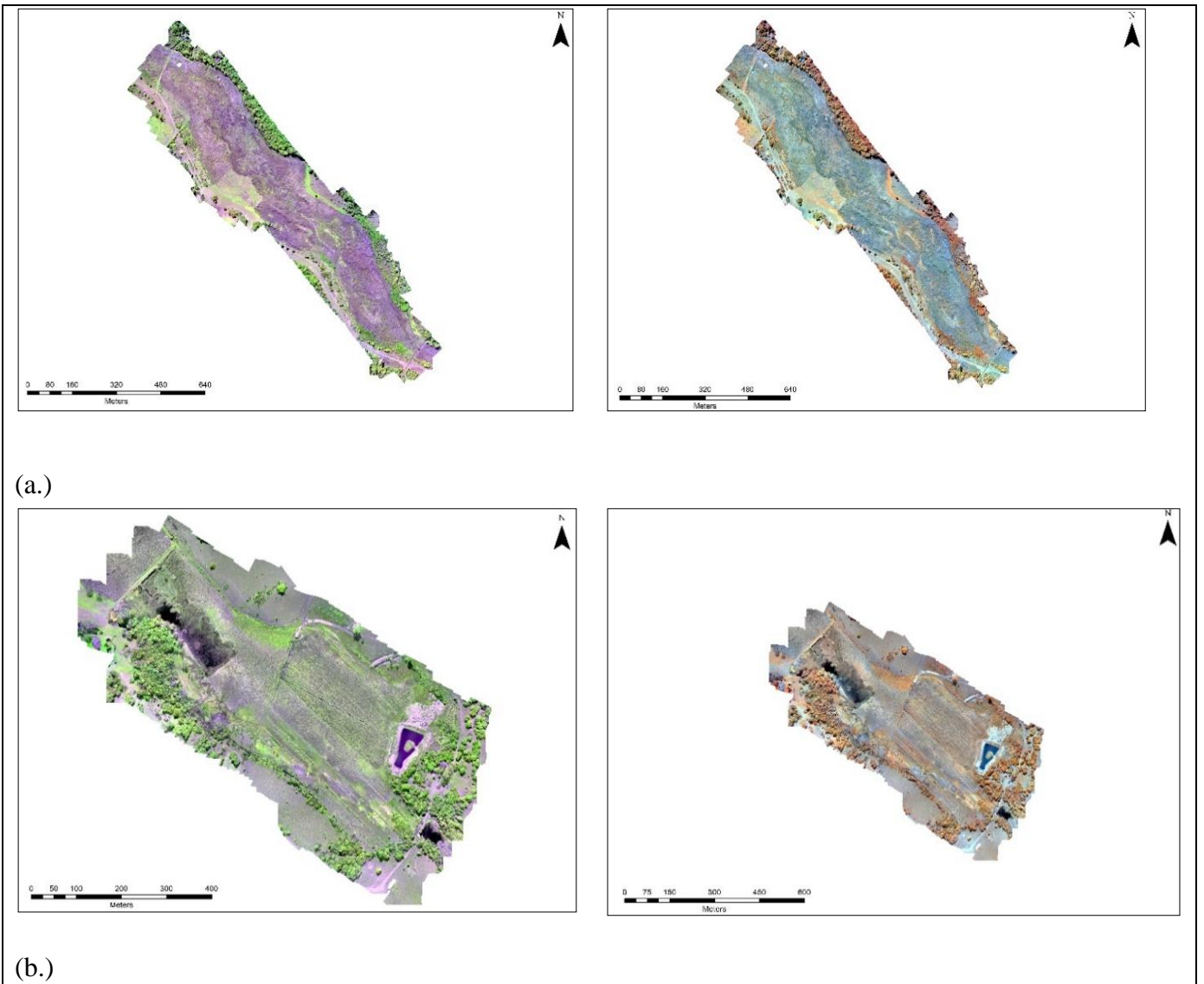
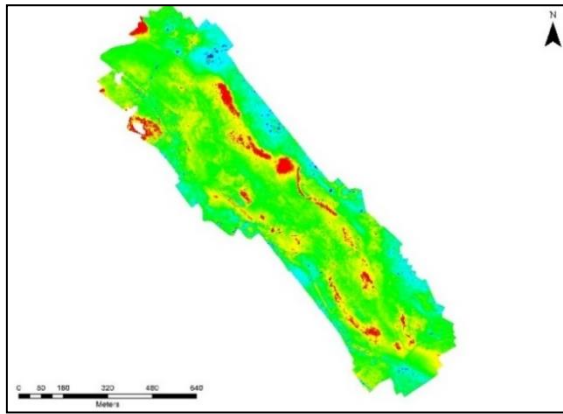
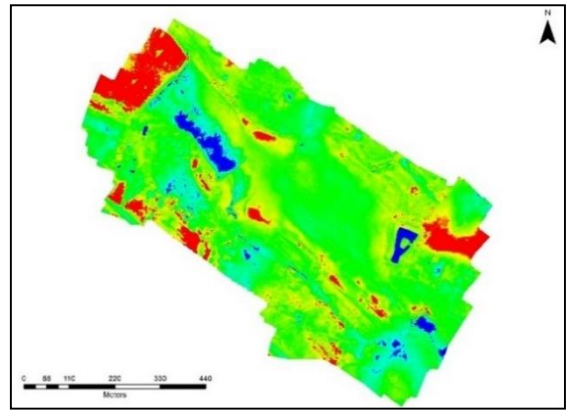


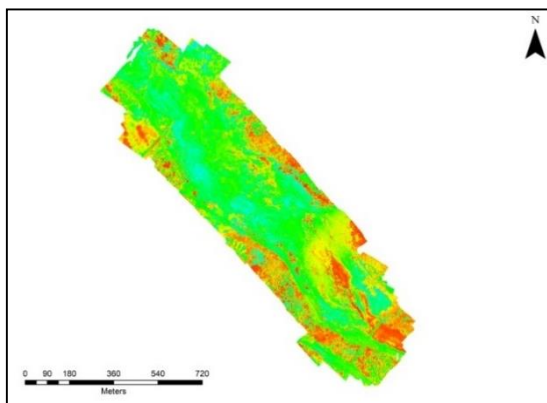
**Figure A 11:** High-resolution multispectral image for Molopo (a.) and Molemane (b.) peat site with RGB: 3, 4, 2 (left) and RGB: 4, 3, 2(right)



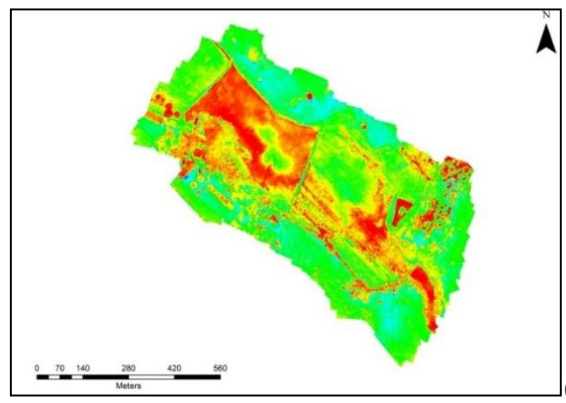
(a.)



(b.)



(c.)



(d.)

**Figure A 12:** Thermal images, May survey for peat sites Molopo (a.) and Molemane (b.) (RGB: 3, 2, 1) and December survey, Molopo (c.) and Molemane (d.) peat sites (RGB: 3, 2, 1)

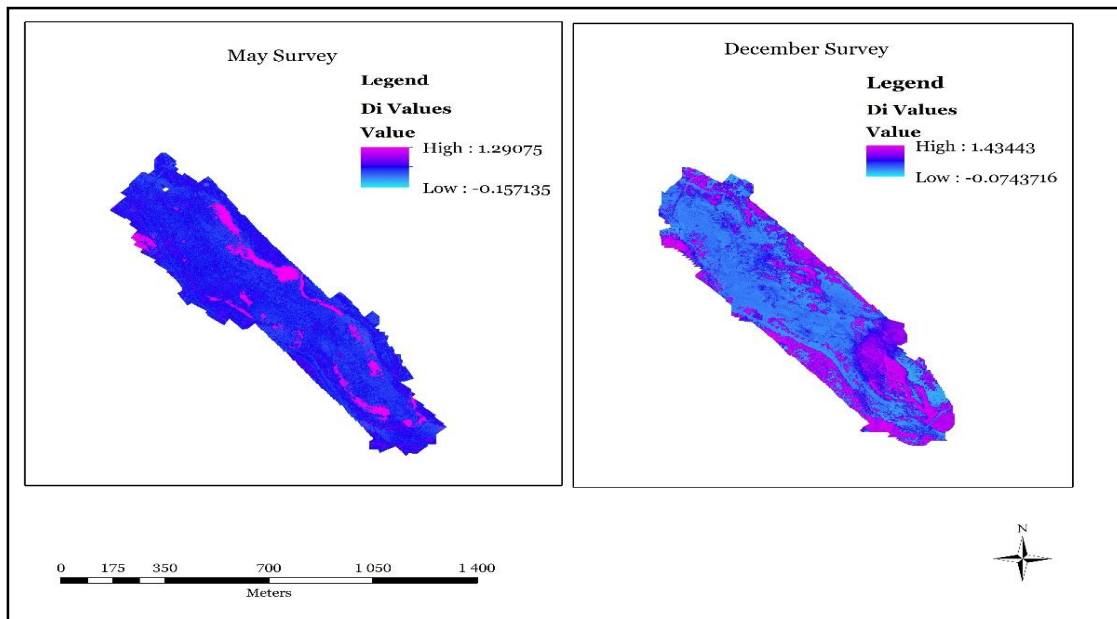


**Figure A 13:** Molopo peat site Di distribution

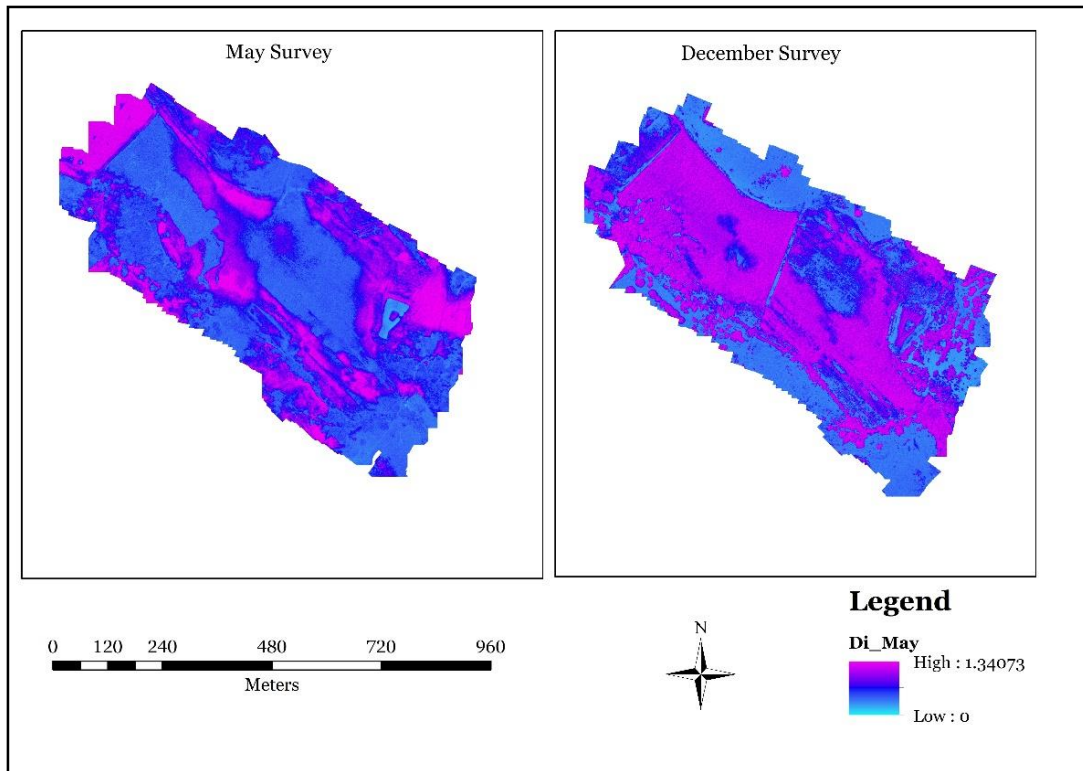
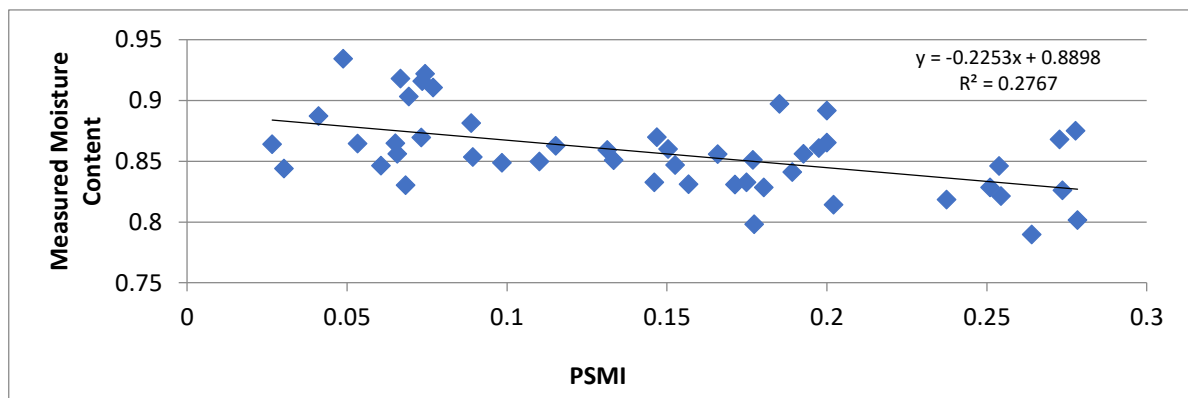
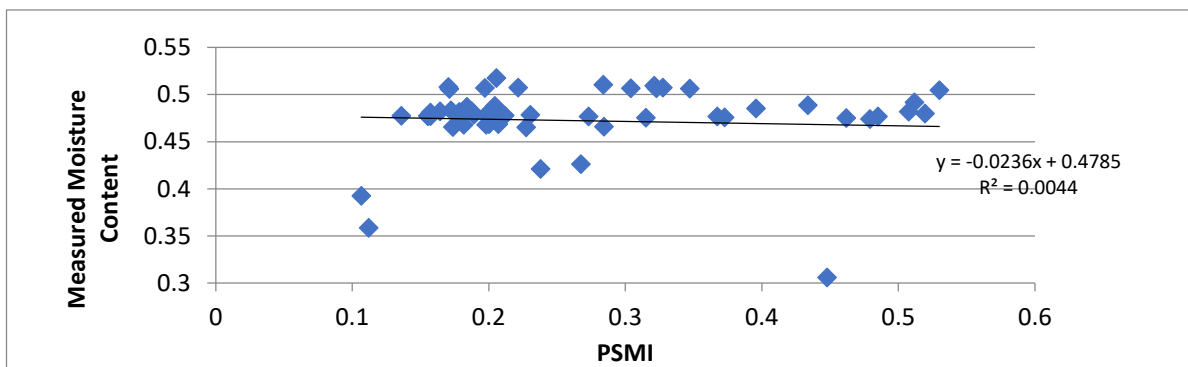


Figure A 14: Molemane Peat site Di distribution



(a.)



(b.)

Figure A 15: Linear regression for soil moisture field measurements and predicted soil moisture from TIR and NIR bands for Molopo site (a.) and Molomane (b.)

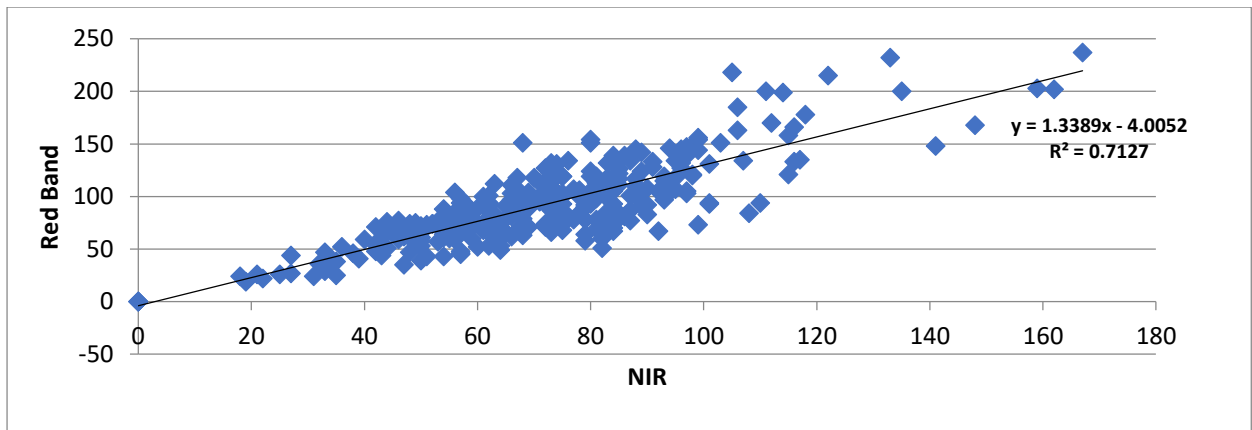


**Figure A 16:** The relationship between Red and NIR band